

UNIVERSITY OF MISKOLC  
FACULTY OF MECHANICAL ENGINEERING AND INFORMATICS



**DESIGN, DEVELOPMENT, AND OPTIMIZATION OF SOLAR  
DRYER FOR WOOD FUELS**

PHD THESES

Prepared by

**Baibhaw Kumar**

Mechanical Engineering (BE),  
Energy Technology-Mechanical (MTech)

**ISTVÁN SÁLYI DOCTORAL SCHOOL OF MECHANICAL ENGINEERING SCIENCES**  
**TOPIC FIELD OF DESIGN OF MACHINES AND STRUCTURES**  
**TOPIC GROUP OF ENERGY AND CHEMICAL ENGINEERING SYSTEMS DESIGN**

Head of Doctoral School

**Dr. Gabriella Bognár**  
DSc, Full Professor

Head of Topic Group

**Prof. Dr. Zoltán Siménfalvi**

Scientific Supervisor  
**Dr. Zoltán Szamosi**

Scientific Co-Supervisor  
**Dr. Gábor L. Szepesi**

**Miskolc**  
**2023**

CONTENTS

CONTENTS.....	I
SUPERVISOR'S RECOMMENDATIONS.....	III
LIST OF SYMBOLS AND ABBREVIATIONS.....	IV
<b>1. INTRODUCTION .....</b>	<b>5</b>
<i>1.1. Background and Context .....</i>	<i>5</i>
<i>1.2. Objectives of the research .....</i>	<i>8</i>
<i>1.3. Thesis layout .....</i>	<i>10</i>
<b>2. TECHNICAL CONTRIVANCES IN SOLAR DRYING OF WOOD .....</b>	<b>12</b>
<i>2.1 Parameters affecting the performance of extant solar wood dryers and their classification .....</i>	<i>12</i>
<i>2.1.1. Basic parameters affecting solar drying of wood .....</i>	<i>12</i>
<i>2.1.2. Classification of wood solar dryers .....</i>	<i>14</i>
<i>2.2. Contrast in numerical modeling and simulation approaches .....</i>	<i>15</i>
<i>2.3. Prevalent design concepts .....</i>	<i>21</i>
<b>3. EXPERIMENTS WITH NATURAL CONVECTION SOLAR DRYER.....</b>	<b>24</b>
<i>3.1. Background Study .....</i>	<i>24</i>
<i>3.2. Design and construction .....</i>	<i>24</i>
<i>3.3. Temperature profiling results .....</i>	<i>25</i>
<b>4. EXPERIMENTS WITH FORCED CONVECTION CABINET TYPE SOLAR DRYER .....</b>	<b>27</b>
<i>4.1. Empirical study on the Forced convection cabinet solar Dryer.....</i>	<i>27</i>
<i>4.2. Energy Analysis .....</i>	<i>30</i>
<i>4.3. Exergy Analysis .....</i>	<i>30</i>
<i>4.4. Uncertainty Analysis .....</i>	<i>32</i>
<i>4.5. ANN modelling .....</i>	<i>33</i>
<i>4.6. Development of the ANN model .....</i>	<i>33</i>
<i>4.7. Parameters of the ANN model .....</i>	<i>34</i>
<i>4.8. Results of experimental investigations .....</i>	<i>35</i>
<b>5. EXPERIMENTS WITH PHASE CHANGE MATERIAL (PCM) .....</b>	<b>41</b>
<i>5.1. Artificial radiation set-up .....</i>	<i>41</i>
<i>5.2. Thermophysical properties of coconut oil as PCM .....</i>	<i>43</i>
<i>5.3. Methodology .....</i>	<i>44</i>
<i>5.4. 4-E Analysis.....</i>	<i>46</i>
<i>5.4.1. Energy analysis .....</i>	<i>47</i>
<i>5.4.2. Exergy analysis .....</i>	<i>48</i>
<i>5.4.3. Economic Assessment .....</i>	<i>49</i>
<i>5.4.4. Environmental Assessment .....</i>	<i>51</i>
<i>5.5. Uncertainty Analysis .....</i>	<i>53</i>
<i>5.6. Results of experimental investigations .....</i>	<i>54</i>

5.6.1.	<i>Temperature</i> .....	54
5.6.2.	<i>Energy gain and efficiency</i> .....	56
5.6.3.	<i>Exergy gain and efficiency</i> .....	57
5.6.4.	<i>Economic assessment findings</i> .....	59
5.6.5.	<i>Environmental assessment results</i> .....	60
5.6.6.	<i>Critical Observations</i> .....	60
<b>6.</b>	<b>SOLAR DRYING POTENTIAL IN HUNGARY: TRENDLINE ASSESSMENT WITH A CASE STUDY</b> .....	<b>63</b>
6.1.	<i>Scope of renewable energy in Hungary</i> .....	63
6.2.	<i>Trendline assesment of solar potential in Hungary and its neighbour countries</i> .....	65
6.3.	<i>Case Study: Real-time Data Assessment of a boiler plant in Miskolc, Hungary</i> .....	68
6.3.1.	<i>Calorific value and moisture content of wood as biofuel</i> .....	68
6.3.2.	<i>Calorific value and moisture content of wood as biofuel</i> .....	69
6.3.3.	<i>Trendline analysis: Moisture content and calorific value</i> .....	70
6.3.4.	<i>Trendline analysis: Production, consumption, and operations</i> .....	71
6.3.5.	<i>Identification of possible remedies via. solar drying</i> .....	71
<b>7.</b>	<b>THESES-NEW SCIENTIFIC RESULTS</b> .....	<b>73</b>
<b>8.</b>	<b>8. FUTURE SCOPE</b> .....	<b>ERROR! BOOKMARK NOT DEFINED.</b>
8.1.	<i>Future prospects on industrial utility</i> .....	76
8.2.	<i>Future research direction</i> .....	78
	<b>ACKNOWLEDGMENTS</b> .....	<b>80</b>
	<b>REFERENCES</b> .....	<b>81</b>
	<b>LIST OF PUBLICATIONS RELATED TO THE TOPIC OF THE RESEARCH FIELD</b> .....	<b>95</b>

**SUPERVISOR'S RECOMMENDATIONS**

Date

Supervisor

LIST OF SYMBOLS AND ABBREVIATIONS

$Q_l$	absorbed energy (W)	$n$	lifespan (years)
$Q_u$	useful energy (W)	$R$	universal gas constant (J/kg.K)
$Q_{st}$	stored energy (W)	$\frac{W_{Tch}}{T_{ch}}$	temperature uncertainty
$Q_l$	lost energy (W)	$\frac{W_{ma}}{\dot{m}a}$	mass-flow rate uncertainty
$\rho$	density (kg/m <sup>3</sup> )	$\frac{W_{Eout}}{E_{out}}$	energy uncertainty
$V_{avg}$	average velocity (m/s)	$N$	payback period (years)
$\beta$	tilt angle [°]	$\phi$	latitude angle
$A_{duct}$	duct area (m <sup>2</sup> )	$f$	inflation rate (%)
$C_p$	specific heat of sawdust (J/kg/K)	<b>Abbreviations</b>	
$T_o$	outlet temperature (°C)	PCM	phase change material
$T_i$	inlet temperature (°C)	PV	photovoltaics
$A_c$	collector area (m <sup>2</sup> )	TES	thermal energy storage
$I_T$	radiation (W/m <sup>2</sup> )	DSC	differential scanning calorimetry
$Q_{ch}$	energy while charging (W)	CRF	capital recovery factor
$Q_{dis}$	energy while discharging (W)	FAC	fixed annual cost
$m$	mass flowrate (kg/s)	SFF	sinking fund factor
$\Delta t$	temperature difference	ASV	annual salvage value
$\eta_{th}$	thermal energy efficiency	AMC	annual operational cost
$T_a$	ambient temperature (°C)	FAC	fixed annual cost
$Ex_{in}$	inlet exergy (W)	EBPT	energy payback time
$Ex_u$	outlet exergy (W)	IP	improvement potential
$i$	interest rate (%)	LOP	lack of productivity
$\eta_{ex}$	exergy efficiency	IC	capital cost of dryer
$L$	latent heat, J/kg	EUR	euros

### 1. INTRODUCTION

#### 1.1. Background and Context

In the 21st century, it is inevitable to look for solutions beyond conventional energy sources. There is a continuous struggle among scientists and industries to address the issue of the energy crisis and the adversities of climate change. In this overall change, biofuels such as wood chips are key players, primarily in heating utilities. However, the particle emissions from wood biomass are higher than those from conventional energy sources. The usage of wood chips for small-scale heating applications has grown considerably in the central European region in the last decade. In the last few years, Germany adopted the emission control act to revive the already existing heating systems and reduce the emission load in the region [1]. The quality of the wood chips is primarily affected by the moisture content in the woods. The moisture reduces the overall fuel efficiency and adds adverse effects such as enhanced carbon monoxide (CO) emissions in the process [2]. The energy properties and chemical compositions of the ash content also decide the slagging and fouling phenomena in industrial boilers. These factors also affect the optimization of the boiler efficiency [3]. An industrial boiler's efficiency depends on several factors which directly or indirectly affect energy efficiency.

Over the years, several models or approaches have been developed in this field to understand the efficiency of boilers. A recent review by Cabeza et al. [4] classified the energy efficiency optimization of boilers into three categories, i.e., Analytic models, Mechanistic models, and Empiric models. These models are used based on the requirements of the optimization. For example, analytical models are used for first-hand approximation, whereas mechanistic models are preferred for accurate calculations. Artificial intelligence models are now being supported with existing models for better insights into the optimization process. The boiler performance could be analyzed with the suggested mathematical and computational models. The performance of the boiler plant with wood chips as a fuel source also depends on the plant operating parameters, the moisture content, size, and storage of the fuel. Thus, an analytical understanding of all these factors is crucial for the overall performance of the boiler plants [5]. Although storage conditions and moisture content of the wood chips considerably affect the boiler performance. Generally, the wet basis moisture content is dried

to a level of 10 – 15%, but it is not yet storage stable. Few researchers addressed this problem, and results showed that for six months of storage with 1.1% dry matter loss with 20% moisture content at 21°C storage temperature. Thus, the moisture content effect also varies under different storage conditions [6].

On the other hand, a simple example demonstrating the challenge in developing wood-based solar drying technologies is rooted in its classification. Wood as fuel can broadly be classified into three main categories: coniferous wood, non-coniferous wood, and wood chips. As per the five-year average data of FAOSTAT (Food and Agriculture Organization Corporate Statistical Database, United States), Europe and America were major coniferous and wood chips producers [7]. In contrast, Asia and Africa lead the production of non-coniferous types of wood, as shown in Figure 1. Thus, it is comprehended that distinct regions of the world have particular types of wood production. Accordingly, the storage and fuel efficiency of the wood supplied for industrial use also differs.

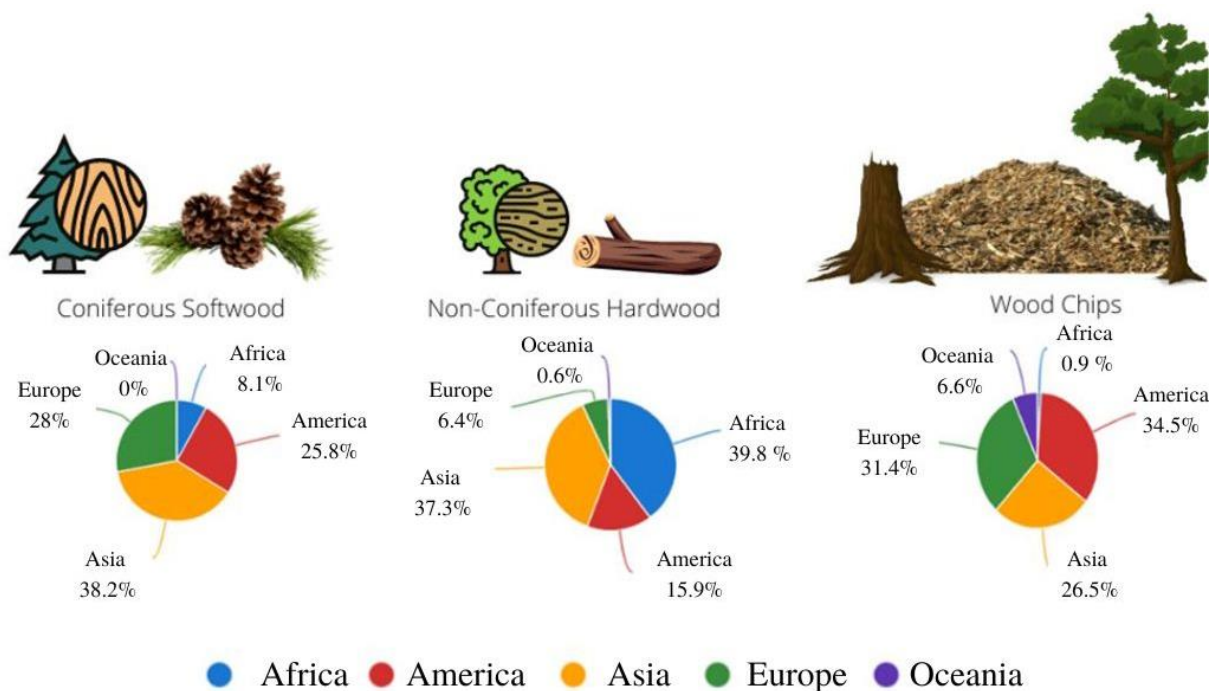


Figure. 1 Wood fuel (coniferous and non-Coniferous) and wood chips production by region at the world level as average for 2015-2020 (Data source: FAOSTAT) [7].

It is important to properly store and dry the wood fuels before utilizing them for several reasons:

- **Reduced moisture content:** Wood fuels, such as firewood or wood pellets, typically contain a significant amount of moisture when freshly cut. This moisture content

affects the combustion efficiency and heat output of the wood. By solar drying, the moisture content can be significantly reduced, leading to more efficient and cleaner combustion in large-scale usage of fuels.

- **Improved energy efficiency:** Solar drying utilizes the sun's energy to remove moisture from the wood, reducing the need for traditional sources like fossil fuels or electricity. This reduces the overall energy consumption and associated costs in the drying process.
- **Prevention of decay and fungal growth:** High moisture content in wood fuels can lead to decay and fungal growth, reducing their quality and energy content. Solar drying helps to lower the moisture content to a level where decay and fungal growth are minimized, thereby preserving the quality of the wood fuels. Optimizing solar dryers can improve the drying process scientifically in several ways.
- **Enhanced energy/exergy efficiency:** By improving the design and operation of solar dryers, it is possible to increase the rate of moisture removal from wood fuels. This can be achieved by optimizing factors such as air circulation, temperature control, solar radiation exposure, and with the usage of phase change materials (PCM).
- **Consistent drying for long-time storage:** Solar dryers can be designed to provide a more controlled drying environment, allowing for consistent moisture reduction across different batches of wood fuels. This helps in achieving uniform drying and ensures consistent quality of the final product. PCMs have evolved as a potential solution for hybridization and continuous drying solution.
- **Monitoring and data analysis:** By incorporating sensors and monitoring systems into solar dryers, it becomes possible to collect data on variables such as temperature, humidity, and airflow. This data can be analyzed scientifically to understand the drying process better, identify optimization opportunities, and make informed decisions regarding drying parameters. Investigating and optimizing solar dryers for wood fuels is important for several reasons:
- **energy sustainability:** Wood fuels are a renewable energy source, and efficient utilization of solar energy for drying can contribute to a more sustainable energy system. Optimizing solar dryers helps in reducing the reliance on non-renewable

energy sources and mitigating the environmental impact associated with conventional drying methods.

- **Economic viability:** Solar drying offers potential cost savings by reducing energy consumption and operational costs. Investigating and optimizing solar dryers can lead to improved efficiency, reduced drying times, and enhanced overall productivity, making wood fuel production more economically viable.
- **Climate change mitigation:** Efficient utilization of wood fuels can help reduce greenhouse gas emissions compared to fossil fuel alternatives. By optimizing solar dryers and promoting the use of properly dried wood fuels, the overall carbon footprint of energy production and utilization can be minimized.
- **Rural development and livelihood improvement:** Wood fuels are often sourced and utilized in rural areas, where access to modern energy services may be limited. By investigating and improving solar drying techniques, it becomes possible to enhance the livelihoods of communities relying on wood fuel production, leading to rural development and improved living conditions.

### 1.2. Objectives of the research

In the context of drying, the solar drying technique for maintaining wood fuel quality is common in many countries with reasonable solar radiation through solar kilns. The solar kiln designing and prototyping started more after the energy crisis of 1970. Lianbai extensively investigated wood drying techniques in China a decade ago. The review suggests that the Chinese kilns for hardwood drying are slower and emphasize larger thermal capacity and a higher rate of air circulation [8]. The effectiveness of solar drying depends not only on input temperature but several factors of the designed solar kiln [9]. The solar insolation varies, and so does the wood moisture content and the atmosphere's humidity. The epochal weather conditions limit the drying rate; thus, heat storage mediums are important in drying technology innovations. Pushendra et al. [10], identified such limitations in their review. The study suggested using PV/T and thermal energy storage mediums to improve the dryer efficiency. Research conducted by Dundar et al. [11] predicts that the requirement for woody biomass demand will rise soon. However, the study on solar drying or wood as biomass and its quality improvement through solar drying is covered to a small extent.

Researchers reviewed the vacuum-drying of wood by categorizing them into four groups: conductive heating vacuum, cyclic vacuum, superheated steam vacuum, and dielectric vacuum [12]. Review work is also available on solar drying techniques, emphasizing types, parameters, and limitations with context on the economic and environmental assessment of various solar dryers [13]. Yi *et al.* [14] presented the progress by reviewing cutting-edge drying technologies, including solar drying, microwave drying, and far-infrared drying at the laboratory and pilot-plant scale for biomass drying. In a recent review work by Lmarani *et al.* [15], the authors identified that the number of publications related to solar wood drying increased in the last five years. However, very limited review articles have been published. Also, they added that the solar drying of “wood” is a complex phenomenon depending on several factors. Therefore, further reviews and research can provide additional insights focusing on solar wood drying. Through this research, the intention is to bridge the gap and, at the same time, provide factual information linking solar energy utilization and the need for improving the fuel quality of wood for its use in process industries. The intrinsic pathways and methodologies researchers worldwide adopted in solar drying of different wood forms are addressed and discussed in detail. In addition, the thesis also explores the solar potential of Hungary through a trendline data assessment of the last ten years. The prime objectives of the research work carried out in this dissertation are as follows:

- To explore and review the classification of solar wood dryers and the various modeling approaches prevalent in the optimization of the drying system performances. In addition, An intrinsic global mapping of wood as biofuel production and review work of the solar drying systems used in various parts of the world can provide insights into the type of wood being stored and dried with distinctive methods.
- To construct and understand the temperature profile for a box-type natural convection solar dryer for drying of wood-chips.
- To develop a forced convection cabinet-type solar dryer and investigate the energy efficiency of the dryer for the three most commonly used wood fuels, i.e., woodchips, sawdust, and pellets.
- To develop a validation model using an artificial neural network (ANN) on MATLAB for the prediction of moisture content during the solar drying process.
- To demarcate the optimization of the solar dryer with and without phase change material (coconut oil) in terms of exergetic and energetic thermal performance.

- To evaluate the economic and environmental impact of hybrid solar drying of wood fuels.
- To identify the solar potential of the Hungarian region and investigate the problems in the quality of wood fuels at the boiler plant operations in Miskolc, Hungary, through trendline analysis of data.
- To propose and suggest potential reforms for the long-term storage and maintenance of the quality of wood fuels in largescale utilities.

### 1.3. Thesis layout

In this thesis, **Section 2** discusses the technical contrivances in solar wood drying (i.e., in-use solar wood dryers, numerical and simulation modeling methodologies, and prevalent design concepts). The prevalent practices of process optimization from a global outlook are discussed and reviewed in this part.

**Section 3** outlines the design and development of the box-type natural convection solar dryer for wood chips. Experimental investigations were conducted to check the rise in temperature and drying rate for open sun v/s box type dryer.

**Section 4** presents the investigations on the newly developed cabinet-type solar dryer for wood fuels (woodchips, sawdust, and pellets). Here, the thermal efficiency of the system was evaluated through numerical calculations, and an Artificial neural network (ANN) model was developed on MATLAB to validate the results and predict the moisture content for the drying system. The experiments carried out for this section were done in the open sun with varying radiation of the sun.

**Section 5** details the 4E assessment, i.e., energy, exergy, environmental and economical for the hybrid dryer with phase change material (PCM). A comparative analysis was performed with and without PCM scenarios under constant radiation supply through the artificial solar source (Halogen Lamps). The efficacy of the coconut oil as PCM and the hybridization of the dryer were analyzed.

**Section 6** presents a case study of solar potential in Hungary. The regional assessment of the solar potential is performed along with the trendline assessment of wood fuels being used in boiler operations from a local company operating in Miskolc, Hungary. The impact of moisture content on the calorific value of the woodchips is presented along with the proposed

solutions/steps that could be taken by the industries using wood biomass for the long-term storage of wood chips using solar drying solutions.

**Section 7** concludes with the new scientific results obtained from the experimental and theoretical investigations of the research work carried out in the dissertation.

### 2. TECHNICAL CONTRIVANCES IN SOLAR DRYING OF WOOD

#### 2.1 Parameters affecting the performance of extant solar wood dryers and their classification

##### 2.1.1. Basic parameters affecting solar drying of wood

Wood, a non-hygroscopic material, cannot reach zero moisture content as it holds back residual moisture in its capillaries even after moisture removal. The moisture removal during solar drying fundamentally goes through two physical processes simultaneously.

Heat Transfer – The transfer of heat for the evaporation of water from the wood.

Mass Transfer – Air temperature, air velocity, humidity, pressure, etc., play a crucial role in the movement of the moisture internally, leading to the mass transfer phenomenon. To understand mass transfer, the mass balancing calculation can be performed using Equation (1) [2].

$$V_o W_o - V_i W_i = -V_s \frac{\partial MC}{\partial t} - V_a \frac{\partial W_o}{\partial t} \quad (1)$$

Any combination of vapor diffusion (in pits and lumens) and bound-water diffusion (in cell walls) operating in sequence or parallel can push water from areas with high to low moisture content, as depicted in Figure 2 (a). Understanding where and how moisture is trapped in wood is essential for a deeper understanding of the drying process. The cell walls and the internal structure of the wood's porous micro-voids contain moisture, as shown in Figure 2 (b).

## 2. TECHNICAL CONTRIVANCES IN SOLAR DRYING OF WOOD

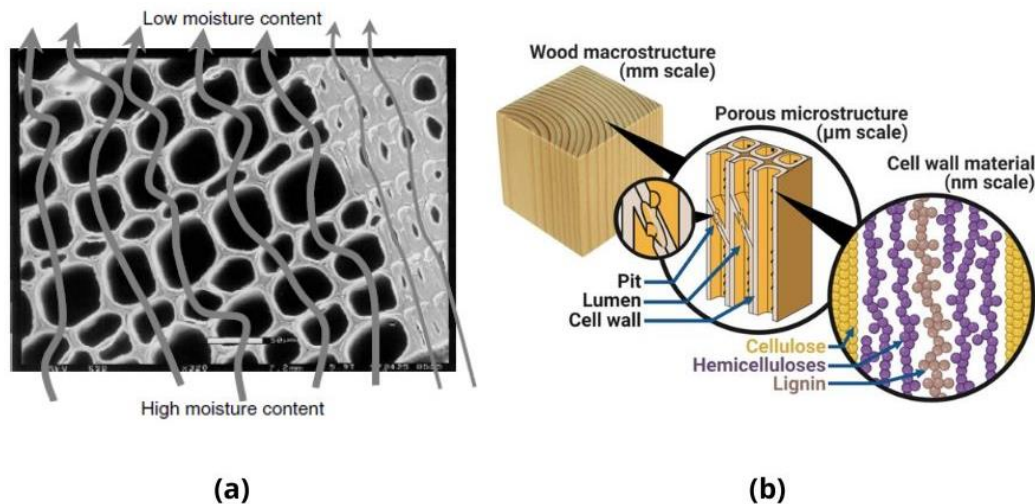


Figure. 2 (a) Moisture diffusion in the hygroscopic range [3], and (b) Moisture trapped at different locations inside the wood [4].

To further understand the solar dryer performance, the energy balancing of the system is inevitable. The input and output conditions of the dryer geometry and the placement of the wood must be investigated. Some of the commonly considered energy balancing involved with optimization analysis are listed below [5]:

- energy balance of the collector glass cover.
- energy balance of the air between the glass cover and absorber.
- energy balance of the absorber plate.
- energy balance of the timber/ wood stack load.
- energy balance of the flowing air inside the kiln.

Also, some geometrical parameters are crucial for the performance enhancement and design consideration of the kiln/dryer. These parameters are:

- conditions of opening vents (size, shape, and numbers ).
- Absorber glass and insulation material (absorptivity).
- Load volume capacity of the drying chamber.
- Timber/wood stack board thickness and placement.
- Season of drying with sky clarity index and solar irradiation.
- Drying air velocity and temperature.
- Accompanied drying defects such as stress/strain.

## 2. TECHNICAL CONTRIVANCES IN SOLAR DRYING OF WOOD

---

### 2.1.2. Classification of wood solar dryers

Different solar dryer models are available depending on the various heat transfer modes. The type of wood, volume of the chamber, and available solar irradiation dictate the design of the kiln/dryer. The method of airflow or the hybridization with thermal energy storage techniques differentiates the dryers. Some recent designs of different solar wood dryers can be found below.

- Natural convection direct type [6]
- Natural convection indirect type [7]
- Forced convection direct type [8]
- Forced convection indirect type [9]
- Hybrid type with PV/T (Photovoltaic/thermal) [10]
- Hybrid type with phase change material (PCM) [11]
- Hybrid type with packed bed thermal storage [12]
- Hybrid type with biomass storage support [13]
- Hybrid type with heat pump support [14]
- Greenhouse-type solar wood dryers [15]
- Semi-Greenhouse type solar wood dryers [2]

The different kinds of solar dryers used for wood-based drying must be classified to understand the solar drying phenomenon in detail. A range of several factors influences the design and construction of these dryers. The reported works show that airflow and energy transfer are the prime factors in classification, as shown in Figure 3. Among the three classifications, in the passive mode, airflow or convection is naturally assisted. In contrast, in the active mode, an external source aids convection. Over the years, due to continuous research, the choice of material, design, construction, and use have evolved.

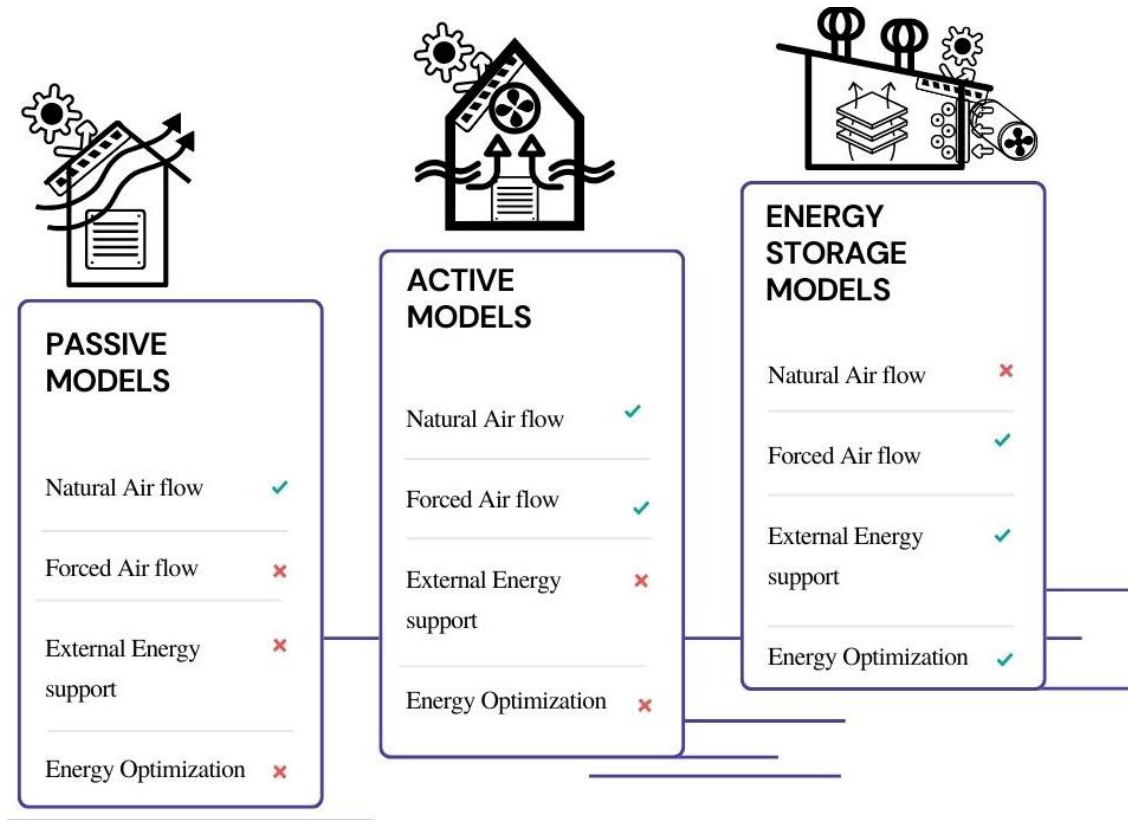


Figure. 3 Classification of solar drying kilns based on airflow and energy storage.

In recent years, much focus has been on developing the third classification type, i.e., the energy storage mode, to enhance the efficiency and provide continuous drying support minimizing the intermittency associated with solar energy. Nevertheless, the basic working principle of heat transfer still governs the dryer's performance. In the energy storage models, convective airflow aids a faster drying rate [16], while energy storage helps optimize energy flow usage [17]. A few reported works use mirror reflectors in cabinet solar dryers for better heat transfer rates [18]. To improve drying efficiency, the use of evacuated tubes has also been noted in drying agricultural products such as cloves to achieve a drying efficiency of 56% [19]. A study even combined the evacuated tubes with photovoltaic/thermal collectors [20]. In view of this classification, numerical and simulation approaches are decided and worked out to estimate the energy efficiency of these dryers.

### 2.2. Contrast in numerical modeling and simulation approaches

Solar dryer performance optimization for different applications/products has been a topic of research interest worldwide. Yet a commercial dryer system with the flexibility to dry (i.e., remove moisture) a range of products with different moisture content is not devised. This is mainly attributed to the different constraints, such as texture, thickness, a wide difference in initial moisture content, and geographical constraints (i.e., solar insolation, relative humidity,

## 2. TECHNICAL CONTRIVANCES IN SOLAR DRYING OF WOOD

---

etc.), etc. of each product. Similarly, as the wood form varies, the challenges associated with solar wood drying also vary. Hence, various methodologies are used to identify critical parameters that affect the drying quality in solar wood drying.

This section discusses and highlights the use of numerical modeling/computational simulations that aids in understanding and assessment of the drying phenomena. It is to be noted that solar drying kilns could be of various designs, sizes, and shapes and with varying modes of operation. Also, the modeling and simulation approaches differ depending on the type of dryer. Furthermore, environmental conditions, such as irradiation, moisture content, and airflow, control the whole process. Therefore, modeling and simulation are challenging yet necessary for optimizing the solar wood drying process. Table 1. discusses a few of the recently developed approaches for modeling and simulation of various forms of wood. It is essential to highlight that a software package is a grouping of related software applications that have been bundled together for distribution and installation. For instance, commercial software programs like ANSYS Fluent/CFX, TRNSYS, and COMSOL Multiphysics are frequently used to simulate drying parameters after experimental investigations for validation. On the other hand, a code is a set of written instructions in a programming language used to build software or a system to address various functional optimization of a drying system. In other words, code is the component needed to produce a software package, whereas a final result ready for use is a software package. In optimizing dryer performance, both are used based on the requirement of the analysis performed.

Conventional optimization tools such as neural networks can be adopted to study the time-dependent acceleration phase of wood drying. Evidence from the reported works suggests that the neural network approach has better control accuracy and helps solve nonlinear time-dependent drying problems [21]. Researchers have also performed experiments for sensitive analysis investigations of wood drying as low as particle level [22]. The influence of moisture content over time on a single wood particle was investigated using the Reaction Engineering Approach (REA) along with the continuum model of experiments. Apart from moisture content, the heat and mass transfer equations are critical in the calculation of the energy efficiency of the dryers. Over the years, FORTRAN software package has evolved into the most commonly used platform for solving nonlinear differential equations involved in energy calculations. Local models developed on FORTRAN can be converted to global models through Gauss iterative models using TRNSYS software [23]. Drying systems that utilize solar collectors as the energy source must have meteorological data analysis.

## 2. TECHNICAL CONTRIVANCES IN SOLAR DRYING OF WOOD

---

Meteonorm is one software that helps estimate environmental parameters such as irradiation of the region [24]. There are also works reported with dryers integrated with latent heat sources. In such systems, it is difficult to predict the actual size of the storage capacity. In this direction, Khouya and Draoui [11] provided an interesting flow chart to calculate the sizing of the alternate heat storage using C++ coding language. The finite element method can be used to study the steady and transient state of wood drying. TRNSYS software can help in simulating the experimental work [25]. In some cases, time-dependent simulations were carried out to study the operational energy (OE) and embodied energy (EE) over 20 years. For this, LNEA (life-cycle net energy analysis) was performed for solar drying of two different kiln designs. Hardwood species drying is energy-intensive, and this approach could be a benchmark in time-valued net energy analysis optimization [26].

During the solar drying of wood, the evolution of stress and strains within the board is a common phenomenon. It affects the quality of the board, and hence a 3-D formulation was prepared to understand the hydrous, thermal, mechano-sorptive, and elastic deformations. ANSYS-CFX10 and FESh++ codes were used to simulate hygro-thermal and mechanical behavioral problems [27]. This study shows that the simulation and modelling approaches are used not only for studying the heat and mass transfer but also for the mechanical properties of the wood. Also, Autengruber et al.[28] present a finite element-based moisture transport model for wood, including free water above the fiber saturation point. The FEM (finite element method) software ‘Abaqus’ performed the simulation for the model. This optimization tool is suitable for potentially observing the moisture behaviour during solar drying. Thermophysical parameters should be considered to develop numerical models for tropical wood drying. FORTRAN 77 language is suitable for obtaining numerical results, and literature suggests the addition of anatomical parameters could be explored in similar investigations of tropical wood drying [7]. Luna et al. [29] carried out modelling of the kiln with energy storage. In this study, several models were developed to simulate different boards. All these models were combined to generate a global model, producing good energy storage simulation results. These are some of the modelling and simulation approaches that could be useful in further developing new models. In addition, the simulation approaches also differed based on the type of wood, ambient conditions, and volume.

Table 1. Observations on few recently developed and validated modelling and simulation approaches in solar drying of wood products.

## 2. TECHNICAL CONTRIVANCES IN SOLAR DRYING OF WOOD

SI. No.	Dryer (Year)	Modelling approach	Software Package/Code	Observations	References
1	Ash wood dryer (2014)	Process neural network approach	Neural Networks based on time varying learning algorithms	Traditional neural network program was extended with process neurons in time domain. A comparison study performed between traditional and proposed mode, reveals that the process neural network has better control accuracy.	[21]
2	Single wood particle drying (2019)	Reaction Engineering Approach (REA) and Continuum Model (CM)	REA codes (based on ordinary differential equations) and CM codes (based on partial differential equations)	Experiments and simulations established that the REA model could be employed to describe heat and mass transfer between particles and the drying agent (where wood is the dried product).	[22]
3	Models divided into three categories: (a) models for drying a single board, (b) models for drying a kiln-wide stack, and (c) models for drying stress and deformation. (2007)	Mathematical model		(a) The single-board drying model employs comprehensive heat and moisture mass transfer equations and can be used to investigate the influence of wood variability. (b) The kiln-wide drying model, which is based on the transfer processes between wood and the drying medium, can examine the influence of drying schedules and wood properties. (c) The stress model can predict stress development in drying and stress relief in final steam	[30]

## 2. TECHNICAL CONTRIVANCES IN SOLAR DRYING OF WOOD

---

				conditioning and post-kiln treatment. An integrated model can optimize drying schedules and develop strategies for high-quality dried timber.	
4	Three direct solar dryer designs used to dry wood, including both greenhouse and semi-greenhouse-types (2021)	Numerical simulation	Fortran v. 95 (software package) with step time of 60s.	The six proposed heat and mass transfer differential equations were solved using computer simulations with a one-minute step count. However, the models verified best for direct dryers but can also be used for indirect dryers with modification in the governing equations.	[31]
5	Solar wood dryer with glazed walls- (2020)	Numerical simulation	Turbo Pascal v. 7 program and Fortran v. 90 (software package)	It is identified that although Turbo Pascal is a fast response program, it has some limitations. Therefore, modern FORTRAN v.90 is recommended in the selected operating conditions.	[32]
6	Dryer consists of a drying chamber, a solar air collector and a packed-bed energy storage (PBES) system (2020)	Numerical simulation	TRNSYS (software package)	The numerical model was prepared using the FORTRAN language, and then the global model was developed using meteorological data on the TRNSYS 18 software. The finite difference methods and Gauss iterative methods were helpful in designing energy transfer equations for the study.	[33]

## 2. TECHNICAL CONTRIVANCES IN SOLAR DRYING OF WOOD

---

7	Simple solar dryer for tropical wood using a collector (2017)	Mathematical model and numerical simulation	FORTRAN and Meteonorm (software package)	The energy and mass balance equations are solved simultaneously using the fourth order Runge-Kutta method in FORTRAN, and the meteonorm software was used for meteorological data collection. Such approaches with a combination of software are more fruitful than experimental investigations, which take longer durations, for example, months.	[8]
8	Timber-drying solar kiln designs (Oxford and Boral kilns) (2015)	Numerical simulation		Fick's law of diffusion for mass transfer and Fourier's law for heat transfer was considered for modeling. Seasonal varying boundary conditions were also accommodated in this model. This approach suits stacked Oxford, and Boral kilns type solar dryers.	[34]
9	Hybrid solar dryer for woody biomass (2020)	Mathematical model		The heat and mass transfer in the porous medium is solved using the implicit finite difference method, which is commonly used. This model can be helpful in combined energy sources such as solar and heat pumps, where energy transfer rate is critical.	[13]

## 2. TECHNICAL CONTRIVANCES IN SOLAR DRYING OF WOOD

---

10	Solar kiln with latent heat energy storage (2018)	Computational drying model	C ++ program (Code enable to simulate the thermal performance of the solar kiln for different weather condition with a time step of 100s)	An interesting flowchart and mathematical model framed to calculate the sizing of the thermal energy storage depending on various parameters of the phase change material. Integration of PCM reduced drying time by 26.5% and process of heat recovery by 47%. Also, the maximum drying efficiency reached 85% which is significant inspiration for future research with this approach.	[11]
----	---	----------------------------	---	--	------

---

### 2.3. Prevalent design concepts

Drying wood or wood-based product is different from drying other agro-products. Though the fundamentals remain the same, the design of solar kilns is drastically different from the standard solar dryers. The wood sizes and volumes are much larger than the other products, such as crops, herbs, spices, fish, dry fruits, etc., typically used in conventional solar dryers. The traditional drying process is not sustainable as it emits carbon dioxide [35]. The wood logs/stacks can take between one to four months, depending on the quality and thickness of the wood being dried. Simo-Tagne and Bennamou [36] studied per cubic meter drying for sawn timber in African cities. The results pointed out that the energy requirement for drying is more for the dense type of wood. Recently, Khouya [10] developed a combined solar drying system using photovoltaics and a heat pump arrangement. The findings revealed that the system reduced the drying time by 18%, with the photovoltaic thermal efficiency ranging between 37-52%. Also, the electricity savings and moisture extraction rates improved by 57% and 39%, respectively. The arrangement of the system, as shown in Figure 4 (a), is a new step in further exploring the idea of hybridization. Ugwu *et al.* [12] demonstrated pebble beds as an energy storage medium for continuous drying in tropical regions, as shown in Figure 4 (b). Interestingly during the off-peak hours, the pebble bed helped in averting the reverse flow of most air, thus maintaining a higher temperature than the ambient inside the

## 2. TECHNICAL CONTRIVANCES IN SOLAR DRYING OF WOOD

---

kiln during the whole day. However, this model is suitable for seasoning timber drying in tropical areas but cannot be replicated everywhere.

Figure 4 (c) depicts the Tagne et al. [37] model of a forced convection wood dryer with in-built fans for drying wood fuel. In this work, the overall efficiency of the dryer was reported as 39%, with a raised temperature of 38°C. The study pointed out that this system could not provide better drying results during the winter season, reflecting the need for the dryers' hybridization. Lamrani and Draoui [38] designed a novel hybrid solar-electrical dryer with a latent heat storage system, as shown in Figure 4 (d). It achieved a notable temperature rise of 4-20 °C overnight. Considering a temperature difference of 5°C, the commercial PCM, RT55, with an average melting temperature of 55°C and heat storage of capacity of 170 kJ/kg, was used. The phase change material (PCM) also helped reduce the drying time to 5 days. Similarly, Khouya [13] designed a hybrid dryer with a heat pump and condensing boiler for drying wood chips, improving the drying efficiency by 92%. Such examples provide wisdom for more research on hybridizing solar dryers for wood drying. Depending on the availability, sodium sulfate decahydrate ( $\text{Na}_2\text{SO}_4 \cdot 10\text{H}_2\text{O}$ ) and sodium chloride (NaCl) can also be used as the thermal storage medium for integrated solar drying. The study [39] suggests sodium chloride (NaCl) as a more effective medium, but for wood drying, it holds potential for investigation. Another possible medium for thermal storage could be glycerol. Ndukwu et al. [40] integrated glycerol as a thermal storage medium with a low-cost active wind-powered active solar dryer. Glycerin ( $\text{C}_3\text{H}_8\text{O}_3$ ) was used as thermal storage material with a transition temperature of 17.8°C. Similarly, commercial PCM were investigated for solar kiln drying [11]. Comparison of the different PCMs used by various researchers is presented in Table 2.

Table 2. Various forms of PCM used in solar drying of wood with their properties.

PCM	Scientific name	Melting temperature	Latent Heat of fusion
Commercial PCM	RT55	55°C	170 kJ/kg
Salt based	sodium sulfate decahydrate ( $\text{Na}_2\text{SO}_4 \cdot 10\text{H}_2\text{O}$ )	32 °C	522 kJ/mol
Glycerin	$\text{C}_3\text{H}_8\text{O}_3$	17.8 °C	-
Commercial PCM	RT64	64 °C	240 kJ/kg
Commercial PCM	RT 82	78-82 °C	170 kJ/kg

## 2. TECHNICAL CONTRIVANCES IN SOLAR DRYING OF WOOD

Commercial  
PCM

Erythritol

118 °C

339 kJ/kg

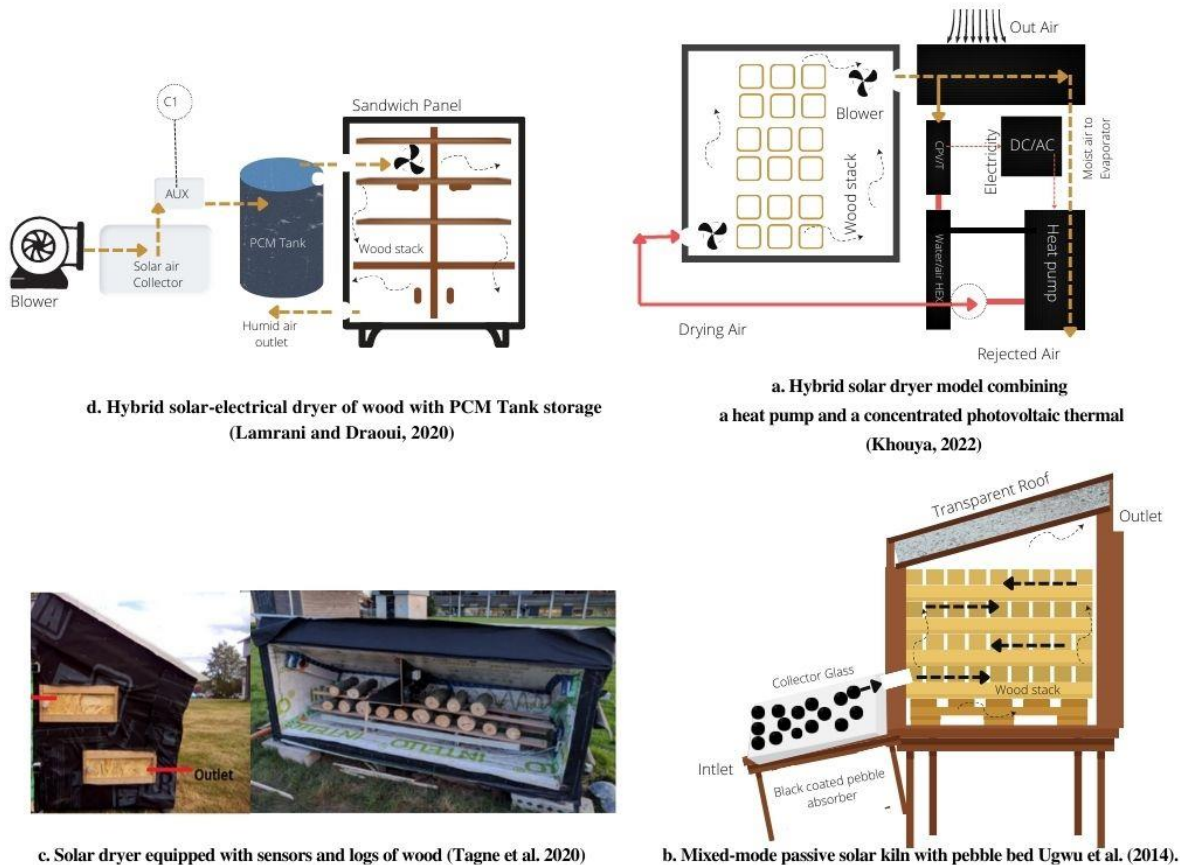


Figure. 4 Distinct solar dryers developed recently for drying various forms of wood. Image adaptation (a) [10] (b) [12] (c) [37] (d) [38].

The energy and exergy efficiency obtained for potato drying were 31.5% and 80.9%, respectively. In African regions with low electrical support, such models can aid the timber drying of tropical woods. Future designs can also consider desert sand as a high-temperature integrated storage medium considering the regional environment [41]. In particular cases, drying wood in sawmills is also of significant concern for process optimization. The profitability of sawmills depends on the quality of the logs produced. The drying stage or scheduling is critical and energy intensive [42]. Vanzetti *et al.*[43] proposed MILP (mixed integer linear programming) models to minimize product delivery delays. The drying process was combined with the by-product production of wood chips as a feedstock for the boiler. This model can further be investigated with solar or integrated thermal storage energy support. The volume of wood, its type, and volume is higher than any other agricultural product. Thermal storage integrated designs are the way forward for efficient drying and judicious energy utilization in future solar dryers.

## 3. EXPERIMENTS WITH NATURAL CONVECTION SOLAR DRYER

### 3.1. Background Study

Open-air solar drying is frequently regarded as the simplest and least expensive drying method. This technique has been around for a while in the area of agriculture and crop production. The main problem with open sun drying is the unpredictable drying rates, and dehydrating takes the most extended amount of time. The final quality is also impacted by uneven heating and varying drying rates. Depending on the customer's precise needs, solar dryers of various designs can manage these unfavorable aspects of open drying. The primary construction factors for a solar drier are the physical parameters, such as drying rate, temperature control, heat ventilation, etc. In this study, a direct-type natural convective lab-scale dryer was designed and developed to understand temperature profiling during different winter seasons. The dryer's air flow is passive in nature and does not require any external fan or blower. The temperature inside the dryer rises during the afternoon and slowly declines with the sunset. This temperature rise gradually increases the dehydration of the product inside the cabinet. The drying efficiency differs for various products and needs different optimal moisture content. Dryers could also be designed based on the size of the agricultural product that needs to be dried. Forced dryers are commonly used in cases where a high heat requirement is required for the faster drying process. The airflow increases the heat transfer inside the chamber, directly affecting the drying rate. The cabinet dryer is mainly used to dry small items such as spices, grapes, banana chips, potatoes, chilly flakes, wood chips, etc. In most cases, it was observed that the drying rate was mainly 2 to 5 times faster than in open sun during models in agricultural products.

### 3.2. Design and construction

The lab-scale cabinet dryer was developed at the institute laboratory of the University of Miskolc. Figure. 5(a) below depicts the 3D view of the dryer (all mentioned dimensions are in millimeters) and Figure. 5(b) shows the realtime arrangement of the experiment with the dryer having the woodchips inside. The dryer's upper part is a transparent glass cover to maximize the heat trap inside the dryer. The inlet and outlet ventilation was provided on the two sides. These ventilation outlets were used to measure the temperature variation inside the

### 3. EXPERIMENTS WITH NATURAL CONVECTION SOLAR DRYER

dryer. The experiment intended to trap the sensible heat inside and its behavior during the experimental hours of the respective days.

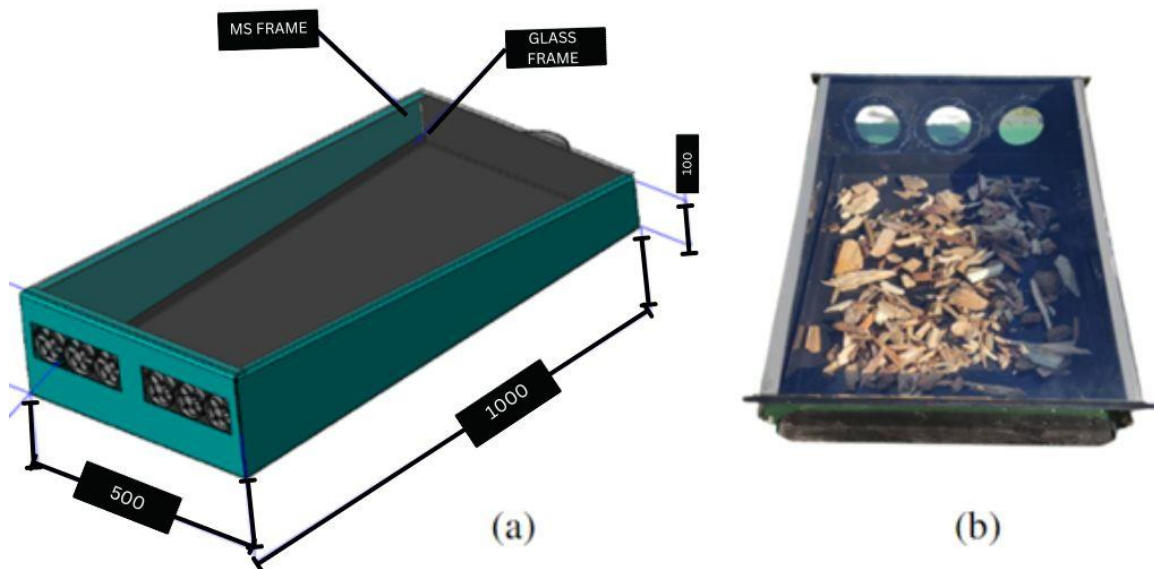


Figure 5 (a) 3D view of the dryer (all mentioned dimensions are in millimeters) (b) realtime arrangement of the experiment with the dryer having the woodchips inside.

#### 3.3. Temperature profiling results

During experiments, various shapes and sizes of the wood chips of grade EN14961 were used in the laboratory. EN14961 is the European grade of solid biomass fuel utilized for various industrial as well as Non-industrial applications. The moisture content measurement was done using a lab-scale moisture measuring instrument. These woodchips are readily available around the forest regions of Miskolc city. The woodchips were pre-soaked for 24 Hrs before sun-drying the chips in a box-type dryer developed at the laboratory.

To understand the wood chips' drying nature, different sizes of the wood chips were kept under observation. The experiments were conducted in November, 2021, when the ambient temperature at the city of Miskolc fluctuated between 10 °C to 25 °C. The observations were made only for 20 days when the sunshine was good with a clear sky and the 4 best days with high irradiation were considered. It was recorded that the maximum temperature reached

### 3. EXPERIMENTS WITH NATURAL CONVECTION SOLAR DRYER

during the tests was 35 °C at the outlet on Day 1. The temperature profiles reveal that the maximum temperature attained inside the dryer was in the afternoon from 12 PM to 2 PM. The temperature drops fast as the sun gets down in the evening. Hourly change of solar radiation also affects the drying phenomenon.

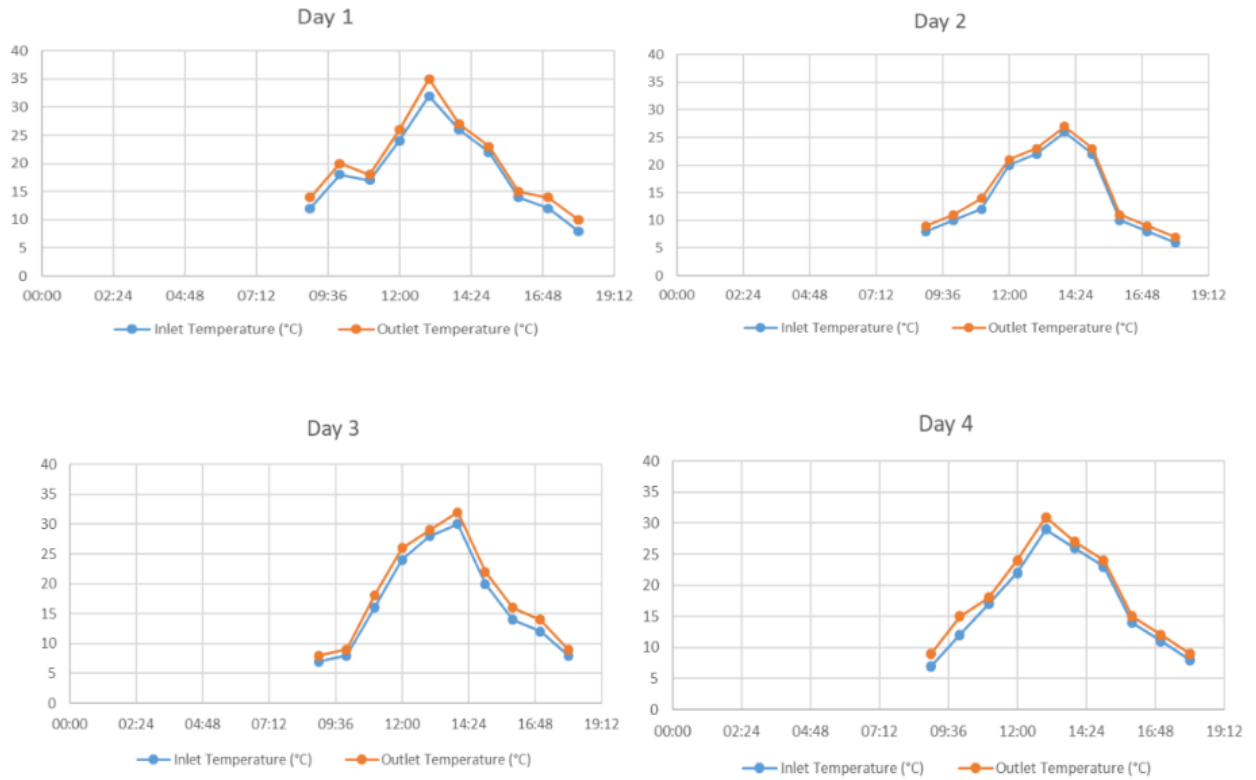


Figure 6. Temperature profiles of the inlet and outlet temperatures at the different days of the experiments.

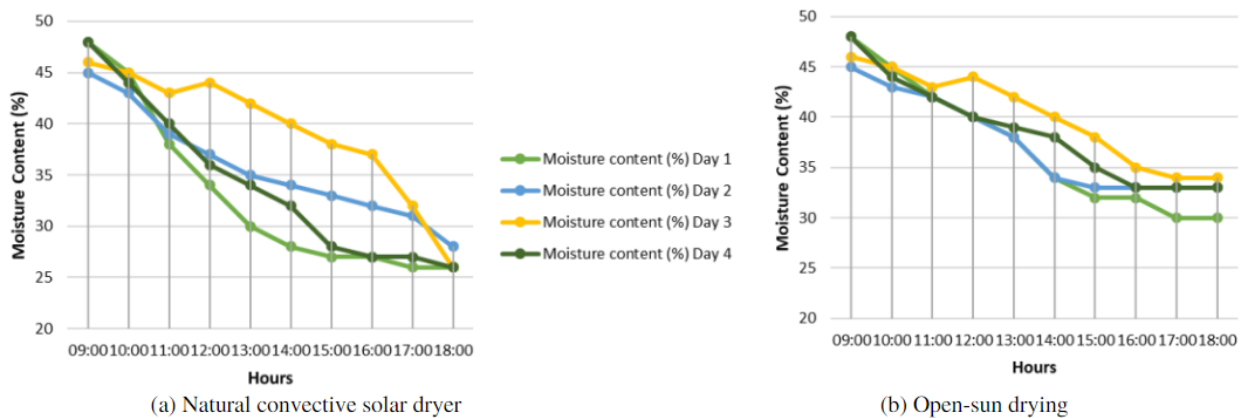


Figure 7. Moisture content decline graph of wood chips for (a) Natural convective solar dryer (b) Open sun drying.

### 4. EXPERIMENTS WITH FORCED CONVECTION CABINET TYPE SOLAR DRYER

Due to their non-hygroscopic nature, wood biofuels cannot be 100% moisture free. However, solar drying can considerably reduce moisture, improving the properties of wood biofuels. Limited studies are available on the solar drying of wood-based biofuels (pellets, sawdust, and woodchips). In our present study, we investigate the drying behavior of biofuels in a combined solar dryer.

The methodology employed in this part of the study included conceptualizing the structure of the forced convection solar dryer, designing the conceived dryer, building the designed dryer, and validating the experimental results with an artificial neural network tool. Energy and exergy analysis was performed for the drying system to evaluate its efficiency. Wood chips, pellets, and sawdust were utilized as the drying product under observation in the drying chamber with three different layers of the tray.

#### 4.1. Empirical study on the Forced convection cabinet solar Dryer

A forced convective cabinet solar dryer was prepared for this study at the University of Miskolc, Hungary. This dryer works on the indirect air circulation model, in which the hot air is collected in the air collector, as shown in the isometric view of the dryer in Figure 8. The dryer's body is made of wooden blocks, which are 2.5 cm thick and well-insulated on all sides. The size of the drying chamber (Length x Breadth x Height) is (80x50x45) cm. Thus, the total capacity of the dryer is 180,000 cm<sup>3</sup>, i.e. 180 litres by volume. The drying cabinet consists of three trays separated by a distance of 7.5 cm. However, the pressure drop across the height was not considered while designing the drying system. On the top of the cabinet, a 50 cm long chimney is placed for the throughput of outlet air. The hot air solar collector attached to the dryer has an inclination of 40°. Transparent glass material is used for the air collector. For the air collector to provide ample air circulation and heat transfer, the length of the collector should be higher than its width [44]. Literature suggests the aspect ratio (Length: Width) be around 2 [45]. Based on (Length x Width), i.e. (40 x 60) cms, the aspect ratio of the proposed collector is 1.5. However, it can be improved further with size

#### 4. EXPERIMENTS WITH FORCED CONVECTION SOLAR DRYER

modification. The latitude angle ( $\phi$ ) of the location where drying is to be done is generally very closely related to the angle of inclination of the collector ( $\beta$ ) or the tilt angle, given that the collector's face must be facing south-north [45]. In general, the inclination angle is given as [46]

$$\beta = \phi + 10^\circ \quad (2)$$

Based on the coordinates of the city of Miskolc, i.e., 48°06'15"N 20°47'30", the inclination angle was kept at 40° due to glass material size constraint. However, it can be improved further to around 60°.

Six inlet holes are provided for the air inlet with a diameter of 2 cm and three outlet holes with a diameter of 6 cm, which are joined to the drying cabinet. All sides of the dryer are painted black for the maximum heat trap inside the cabinet. The dryer's back view shows that the three trays consist of three different drying products. The bottom trays consist of woodchips, the middle one sawdust, and the top tray consists the pellets. Table 3. depicts the design considerations considered in the experimental setup. These parameters are crucial for getting clear insights into the experiments and the various materials involved in the study.

Table 3. Design items and descriptions considered during the experiments.

<b>Item</b>	<b>Details</b>	<b>Units</b>
Drying Products	Woodchips, Sawdust, Pellets	-
Weight of Product	1	Kilograms for each
Duration of Experiment/day	10 A.M. – 3 P.M.	Hours
Thickness of walls	2.5	cm
Thickness of collector glass	0.5	cm
Transmissivity of glass	0.89	Approx value
Number of trays	3	-
Capacity of Dryer	180	Liters
Type of air flow	Forced Convection	AC power supply
Load capacity	6	kg
Drying time	5	Hrs

#### 4. EXPERIMENTS WITH FORCED CONVECTION SOLAR DRYER



Figure 8. Experimental setup of the solar dryer for the investigations.

The experiments were carried out in the first and second week of October 2022 and best irradiation results were considered for calculations. The whole body of the dryer and the collector is made of wooden blocks, and sealant was used to fill the gaps to avoid heat loss from the system. The body was coated with black paint to enhance heat absorptivity. Experiments were conducted during the prime sunshine hours of the day, i.e., 10 A.M. to 3 P.M. The highest Radiation mainly was recorded between 12-1 P.M. Henceforth; the temperature rise inside the collector and dryer was also maximum during these hours. The anemometer measured the air inlet speed, which was controlled by the fan's speed at the top of the chimney. For all experiments, the air inlet speed was maintained at 2 m/s. An AC-powered fan was used at the top chimney to maintain this air flow rate. A multichannel data logger measured the temperature at six different locations of the inlet and outlets of the system. The relative humidity was measured using an (RH) meter valid in the range of 10-90 %. The sample's initial and end weights and moisture content were measured on the weight and moisture balances. All these apparatuses were utilized to take measurements as per the required parameters described in the methodology section.

#### 4.2. Energy Analysis

The performance of the solar dryer is determined by the energy and exergy efficiency of the system. The efficiency of the dryer is coherent with the thermal efficiency of the solar air collector attached to the dryer. The temperature difference at the inlet  $T_i$  ( $^{\circ}\text{C}$ ) and outlet  $T_o$  ( $^{\circ}\text{C}$ ) of the collectors is used to calculate the useful heat energy  $Q_u$  of the collector, which is represented in Equation 1.  $C_p$  is the specific heat capacity of air at known temperature ( $\text{kJ/kg}\cdot\text{K}$ ) and ( $\dot{m}$ ) be the mass flow rate of air at a given temperature ( $\text{kg/s}$ ) [47].

$$Q_u = \dot{m}C_p(T_o - T_i) \quad (3)$$

The mass flow rate can be calculated as the product of the air density  $\rho$  ( $\text{kg/m}^3$ ), average air velocity  $V$  ( $\text{m/s}$ ) at the inlet of the collector, and the cross-section area  $A_{\text{collector}}$  ( $\text{m}^2$ ) of the duct [47] [48].

$$\dot{m} = \rho VA_{\text{collector}} \quad (4)$$

The amount of solar radiation absorbed by the collector is the amount of heat input to the system. The heat input  $Q_i$  is the product of solar Radiation  $I_T$  ( $\text{W/m}^2$ ) falling on the collector and the surface area  $A_c$  ( $\text{m}^2$ ) on which the radiation is falling [49]. Considering the transmissivity ( $\tau$ ) of the glass cover as 0.89 and assumed efficiency ( $\eta$ ) of 0.9.  $Q_i$  is the proportion of total incident radiation received ( $I_T$ ) on the air collector [45].

$$Q_i = I_T A_c \quad (5)$$

The ratio of useful heat in the system to the input heat energy falling on the collector gives the thermal efficiency for the solar air collector. The thermal efficiency of the collector influences the temperature inside the drying chamber directly. The drying rate of the wood fuel enhances with better efficiency [49].

$$\eta_{\text{th,c}} = \frac{\dot{m}C_p(T_o - T_i)}{I_T A_c} \quad (6)$$

#### 4.3. Exergy Analysis

The concept of exergy gain is based on the second law of thermodynamics. Thermal systems constitute available and unavailable energy parts known as "exergy" and "anergy"

respectively. Exergy efficiency is defined as the proportion of energy or exergy in the fuel utilized to make the product. Exergy analysis's primary goal is to calculate the exergy destruction in various thermal system components [50]. The exergy gain can be defined as the rise in exergy during the airflows inside the collector. Equation (5) gives the exergy increase where,  $\frac{\rho_o}{\rho_i}$  is the ratio of air density at outlet and inlet, and  $R$  is the air gap Rayleigh number [51]. The inlet exergy depends on solar radiation and the absorbing surfaces [49]. The  $T_s$  temperature of solar intensity was considered as 5600 K, whereas  $T_a$  is the ambient temperature in Kelvin as the  $C_v$  is in (J/kg·K). The ratio of the increase in exergy outlet and the inlet gives the exergy efficiency. The dryer performs better with better exergy efficiency [49] [52].

$$Ex_u = \dot{m} \left[ C_p (T_o - T_i) - T_a \left( C_v \ln \left( \frac{T_o}{T_i} \right) - R \ln \left( \frac{\rho_o}{\rho_i} \right) \right) \right] \quad (7)$$

$$Ex_{in} = \left[ 1 + \frac{1}{3} \left( \frac{T_a}{T_s} \right)^4 - \frac{4}{3} \frac{T_a}{T_s} \right] I_T A_c \quad (8)$$

$$\eta_{th} = \frac{Ex_u}{Ex_{in}} \quad (9)$$

The type of material, the level of bound and unbound moisture, whether they are hygroscopic or non-hygroscopic, and the physical characteristics of the air utilized all impact how much moisture can be removed and then how efficiently. Non-hygroscopic materials can be dried to a moisture level of zero whereas hygroscopic materials will always have some residual moisture. The Moisture content ( $MC$ ) helps plot the process's drying curve. The drying curve could be plotted  $MC$  (Wet/Dry) v/s Time, drying rate v/s  $MC$  or drying rate v/s time. In the experiments,  $MC$  was calculated on moisture (wet basis) using the moisture balance as the initial  $M_i$  and final  $M_f$  values pre and post-experiment [53]. Also, the moisture ratio  $MR$  is calculated as the ratio of  $M_t$  (moisture content at any time) v/s  $M_o$  (moisture content initial) [54].

$$MC = \frac{(M_i - M_f)}{M_i} \cdot 100 \quad (10)$$

$$MR = \frac{M_i}{M_o} \quad (11)$$

The amount of moisture removed  $m_{water}$  (Kg) can be calculated considering the mass of the product to be dried ( $m_i$ ) (Kg) and the Heat required to evaporate the water is given as  $Q$  (KJ).  $m_{water} h_{fg}$  represents consumed energy to evaporate water from the drying product [49]. The overall drying efficiency of the system is a ratio of v/s as shown in equation (12) where there are additional ways of heat source other than solar, which is not applicable in the present study.

$$m_{water} = \frac{m_i(M_i - M_f)}{(100 - M_f)} \quad (12)$$

$$Q = m_{water} h_{fg} \quad (13)$$

$$\eta_{system} = \frac{m_{water} h_{fg}}{I_T A_c + E} \quad (14)$$

#### 4.4. Uncertainty Analysis

Analysis of uncertainty is used to identify the errors committed during the investigation. It is crucial to measure observed variances between measured values of an important parameter and its real value. The measurement uncertainties of all the linked independent variables are used to compute the uncertainty in a result [55]. In present experimental setup, the weighing balance machine had accuracy of  $\pm 0.1$  g. The humidity meter had  $\pm 2.5\%$  of RH (Relative Humidity). The pyranometer had sensitivity of  $\pm 0.1$  mV/Wm<sup>2</sup>. The moisture balance had readability of 0.001 grams. The anemometer gives accuracy of 0.1 m/s in the working range of (0.3 to 20 m/s). All the measuring instruments were adequately calibrated before the experimental trials. The readings collected during measurements for this investigation were within an acceptable limit because the uncertainty values found during experimentation in the case of instrument performance were relatively minimal.

### 4.5. ANN modelling

In recent times, artificial neural network (ANN) has evolved as useful computational software for modeling drying processes. Solar drying of various products involves various dependent variables such as radiation, temperature, humidity, etc. Researchers worldwide use the ANN tool for testing and validation of the drying performance of solar dryers. The ANN-based models can predict the heat transfer coefficient [56], moisture ratio, moisture content, or drying rate depending on the requirements and available parameters [57]. Compared to other theoretical and practical modeling methodologies, ANNs may have advantages in simulating these devices, including high accuracy, generalization ability, and quick data insights [1]. Despite the basic assumptions in ANN-based modeling, using ANNs reduces solving complex mathematical models. In addition, fewer experiments are necessary to determine the input/output linkages compared to experimental investigations. Consequently, time and money could be saved by system modeling using ANN. ANN processes the dataset fed into the system mathematically in the form of nodes/neurons. The model consists of input layers as the variables affecting the model, and the output layer is based on the output desired for the prediction. The researcher decides on the hidden layer of the model per the problem's intricacies. Training, validation, and testing are three stages of using ANN models. Training and validation stages involve both the input as well as target data. However, the testing is performed only with input data to see the model's suitability.

### 4.6. Development of the ANN model

The dryer's performance largely depends on the final moisture content of the dried product. It is helpful for researchers to develop a model to predict final moisture through neural network simulation. Bala *et al.* predicted the performance of the solar tunnel dryer using a multilayered neural network technique [58]. The model was trained using a backpropagation algorithm utilizing data on the solar drying of jackfruit bulbs and leather. Similarly, the present study is designed for the wood biofuels. One hidden layer was selected in the model under Levenberg-Marquardt for training the mean square error regression in MATLAB2017b software. The Levenberg-Marquardt algorithm, which is created especially to minimize the sum of square error, is useful in similar predictions. As a first-choice supervised learning approach, the `trainlm` is frequently the quickest propagation algorithm in the toolbox, albeit it does use more memory than other algorithms [59]. It is applied in the current analysis. The model was trained with random data set from the experiments with 10,000 iterations with tan-sigmoid activation function for hidden neurons and `purelin` for linear output neurons. The

test, train, and validation curves are presented in the results section. After several hits and trial runs the best performance curve was plotted.

#### 4.7. Parameters of the ANN model

The dryer's performance largely depends on the final moisture content of the dried product. It is helpful for researchers to develop a model to predict final moisture through neural network simulation. Bala et al. predicted the performance of the solar tunnel dryer using a multilayered neural network technique [58]. The model was trained using a backpropagation algorithm utilizing data on the solar drying of jackfruit bulbs and leather. Similarly, the present study is designed for the wood biofuels. Figure 9. depicting the ANN model developed for prediction of the final moisture content based on the experimental data collected during the experiments mentioned in Table 4. The five input variables affecting the process were selected as solar radiation, inlet and outlet temperature, and relative humidity. One hidden layer was selected in the model under Levenberg-Marquardt for training the mean square error regression in MATLAB2017b software. The Levenberg-Marquardt algorithm, which is created especially to minimize the sum of square error, is useful in similar predictions. As a first-choice supervised learning approach, the trainlm is frequently the quickest propagation algorithm in the toolbox, albeit it does use more memory than other algorithms [59]. It is applied in the current analysis. The model was trained with random data set from the experiments with 10,000 iterations with tan-sigmoid activation function for hidden neurons and purelin for linear output neurons. The test, train, and validation curves are presented in the results section. After several hits and trial runs the best performance curve was plotted.

Table 4. Experimental parameter and their range considered for designing the ANN model.

<b>Parameters</b>	<b>Range</b>	<b>Units</b>
Solar Radiation	100-1100	W/m <sup>2</sup>
Inlet Temperature	18-32	°C
Outlet Temperature	20-60	°C
Initial Moisture content (wet basis)	32-36	%
Final moisture content (wet basis)	16-28	%
Relative Humidity	25-75	%

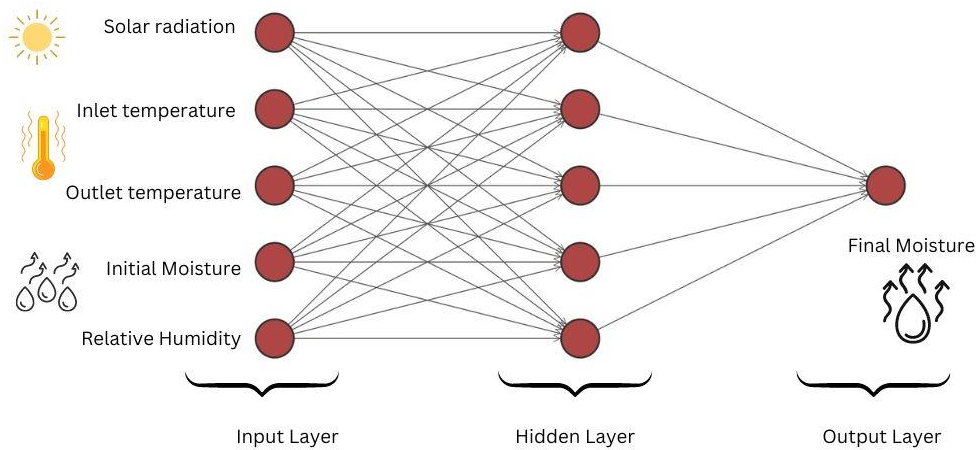


Figure 9. Pictorial depiction of the ANN model developed.

#### 4.8. Results of experimental investigations

The experiments were performed at the University of Miskolc, Hungary, on twenty sunny days in October 2022 and the best irradiation days were considered as three days. The solar radiation measurements reflect the consistency of average radiation above  $600 \text{ W/m}^2$ . However, sudden drops can be seen in the graph of Figure 10. The radiation values dropped suddenly because of the cloudiness or low sky-clarity index. Among the three-day experiments, the third day recorded the highest radiation value of  $1100 \text{ W/m}^2$ . The consistency in good solar radiation helps in the rapid rise of temperature inside the collector and drying chamber, leading to better drying rates for the solar dryer.

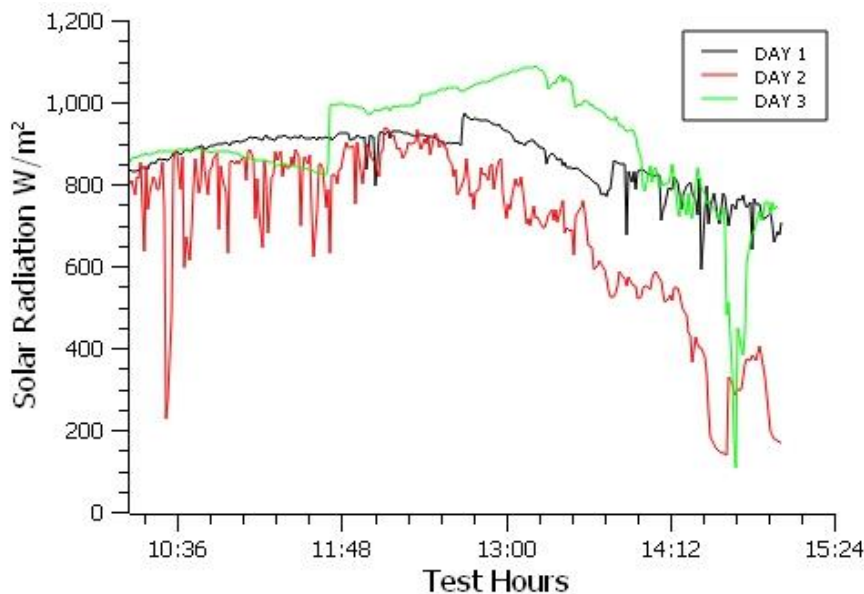


Figure 10. Solar radiation data collected for the three-day experimental setup.

#### 4. EXPERIMENTS WITH FORCED CONVECTION SOLAR DRYER

Temperature rise is critical in the drying of agricultural products. The data logger and K-type thermocouple sensors were installed in the system at different locations. The collector's inlet and outlet temperature determine the air collector's efficiency. Considering no losses due to good insulation, the outlet temperature of the collector is the inlet of the drying chamber. In the three-day experiments, the maximum temperature achieved was 60°C at around 1100 W/m<sup>2</sup>. The complete temperature rise was observed between 12-2 P.M. During total experimental hours, the temperature gradient between the ambient and inside the chamber was around 10°C, which aided in the continuous drying of the wood products. There was little temperature difference between the top layer and bottom layer of the drying chamber. However, the RH value differed by 4-5 % occasionally. Figures 11,12 and 13 represent the temperature profile of the system for the testing hours during Days 1,2 and 3, respectively.

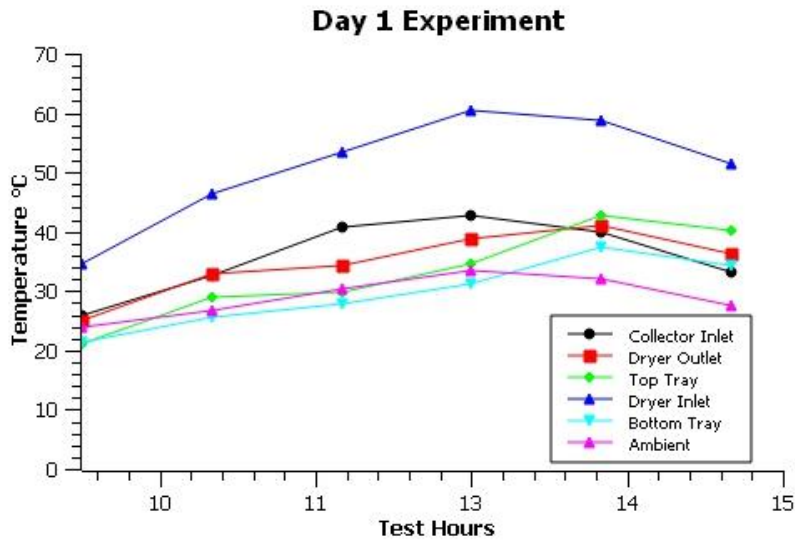


Figure 11. Temperature profiles for the first-day experimental setup of the dryer.

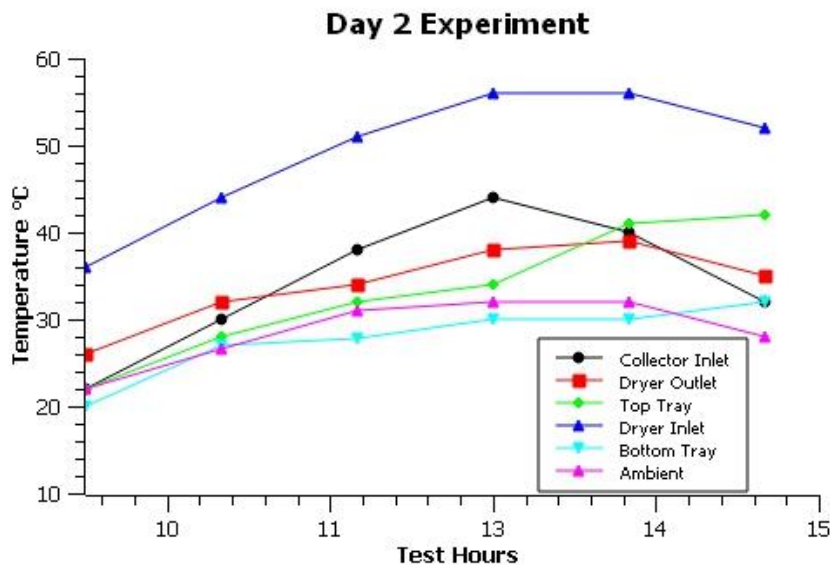


Figure 12. Temperature profiles for the second-day experimental setup of the dryer.

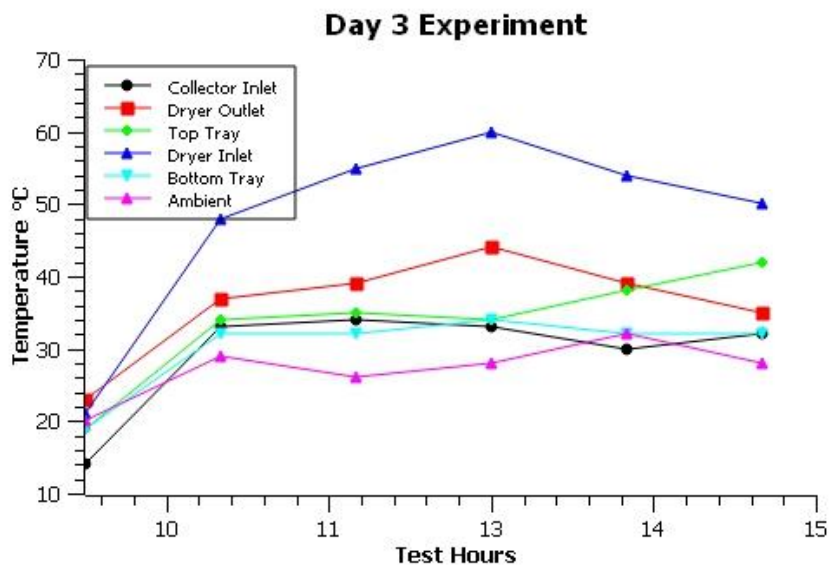


Figure 13. Temperature profiles for the third-day experimental setup of the dryer.

The instantaneous thermal efficiency of the air collector ranged 14.77% to 55%, as shown in Figure 14. The ambient temperature fluctuated between 18-32°C. The thermal efficiency dropped between 11 A.M. and 1 P.M. However, the efficiency constantly rose after that period. The possible reason could be temperature stability was achieved during this period. Figure 15. Depicts the variation of useful heat gains  $Q_u$  of the solar collectors and the ratio of the change in temperature ( $\Delta T$ ) to solar radiation ( $^{\circ}\text{C m}^2/\text{W}$ ) with the drying time of the experiment. The ratio of ( $\Delta T$ ) to solar radiation ( $^{\circ}\text{C m}^2/\text{W}$ ) was used as a basis to compare the trend shown in Figure 15. The hourly heat gain  $Q_u$  range was recorded as (201.65 -

420.55) Watts. The total heat gain sum for Day1, 2 and 3 is 1495.57, 1663.62 and 2050.13 Watts, respectively.

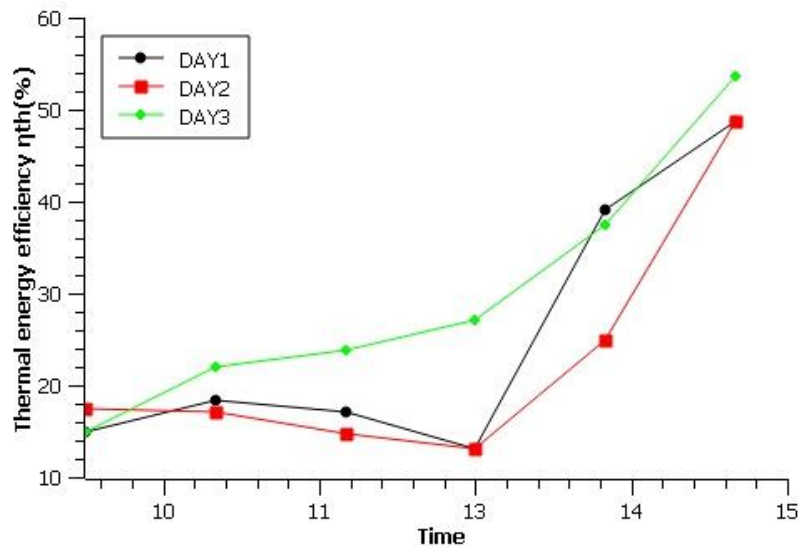


Figure 14. Thermal energy efficiency calculated on an hourly basis for the three-days.

The exergy gain and the exergy efficiency calculations are critical in understanding the thermal performance of the air collector. The performance of the drying chamber is directly proportional to the collector's performance. The energy utilized or the gain improved from morning to afternoon hours is indicated in Figure 16. The value of exergy gains enhanced from 76.26 Watts to 408.57 Watts during the experiments. The calculations were carried out as per the description of the study mentioned in section 4.2. The exergy efficiency improved significantly from 4.8 % to 51.1 % from the first to the last hour, respectively. In addition, the Moisture ratio trends for the three wood fuels are plotted in Figure 17. The rapid loss of moisture content is evident in the wood pellets and sawdust samples. The high porosity level in these two fuel forms aids the fast internal migration of the surface water from the wood fuel. At the same time, the woodchip's surface water evaporation takes place slowly. Also, better exergy and long hours of continuous during can provide better results and insights on the drying behavior. The relative humidity (RH) measured for the samples during early hours was as high as 75%. However, the RH values kept fluctuating at the three levels of the tray primarily because of the different nature and drying rates of the three wood fuel samples.

#### 4. EXPERIMENTS WITH FORCED CONVECTION SOLAR DRYER

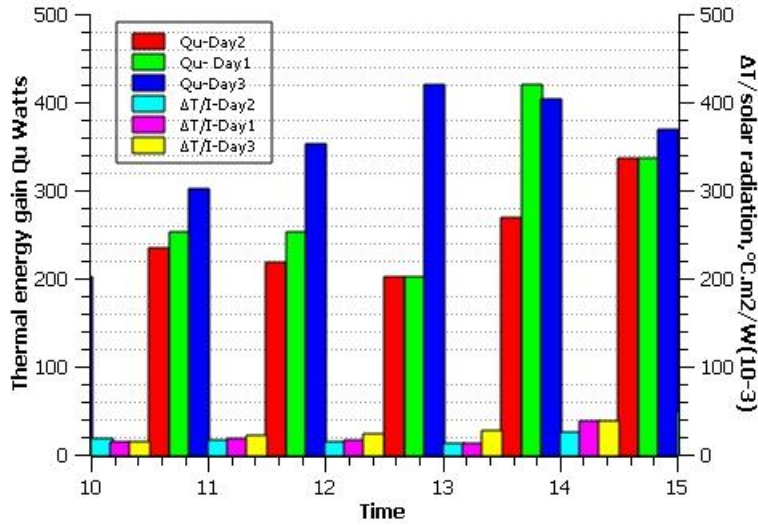


Figure 15. Thermal energy gain and the  $\Delta T$ /solar radiation are calculated on an hourly basis.

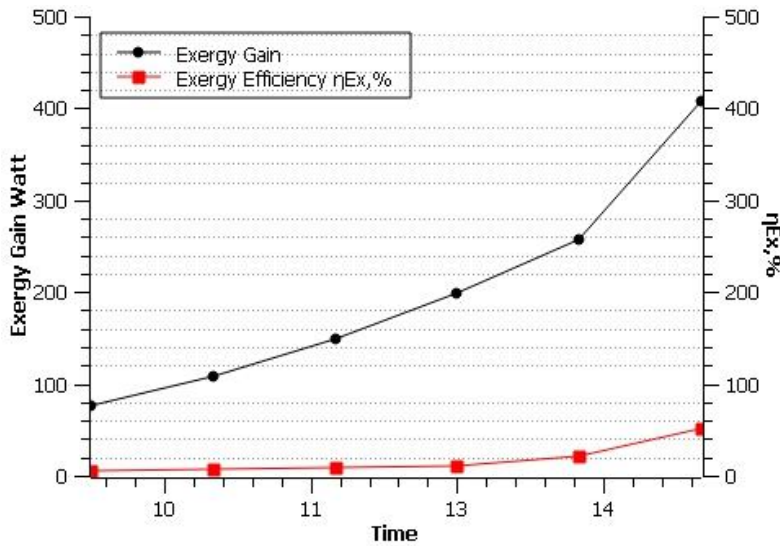


Figure 16. Exergy gain and Exergy efficiency are calculated on an hourly basis.

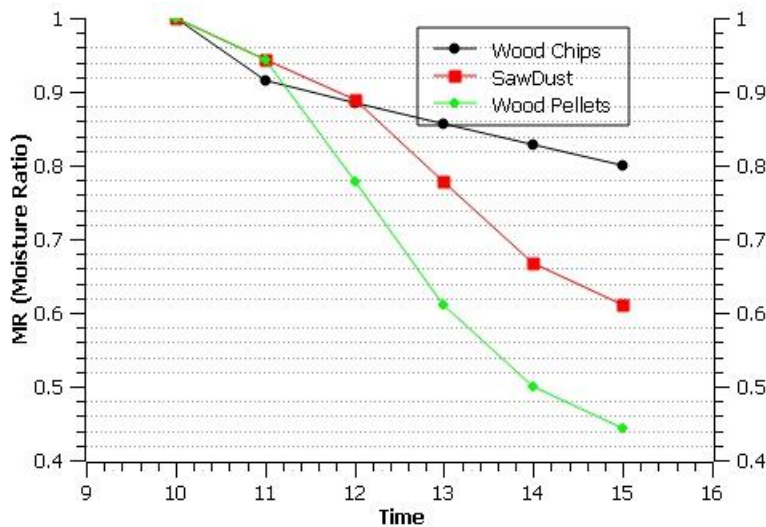


Figure 17. The moisture ratio was calculated for the wood chips, sawdust, and pellets.

#### 4. EXPERIMENTS WITH FORCED CONVECTION SOLAR DRYER

The ANN model is explained in section 4.5. and that was employed in the NN-tool of MATLAB software to validate and predict final moisture content. The Coefficient of correlation (R) gives the goodness of the model. The training, validation, test, and overall values were found to be 1, 0.995, 0.970, and 0.990, reflecting the confirmation of the model shown in Figure 18. The predicted values were found to be coherent with the experimental dataset. The training was completed in 2<sup>nd</sup> iteration when the validation samples of mean square error reached the optimum value. The best validation performance was 2.4949 at epoch 993, where the epoch measures the number of times all training vectors are used once to update the weights.

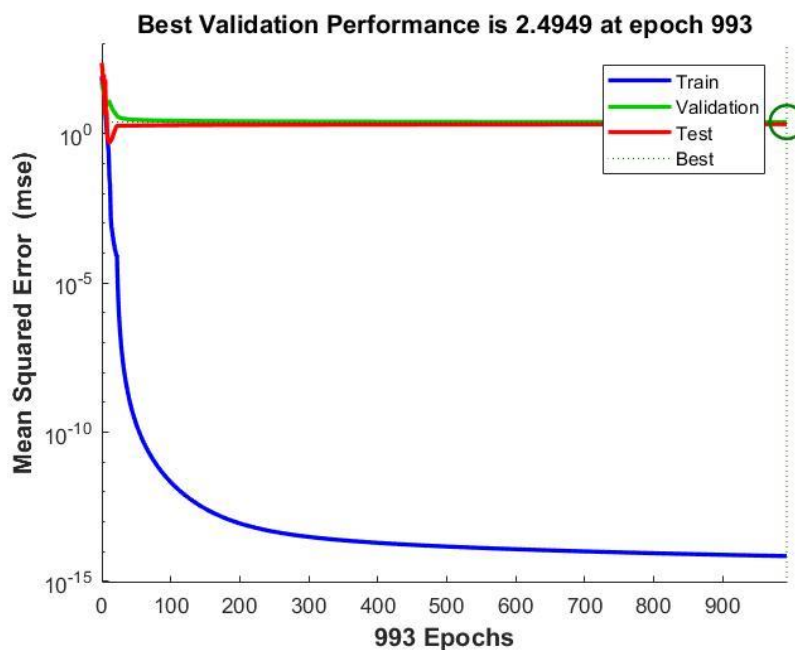


Figure 18. Root mean square error (MSE) plot for the ANN model.

In the above model, (ANN) is employed to forecast the performance of combined solar dryer. While ANN has previously been applied to predict drying performance in fruits, vegetables, and various agricultural/biomass products, its application to wood fuels is a novel contribution highlighted in this research. Notably, the model is highly adaptable, allowing for modifications in input vectors, target vectors, and weights to fine-tune predictions for specific drying conditions, thus mirroring the presented model's versatility. An impressive achievement of this study is the development of an ANN model with a remarkably high R-squared ( $R^2$ ) value of 0.99, signifying its exceptional precision in predicting moisture content. Furthermore, this adaptable approach holds promise for predicting an array of other critical drying parameters, such as solar radiation, moisture ratio, and heat transfer coefficient, underscoring its potential for wide-ranging applications in the field.

### 5. EXPERIMENTS WITH PHASE CHANGE MATERIAL (PCM)

#### 5.1. Artificial radiation set-up

The cabinet dryer developed for this study is made up of wooden blocks as walls of the dryer. Figure 19. comprises the schematic illustration, where the working mechanism and the real-time pictorial view of the dryer are shown. It consists of three prime chambers, namely, the collector chamber for trapping hot air and its transmission with the help of an exhaust chimney fan. The drying chamber (Length x Breadth x Height) is (80 x 50 x 45) cm in size and has three layers of trays consisting of one kilogram of the samples of woodchips, sawdust, and pellets each. Similarly, the bottom chamber below the drying chamber is for hybrid support of thermal energy coming out of the phase transition of PCM, i.e., Coconut oil. The volume of the drying chamber and the PCM material chamber is 180 liters. The airflow for drying occurs through six holes at the collector inlet of 2 cm diameter and three outlet holes in the drying/PCM chamber with a six cm diameter each. A power supply chimney fan circulated the hot air for consistent drying with an airflow of 2 m/s regulated using an anemometer. The collector was placed for the inlet airflow at the top for the "without PCM" scenario, as shown in Figure 19 (a), and at the bottom chamber only during the "with PCM" scenario of experiments, as shown in Figure 19 (b).

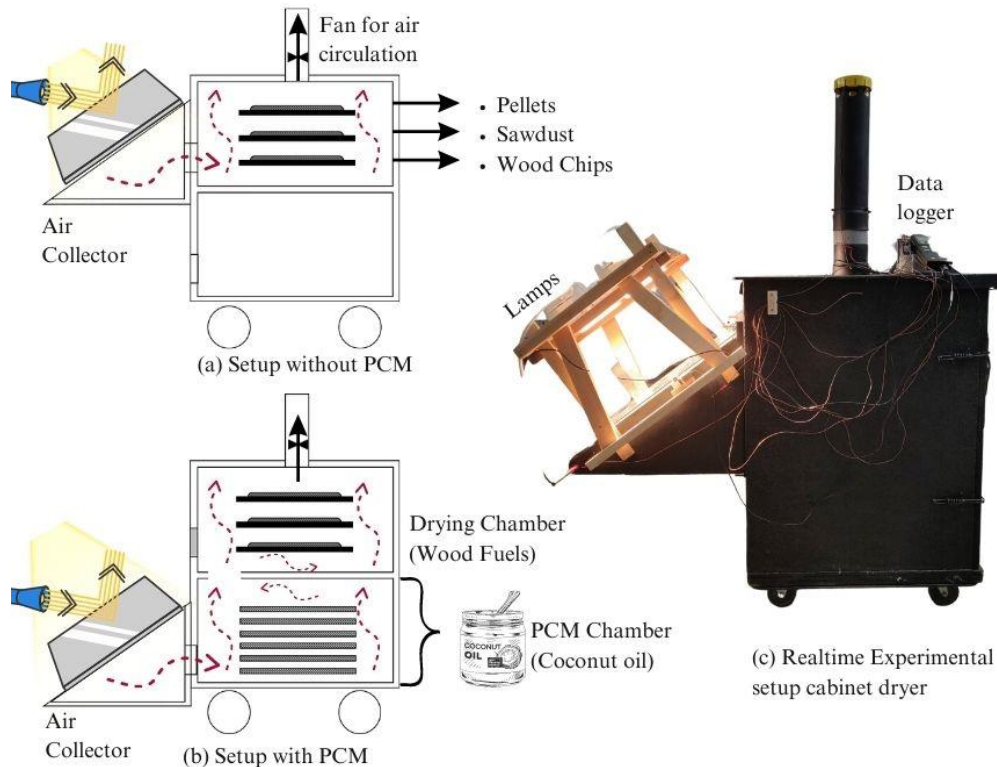


Figure 19. Schematic description of the (a) dryer without PCM chamber, (b) dryer with PCM chamber, and (c) Real time cabinet dryer pictorial view.

For two prime scientific reasons, it was decided to perform the trials with an artificial solar source (i.e., halogen lights) rather than outdoor environmental conditions. Foremost, because of alterations in weather and cloud cover, radiation levels during studies with the sun might fluctuate significantly during the day. The solar dryer's energy and exergy efficiency may fluctuate due to this unpredictability, making it challenging to gauge and contrast performance under various circumstances precisely. It is feasible to create an artificial sun that emits rays in a predictable and regulated manner, making it possible to evaluate energy and energy efficiency with greater accuracy and dependability. Secondly, a potential method for improving solar dryers' efficiency is using phase change material (PCM) for continuous drying. However, because of the variations in radiation levels, it might be challenging to assess PCM's efficacy in the normal sun. It is feasible to examine the performance of the solar dryer with and without PCM under constant and regulated settings by employing an artificial sun, giving a more precise evaluation of its efficacy.

In order to generate constant radiation for the air collector, four halogen reflector lamps of 500 Watts capacity were placed above the collectors with the help of wooden frames. Last but not least, using a halogen lamp offers a more regulated and reproducible experimental

setting, enabling more precise and trustworthy evaluations of the effectiveness of the solar dryer. This can enhance the study's scientific rigor and boost trust in the findings.

### 5.2. Thermophysical properties of coconut oil as PCM

In order to better understand how PCM might be applied to solar thermal devices such as solar heating systems, dryers, greenhouses, etc., many empirical forms of research have been performed. Research shows that the performance of all applications, in most cases, improves using PCMs. A technology that has greatly benefited from this is the combined PV-Thermal systems (PVT), with some sources reporting an impressive increase in the overall efficiency of over 40% [60]. For temperatures above 20°C, coconut oil PCM, coconut oil nano-PCM, and coconut oil nano-PCM embodied in metal capsules can be utilized as temperature regulators. While the latent heat discharging process occurs at a relatively low temperature of (16–18°C), the latent heat charging process occurs between 20–25°C. Therefore, it should be possible to extract this latent heat during the night hours of drying to supply continuous heat to the dryer. Coconut oil is non-corrosive to metal containers, has a comfortable melting point, a high latent heat capacity, and has little to no supercooling during the phase change process. One of the many instruments used by researchers to verify various kinds of organic and non-organic phase change materials is differential scanning calorimetry (DSC). Data on the melting temperature, freezing temperature, latent heat, and specific heat capacity are typically collected using DSC measurements. These parameters are vital in understanding the performance of the PCM as a TES media [61]. Safira *et al.* [62] investigated the thermal properties of coconut oil based on DSC studies for building energy storage applications. The experiments involved examining the addition of graphene that affected the thermal storage properties of the samples. Figure 20 is a modified schematic of the experimental results of this study depicting the two crucial phases of the solidification and melting of the coconut oil. The area under the curve can be used to calculate the latent heat of melting or solidification based on the endothermic or exothermic reactions. Though coconut oil as PCM is cheap and readily available, its performance as a thermally efficient PCM is not yet explored extensively. The energy assessment of the dryer "with" and "without" will reveal the utility of coconut oil as a potential PCM for the solar drying of wood fuels. Some of the critical characteristics and thermal properties of coconut oil are mentioned in Table 5.

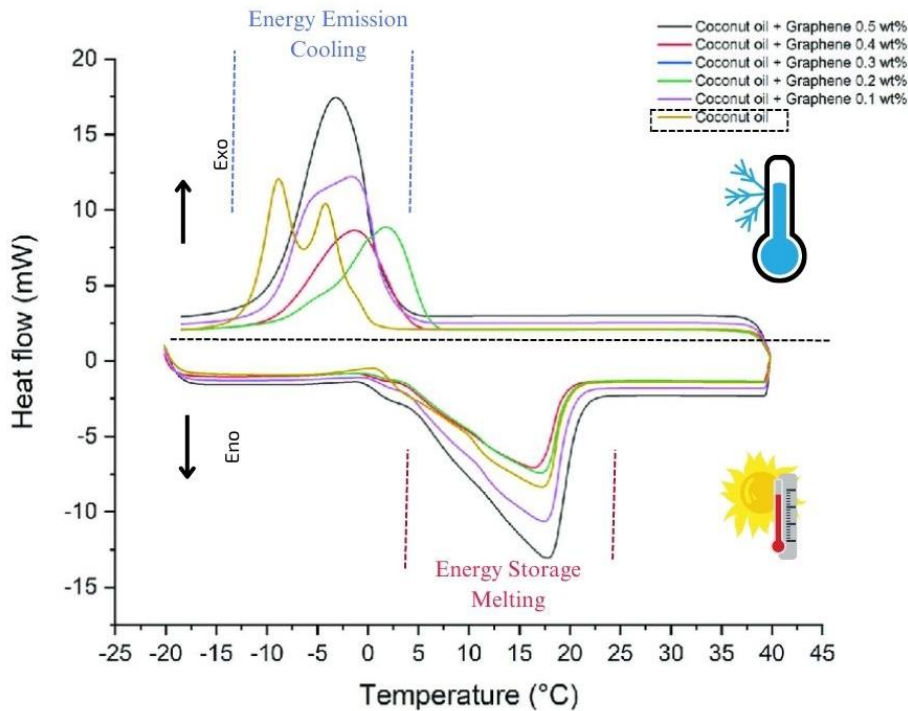


Figure 20. DSC curves of coconut oil during the phase change transformation (Adapted and recreated from source: [62]).

Table 5. Thermal properties of coconut oil used in the investigation [63] [64] [65].

Thermal Properties	Coconut Oil	Air
Density ( $\text{Kg m}^{-3}$ )	916	1.137
Melting Point ( $^{\circ}\text{C}$ )	22-26	-
Heat of Fusion ( $\text{kJ kg}^{-1}$ )	103.25	-
Thermal conductivity ( $\text{W m}^{-1}\text{K}^{-1}$ )	0.161	0.0024
Specific heat ( $\text{kJ kg}^{-1}\text{K}^{-1}$ )	$0.62+0.1006 T$	-
Viscosity (cSt)	20	-
Moisture content ( $\text{mg kg}^{-1}$ )	1	-

### 5.3. Methodology

In this section, investigations on the thermal efficiency and exergy of wood fuel drying systems using phase change material are discussed. Specifically, woodchips, pellets, and sawdust are used as our sample wood fuels and compared their drying performance using the proposed hybrid solar dryer with the performance of an open-sun drying system. Historically, waste streams from timber and other industries have formed the backbone of processed wood fuels. However, in recent years, the production of wood chips, pellets, and sawdust fuel for blending with coal have entirely relied on fast-growing tree crops [66]. Considering the high demand [67], it is inevitable to maintain the moisture content of these wood fuels [68]. The

goal was to propose an economically viable and environmentally sustainable drying solution for industrial applications.

During charging and discharging cycles, phase-change materials like coconut oil can store and release thermal energy [63]. The PCM is heated throughout the charging cycle, changing from a solid to a liquid phase and absorbing heat in the process. This cycle is influenced by temperature since hotter temperatures enable quicker and more effective charging. When the liquid oil cools down throughout the discharging cycle, it solidifies, releases the heat trapped inside, and becomes usable. Temperature also influences this cycle since slower and less effective heat release occurs at lower temperatures. A heat storage medium, such as a micro [69] or macro [70] encapsulate that can absorb and transfer the released heat to a desired location or process must be placed optimally to extract latent heat from the PCM. The heat that has been stored can be used in this way.

The proposed hybrid solar dryer consisted of a drying chamber with three layers of one-kilogram samples of each wood fuel product and an additional bottom chamber with eight layers of PCM trays. A data logger with K-type thermocouples recorded the temperature data throughout the experiment. The current study focused on improving energy efficiency and evaluated the economic and environmental performance of the proposed drying system. To assess the economic viability of our proposed drying system, an economic analysis was performed that considered the initial investment, operational costs, and payback period. Furthermore, to evaluate the environmental impact of the proposed system, the reduction in carbon footprint was measured and compared to the open-sun drying system, as shown in Figure 21. The three kinds of wood fuels were acquired from a local supplier in Miskolc, Hungary. The sample fuels were kept for 24 hours with sprinkled water to observe the moisture.

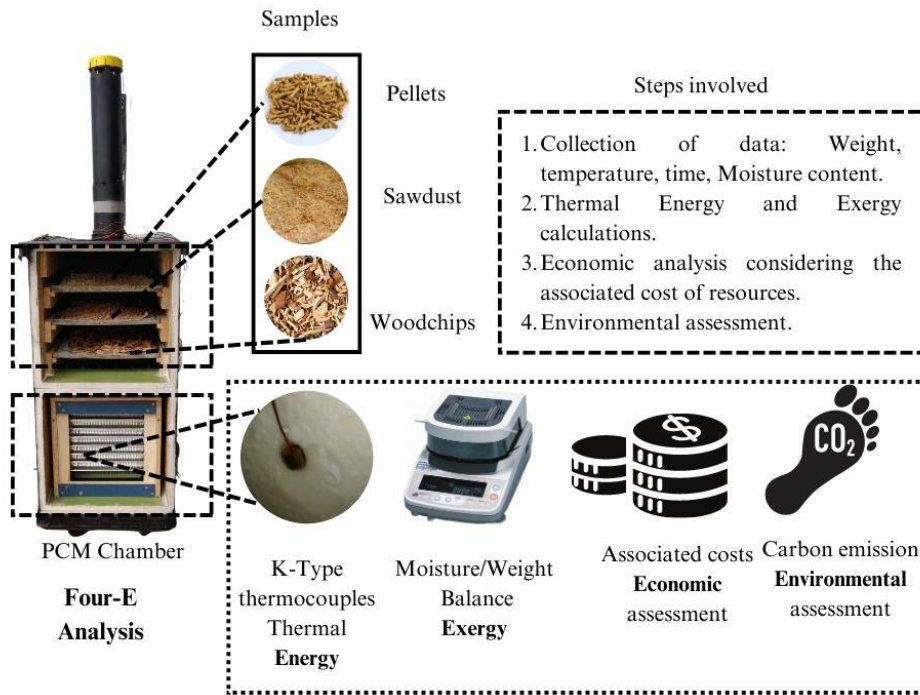


Figure 21. The four-E (Energy, Exergy, Economic and Environmental assessment methodology adopted for the present study.

The moisture content was measured on the moisture balance machine (readability of 0.001 grams). The initial moisture content was measured as 45%, 37%, and 39% for wood chips, pellets, and sawdust samples, respectively, on a wet basis. Four (DELL082) Halogen reflectors of 500 Watts were used as the radiation sources. Xenon lights could also be used for such experiments but were not used due to unavailability in the local market. The pyranometer (SOLART-SYS) was used for irradiance measurement, and the instrument had a sensitivity of  $\pm 0.1$  mV/Wm<sup>2</sup>. After measuring the moisture, air velocity, and irradiance, the three samples were measured for one-kilogram samples on a weighing machine (sensitivity  $\pm 0.1$  grams). These samples were then placed, and the drying of the samples was observed for a duration of 22 hours. This period was selected because, after 20 hours, the system's temperature returned to normal since the lamps got switched off. The four-E analysis is performed from these observations to understand the feasibility of solar drying of wood fuels.

#### 5.4. 4-E Analysis

For optimal effectiveness, it is crucial to comprehend solar dryers' thermal energy and exergy efficiency. The quantity of energy used efficiently to dry the product in a solar dryer is determined by thermal energy efficiency. One can assess the effectiveness of the solar dryer in converting solar energy into usable heat energy for drying by knowing the thermal energy

performance. These experiments can assist in improving the solar dryer's construction to increase utility and decrease energy losses for drying wood biofuels.

On the other hand, exergy efficiency describes the solar dryer's energy caliber. Exergy determines the most useful work that can be done with the energy by accounting for the irreversibility in the system, such as heat losses from convection and radiation [71]. In previous investigations, authors performed experiments for the wood biofuels in open weather conditions for open sun drying [72], box-type natural convection drying [6], and forced convection drying in cabinet dryers with open sun and varying radiation conditions [73]. Understanding exergy performance allows one to assess the caliber of the energy consumed and locate opportunities for exergy loss reduction, both of which contribute to the system's total effectiveness. Simultaneously, conducting an economic analysis of solar drying of wood fuels can offer essential insights into the production and dissemination of wood biofuels and assist in developing more efficient and sustainable techniques for their production. The subsections of Section 5.4. broadly address these issues and describe the methodology used in the experimental analysis of the energy, exergy, and economic assessment of the dryer.

#### 5.4.1. Energy analysis

A solar dryer's efficiency can be assessed using energy and exergy analysis for the overall system. For the energy analysis, the first law of thermodynamics, the overall energy balance equation is formulated with three prime assumptions, which are [74][75]:

- The system remains in a steady state.
- The thermal parameters of the air are considered constant during the experiments.
- The transmissivity of the glass cover is 0.89.

The overall energy balance is mentioned in Eqn. (1) where,  $Q_i$ ,  $Q_u$ ,  $Q_{st}$ , and  $Q_l$  are the absorbed, useful, stored and lost energy of the system respectively [76].

$$Q_i = Q_u + Q_{st} + Q_l \quad (15)$$

As the radiation is supplied to the hot air collector, it generates  $Q_u$  amount of heat which is given as;

$$Q_u = \rho V_{avg} A_{duct} C_p (T_o - T_i) \quad (16)$$

The incident energy absorbed on the surface of the collector  $Q_i$  ;

$$Q_l = I_T A_c \quad (17)$$

Two cycles of the phase change take place during the operation. First is charging, where the frozen oil melts down and stores the energy, and the second is discharging, where the oil again freezes in the absence of heat supply and releases heat. Thus, the total PCM stored heat flux  $Q_{st}$  for the PCM charging and discharging period can be given as [76]:

$$Q_{ch} = \left[ m_{PCM} C_{p,s} (T_m - T_{i,ch,PCM}) + m_{PCM} L + m_{PCM} C_{p,l} (T_{f,ch,PCM} - T_m) \right] / \Delta t_{ch} \quad (18)$$

$$Q_{dis} = \left[ m_{PCM} C_{p,l} (T_m - T_{f,dis,PCM}) + m_{PCM} L + m_{PCM} C_{p,s} (T_{i,dis,PCM} - T_m) \right] / \Delta t_{dis} \quad (19)$$

Thus, the ratio of the useful energy to the incident absorbed energy gives the thermal efficiency of the air collector can be given as Eqn. (6),

$$\eta_{th,c} = \frac{\rho V_{avg} A_{duct} C_p (T_o - T_i)}{I_T A_c} = \frac{\int Q_u}{\int Q_l} \quad (20)$$

Similarly, the thermal efficiency of the PCM storage chamber can be evaluated as;

$$\eta_{PCM} = \frac{\int Q_{dis}}{\int Q_{ch}} \quad (21)$$

#### 5.4.2. Exergy analysis

Exergy is a unit of measurement for the effectiveness or usefulness of energy in a system for carrying out useful actions. It is described as the most work a system can generate as it achieves balance with its surroundings. Exergy is a more useful measure for evaluating the effectiveness and viability of energy conversion processes because it considers both the amount and the quality of energy in a system. The second law of thermodynamics provides the basis for the exergy balance equation, as shown in Eqn. 22, with assumptions kept identical to the energy analysis [77].

$$Ex_u = \dot{m} \left[ C_p (T_o - T_i) - T_a \left( C_v \ln \left( \frac{T_o}{T_i} \right) - R \ln \left( \frac{\rho_o}{\rho_i} \right) \right) \right] \quad (22)$$

$$Ex_{in} = \left[ 1 + \frac{1}{3} \left( \frac{T_a}{T_s} \right)^4 - \frac{4 T_a}{3 T_s} \right] I_T A_c \quad (23)$$

$$\eta_{ex} = 1 - \frac{Ex_{in} - Ex_{out}}{Ex_{in}} \quad (24)$$

### 5.4.3. Economic Assessment

A comprehensive economic analysis of solar dryers can help create more efficient and affordable processes for creating woody material biofuels. Though the experimental work demonstrated in this paper is limited to a lab-scale dryer, the basic calculations performed here can provide a benchmark for further extrapolation in large-volume storage and drying of woodchips, sawdust, pellets, etc. The price of the hot air generated by the solar dryer can be determined by dividing the system's overall cost, which includes the price of components, installation, and upkeep, by the total volume of hot air generated during the system's lifespan. Solar dryers typically last between 10 and 15 years, though the device's lifespan will rely on its robustness and maintenance [78].

In addition to the original investment cost, the system's operational expenses should be considered, including the cost of energy storage, fallback systems, and maintenance. These expenses can be added to the price per kg of heated air to determine the total manufacturing cost accurately. A financial metric used to describe solar dryers, the capital recovery factor (CRF), shows the yearly payment necessary to recover the solar dryer's capital cost over the course with experiments interest rate ( $i$  %) of its useful lifespan of  $n$  years [76].

$$CRF = \frac{i(1+i)^n}{(1+i)^n - 1} \quad (25)$$

The CRF stands for the yearly contribution that must be made to cover the solar dryer's capital cost, which includes the price of components, labor, and implementation. The CRF considers the time value of money or the reality that a single Dollar/ Euro received in the future is worth less than a Dollar/Euro received today. In addition, the fixed annual cost (FAC) can be determined by multiplying the CRF by the capital cost of the dryer, i.e., IC [79].

$$FAC = IC(CRF) \quad (26)$$

The salvage value of the drying system is usually considered as 20% of the capital cost [80].

$$SV = 0.2 \cdot IC \quad (27)$$

Other important considerations are the sinking fund factor (SFF) and annual salvage value (ASV). In the case of a solar dryer, the SFF stands for the sum of funds that must be set aside a

year, considering the possibility of earning interest, to accumulate the initial investment during the dryer's lifespan.

$$SFF = \frac{i}{(1+i)^n - 1} \tag{28}$$

$$ASV = SFF * SV \tag{29}$$

The annual maintenance cost can vary as per the electricity consumed for forced convection through the fan. This can vary where large amount of wood fuels are kept depending on the volume. Also, the fixed annual cost can be multiplied by a factor; for example, 15% is suggested by literature [79] [80] but could be increased based on operations.

$$AMCE = 0.15(FAC) + CE(CRF) \tag{30}$$

Hence, the annual cost can be given as [81],

$$AC = FAC + AMC - ASV \tag{31}$$

Finally, the cost of one kg of hot air generated by the dryer can be given as,

$$CPL = \frac{AC}{M} \tag{32}$$

Table 6. presents the costs associated with the dryer giving the IC value as 279 EUR. These associated costs were noted for the dryer developed for the present study. The mentioned costs were used for the calculations based on which the results are presented in in Section 4. It should be noted that this analysis do not consider the costs of lamps because the authors have considered the normal sun drying situation for the economic assessment of the dryer.

Table 6. Economical costs associated with the dryer.

Item No.	Material	Approximated Costs (€)
1	Wooden Blocks	82
2	Sample Perforated Trays	12
3	PCM material	16
4	Glass Cover	8
5	Insulation	5
6	Convection Fan	12
7	Wheels	20
8	Spray Paint	17
9	PCM trays	7
10	Labor Charges	100

Another important factor is the payback period ( $N$ ) given as with ( $i$ ) as the interest rate of 12% and ( $f$ ) as the inflation rate of 6% considered in the present study [82].

$$N = \frac{\ln\left(1 - \frac{IC}{S}(i - f)\right)}{\ln\left(\frac{1+f}{1+i}\right)} \quad (33)$$

It enables a comparison between the solar dryer's cost and its benefits. This allows decision-makers to compare the solar dryer's cost-effectiveness to other drying techniques. It helps potential investors make an informed decision about investing in a solar dryer. If the payback period is relatively short, the investment is considered more attractive as it can generate returns quickly.

#### 5.4.4. Environmental Assessment

Wood fuels like woodchips, pellets, and sawdust must be dried, which is costly and energy-intensive. Due to its potential to lower energy usage and CO<sub>2</sub> emissions, the use of solar dryers for drying wood fuels is growing in favor as the world advances toward sustainable and renewable energy sources. Limited assessments have been performed on studies concerning the drying of wood fuels. With this assessment, the authors intend to assess the sustainability aspects of this drying approach. However, the volume of the product and the PCM is relatively small compared to the industrial scale, yet this investigation could be helpful for future investigations.

To evaluate the environmental effects of solar drying wood fuels, several factors must be considered, including the energy payback time, CO<sub>2</sub> emissions annually, specific energy consumption, sustainability index, and improvement potential. The energy payback time (EPBT) is the time the solar dryer takes to generate the same amount of energy used in production. The shorter the EPBT, the more sustainable and environmentally friendly the solar dryer is considered; it can be calculated as shown in Eqn. (20) [83]. In Table 7, the embodied energy of the various parts used in manufacturing the dryer are presented with a combined grand 653.87 kWh. Also, the annual energy output is calculated as the product of overall thermal efficiency, radiation, collector area, sunshine hours and working days in a year [84].

$$EBPT = \frac{\text{Embodied Energy}}{\text{Annual Energy Output}} \quad (34)$$

Table 7. Embodied energy for the specific parts of the dryer.

Material	Quantity (In kg)	Embodied Energy co-efficient (kWh/kg)	Total Energy (kWh)	Ref.
Wooden Plywood	25	11.9	297.7	[85]
Aluminum Trays	3.5	22.0	77.1	[85]
Glass	1.5	7.2	10.9	[85]
LDPE DC Fan	0.5	28.5	14.2	[86]
HDPE Wheels	1.5	28.5	42.7	[86]
Spray Paint	5	34.4	172.2	[85]
PCM trays	0.5	78.7	39.3	[85]

CO<sub>2</sub> emissions per year can also be calculated to determine the greenhouse gas emissions associated with the production and operation of the solar dryer. By comparing these emissions with those generated by conventional drying methods, decision-makers can evaluate the potential environmental benefits of solar drying [83].

$$CO_2 \text{ emissions per year} = \frac{\text{Embodied Energy} \times 0.98}{\text{Lifetime}} \quad (35)$$

Specific energy consumption (SEC) is another important parameter that can help assess the efficiency of the solar dryer. It is the amount of energy consumed per unit of wood fuel dried. Lower SEC values indicate a more efficient and environmentally friendly solar dryer [87][88].

$$SEC = \frac{E_{\text{electricity}}}{m_w} \quad (36)$$

$$\text{where, } m_w = \frac{(M_o - M_f)}{(100 - M_f)} \times W_o \quad (37)$$

The sustainability index (SI) is a comprehensive metric that considers the environmental, social, and economic aspects of solar drying of wood fuels. The lack of productivity (LOP) can help researchers and industry professionals evaluate the overall sustainability and environmental impact of using solar dryers for drying wood fuels [87].

$$SI = \frac{1}{\eta_{ex}} \quad (38)$$

$$LOP = \frac{Ex_{loss}}{Ex_o} \quad (39)$$

Finally, the improvement potential (IP) may be used to pinpoint areas where the solar dryer can be improved to become more effective and ecologically friendly. The solar dryer's design

and operation may be improved using this knowledge to lessen its negative environmental effects [87].

$$IP = (1 - \eta_{ex}) \times Ex_{loss} \quad (40)$$

The findings of this evaluation can help direct future research and development efforts toward developing solar dryers that are more effective and sustainable, as well as assist practitioners in the biomass/wood fuel business in making decisions on the possible application of solar dryers for the drying of wood fuels.

### 5.5. Uncertainty Analysis

Analysis of uncertainty is required to demonstrate the accuracy of the experiments. Errors in this investigation were analyzed based on the measurement uncertainties and the sensitivity of the equipment. The weighing balance machine in the current experimental setup has an accuracy of 0.1 grams. The relative humidity (RH) reading on the humidity meter was  $\pm 2.5\%$ . The pyranometer was  $\pm 0.1$  mV/Wm<sup>2</sup> sensitive. The moisture balance had 0.001-gram readability. In its operating range of (0.3 to 20 m/s), the anemometer provides an accuracy of 0.1 m/s. The thermocouples had a sensitivity of  $\pm 0.5^\circ\text{C}$ . Before the experimental trials, all the measurement devices were properly calibrated. In addition, the temperature uncertainty, mass-flow rate  $\frac{W_{\dot{m}a}}{\dot{m}a}$ ,

energy gain  $\frac{W_{Eout}}{E_{out}}$  and thermal efficiency  $\frac{W_{\eta}}{\eta}$  were calculated as [75] [76];

$$\frac{W_{Tch}}{T_{ch}} = \sqrt{(M_{acc})^2 + (P_{error})^2 + (R_{loss})^2} \quad (41)$$

$$\frac{W_{\dot{m}a}}{\dot{m}a} = \sqrt{\left(\frac{W_{Vavg}}{V_{avg}}\right)^2 + \left(\frac{W_{Ta}}{T_a}\right)^2 + \left(\frac{W_{Pa}}{P_a}\right)^2} \quad (42)$$

$$\frac{W_{Eout}}{E_{out}} = \sqrt{\left(\frac{W_{\dot{m}a}}{\dot{m}a}\right)^2 + \left(\frac{W_{Tin}}{T_{in}}\right)^2 + \left(\frac{W_{Tout}}{T_{out}}\right)^2} \quad (43)$$

$$\frac{W_{\eta}}{\eta} = \sqrt{\left(\frac{W_{\dot{m}a}}{\dot{m}a}\right)^2 + \left(\frac{W_{Tin}}{T_{in}}\right)^2 + \left(\frac{W_{Tout}}{T_{out}}\right)^2 + \left(\frac{W_I}{I}\right)^2} \quad (44)$$

The values of flow rate, energy gain by the air, and thermal efficiency are associated with an uncertainty of  $\pm 5.88\%$ ,  $\pm 6.23\%$ , and  $\pm 5.44\%$ , respectively. The data gathered during

measurements for this experiment were within an acceptable range since the instrument performance-related uncertainty values discovered during experimentation were quite low.

### 5.6. Results of experimental investigations

The present work attempts to understand the role of constant radiation supply in the two scenarios (with and without PCM). The collector size had a limitation to fit four lamps on top of it. Hence, the maximum radiation-achieved was  $755 \text{ W/m}^2$  by placing it at a distance of 1.5 meters on top of the collector. The size of the collector and the radiation may vary for large-scale practical applications. In Hungary (city Miskolc), where the experiments are conducted, the value of the global radiation at midday throughout the winter half-year (from October to March) ranges between  $250$  and  $600 \text{ W/m}^2$  [89]. It is between  $600$  and  $1000 \text{ W/m}^2$  from April to September, which is the summer season making the radiation value of  $755 \text{ W/m}^2$  nearly realistic with a fixed mass flow rate of  $0.016 \text{ kg/s}$  for both scenarios, i.e., (with and without PCM).

#### 5.6.1. Temperature

The radiation of  $755 \text{ W/m}^2$  was maintained during the experimental hours (charging period) between 10 A.M. to 1 A.M. of the post-day. After 15 hours, the lamps were switched off to observe the dryer's behavior during the PCM's discharging period. During experiments, the temperatures were measured constantly through the data logger and temperature sensors. The hourly temperature distribution of the dryer is plotted against time and radiation in Figure. 22(a) without PCM and Figure.22 (b) with PCM. The radiation curve, which drops suddenly at 1400 hrs., is due to the switching off the halogen lamps. For both conditions, the highest collector outlet temperature achieved was around  $70^\circ\text{C}$  and drops to  $18^\circ\text{C}$  in just three hours from (15:30 hrs to 18:30 hrs) at the outlet of the collector box. The ambient temperature remains constant at about  $18^\circ\text{C}$  for both (with and without) scenarios. For the without PCM experiments, the temperature profile of all sensors slump rapidly to lower temperatures as observed in Figure 22(a) and 22(b).

## 5. EXPERIMENTS WITH PHASE CHANGE MATERIAL

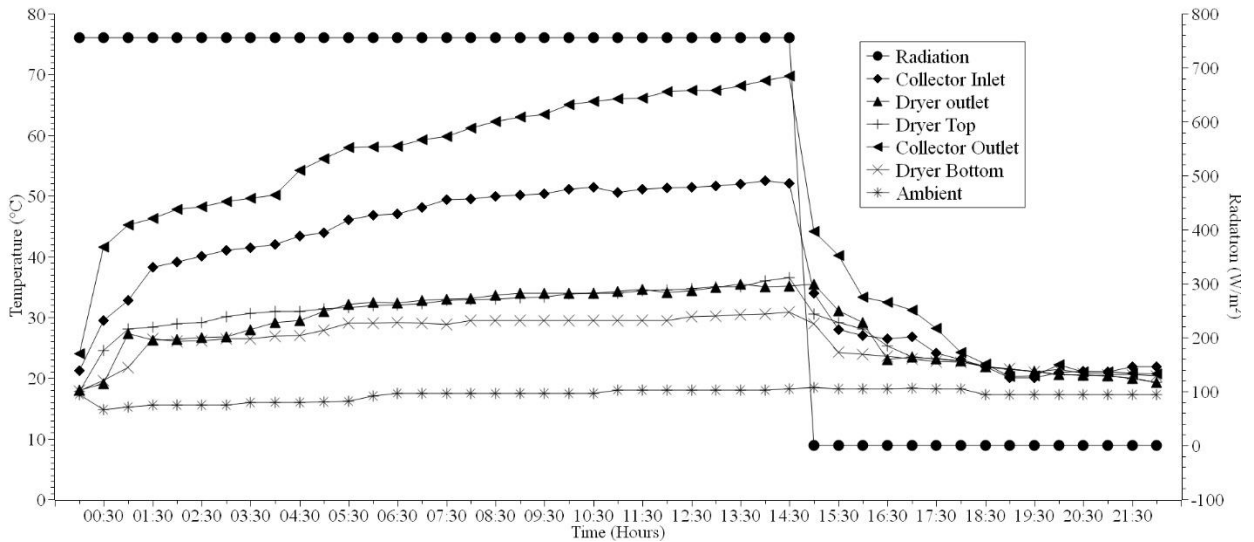


Figure 22 (a). Temperature and radiation profiles during experiments without PCM.

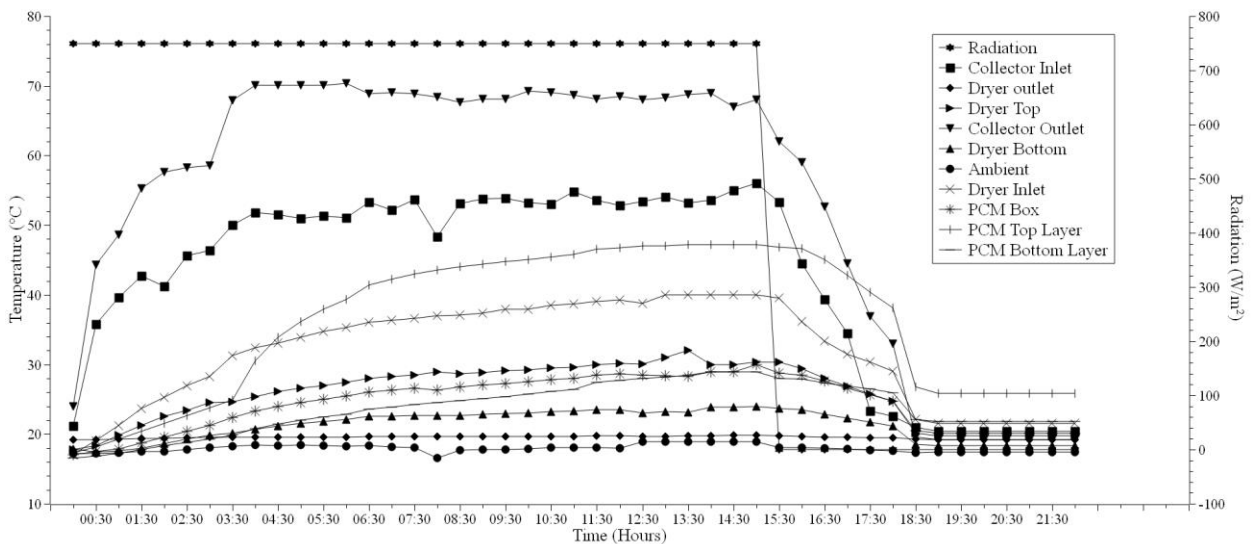


Figure 22 (b). Temperature and radiation profiles during experiments with PCM.

On the contrary, in the PCM condition, as the coconut oil solidifies and releases the stored energy, the slump in trend is not observed, and the various parts of the dryer retain some heat. The collector outlet temperature gradually lowers from 15:30 hrs to 18:30 hrs (from 70°C to 25°C). The temperature was deprived gradually and reached below 30°C after 3 hrs of switching off condition compared to without PCM condition where it goes down 30°C just after one hour. After the first three hours, the dryer outlet, i.e., near the chimney, was maintained at above 40°C (without PCM) while it was above 50°C until switching off condition. In similar research on the solar drying of wood, Tagne and Azese [90] developed a dryer with thermal energy storage at two locations in France. The maximum air temperature achieved was 78°C. Another solar greenhouse dryer developed by Alberto *et al.* [91] for drying woodchips attained a maximum temperature of 59.9°C with a temperature gradient of ambient and inside as 25.2°C. Also, with a

black pebble bed as thermal energy storage for drying timber, the maximum temperature achieved was  $61.7\text{ }^{\circ}\text{C}$  [12]. This observation reflects the performance of coconut oil as a notable potential heat storage material. However, it's also crucial to calculate the energy and exergy performance of the dryer during the experiments, which are discussed in further sections.

### 5.6.2. Energy gain and efficiency

When evaluating the efficacy and cost-effectiveness of the system, it is crucial to consider the energy gain and energy efficiency of a solar drier. The solar drier is more desirable for drying applications due to higher energy gain or efficiency, resulting in faster drying rates, more drying, lower energy usage, and smaller system sizes. The thermal performance of the dryer was evaluated with and without PCM conditions, as shown in Figure(s) 23(a) and 23(b). It observed that the useful heat gain was prolonged with some amount of heat (300 Watts) until

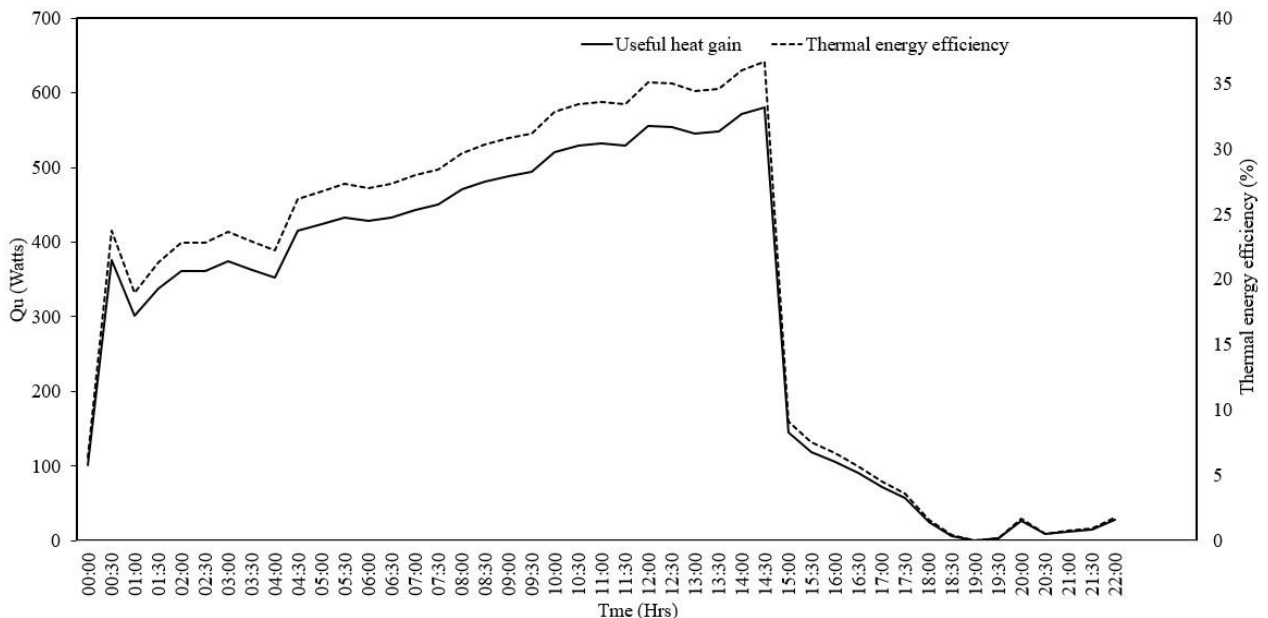


Figure 23(a). Useful heat gain and thermal energy efficiency against time (without PCM).

18:00 hours as the temperature gradient was maintained. During the PCM discharging (solidification), the PCM retains some amount of heat (300 Watts) for 3-4 hours, and then as the temperature gradient nullifies, the efficiency slumps down.

For the without PCM condition, the sudden surge can be observed in Figure. 23(a) with a heat gain of up to 600 Watts and maximum efficiency of 37%. During the PCM (Figure. 23(b)) experiments, the heat gain remains steady and below 600 Watts, and efficiency remains between 30–35%. However, the efficiency steadily drops to below 10% only after 3–4 hours after the radiation is turned off completely. The energy efficiency during the four hours of heat retention

in the case of PCM, the efficiency increases by 63.64%. In general, studies [90] and [37] suggest that the energy efficiency of solar wood dryers is in the range of 30–40%, thereby validating the utility of coconut oil and hybridization of the dryer.

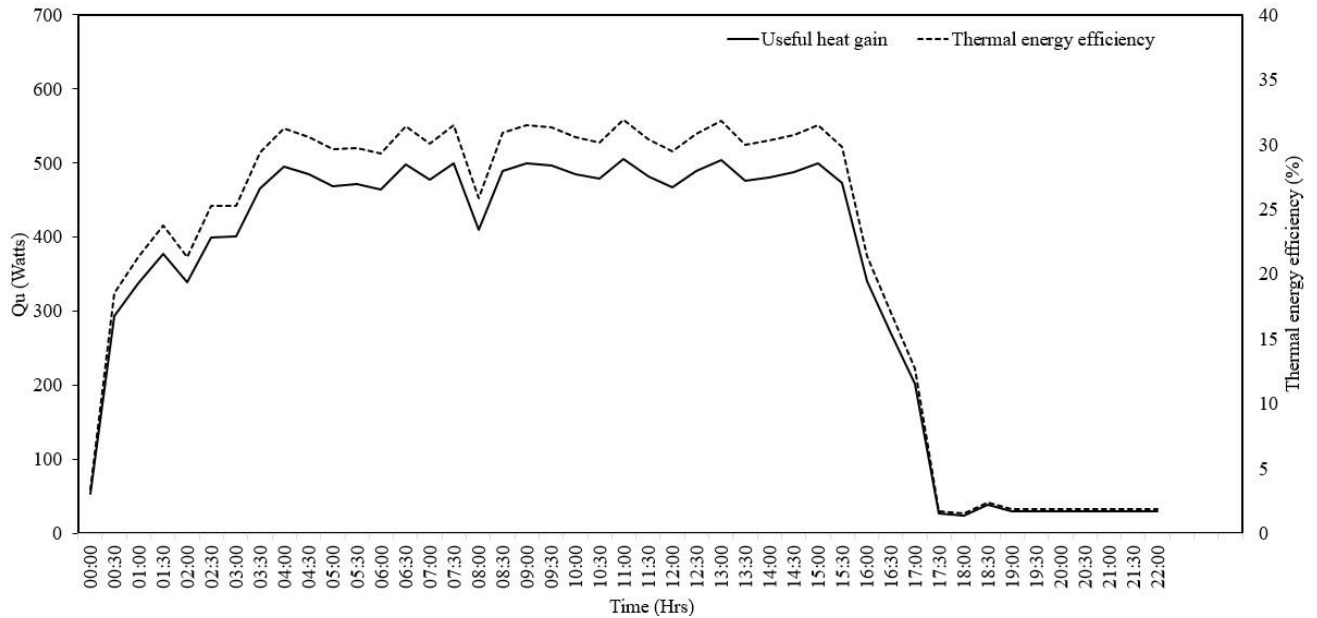


Figure 23 (b). Useful heat gain and thermal energy efficiency against time with PCM.

### 5.6.3. Exergy gain and efficiency

Exergy analysis is frequently used to pinpoint inefficient and energy-wasting areas in a system and to improve its setup and operation for optimum energy effectiveness. Exergy values in a system may fluctuate due to several variables, including temperature, pressure, flow rate, component effectiveness, and irreversibility. Optimizing the functionality and effectiveness of energy exchange systems requires a thorough understanding of these variations and their underlying causes. Figure 24(a) reflects that during the experiments without PCM, with highest exergy efficiency between 14.4–14.5% and drops down to below 30% during off radiation hours.

## 5. EXPERIMENTS WITH PHASE CHANGE MATERIAL

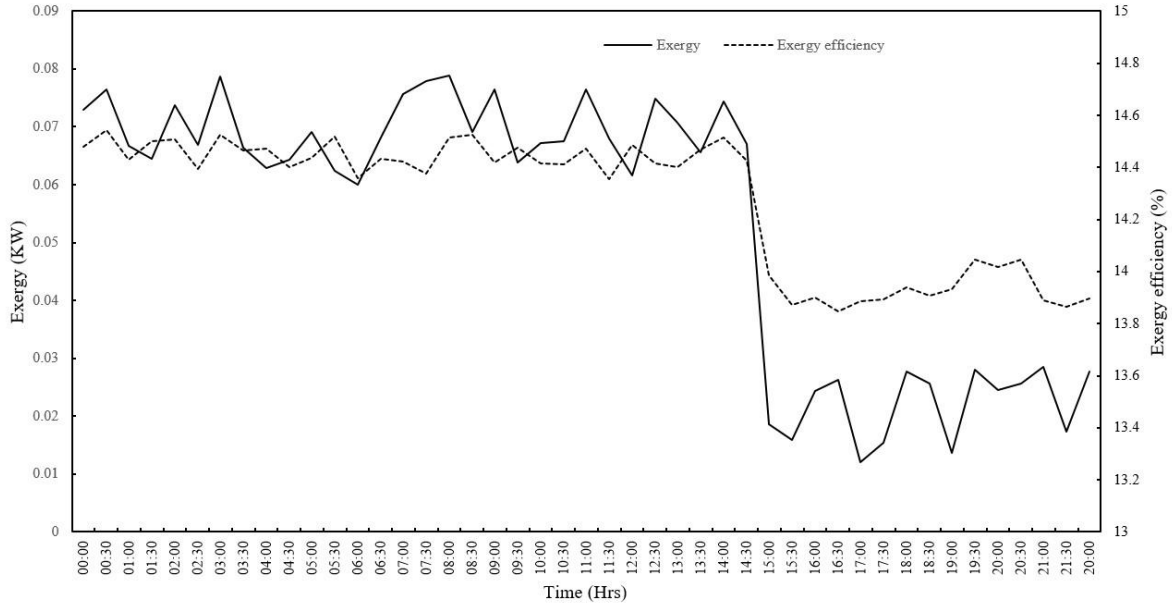


Figure 24(a). Exergy gain and exergy efficiency against time without PCM.

Conversely, for the with PCM experiments, the exergy efficiency fluctuated between 14.1–14.6% during the charging period of PCM and slumped to 13–13.9% during the discharge period of PCM. The exergy was much higher, with PCM conditions reaching 0.012 kW. The fluctuations observed in Figure. 24(b) could be due to pressure variation between the PCM storage chamber at the bottom and the drying chamber of the samples. In the large-scale

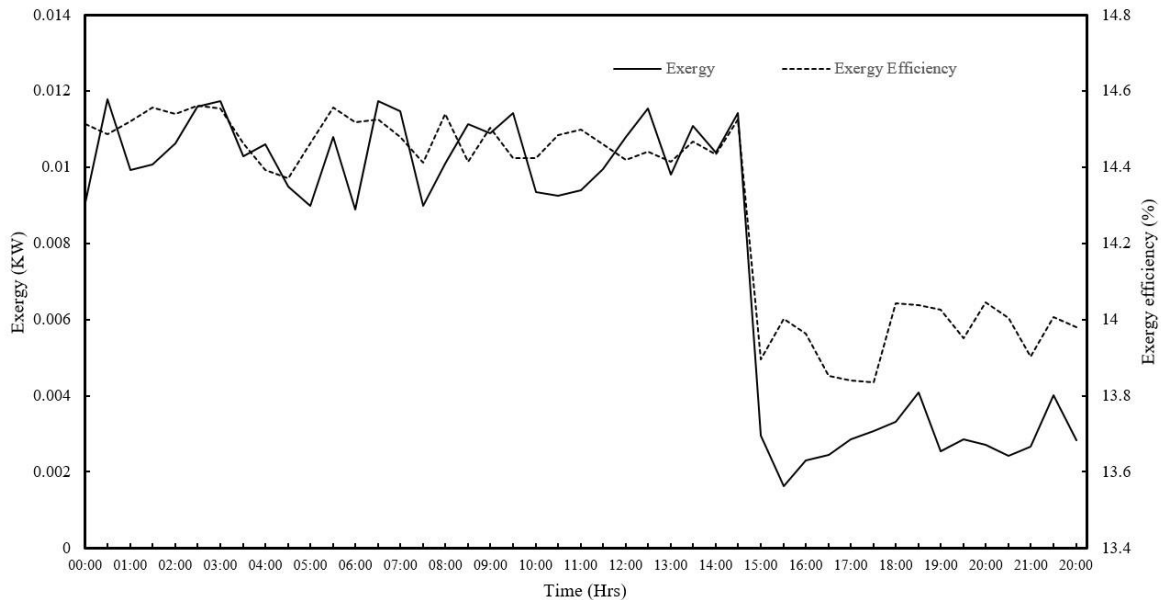


Figure 24 (b). Exergy gain and exergy efficiency against time with PCM.

industrial drying of wood chips, the drum drying system (DDS) (conventional dryer) with capacity ranging between 10 and 180 t/h (wet product). With the temperature rising to 260°C, the energy and exergy efficiencies were calculated as 34.07% and 4.39%, respectively [92].

However, limited research covered the exergy aspect while designing/developing solar-based drying systems specifically for wood fuels. It is important to note that the drying material's thermal and chemical properties influence a solar drying system's exergy efficiency. The exergy efficiency of drying might vary depending on the material's composition, moisture level, and specific heat capacity.

#### 5.6.4. Economic assessment findings

The conclusions of the economic study were informative. The considered solar dryer with a ten-year lifetime and a 12% interest rate has a CRF of 0.172. This indicates that the capital investment's equivalent yearly cost is 17.2% of the initial investment. Researchers may compare the cost of the solar dryer to other drying techniques by using this CRF value to determine the yearly cost of the solar dryer, which includes both capital and operational expenditures. For the entire experimental setup, our initial capital expense was 279 EUR (Euros). As a result, it was determined that the fixed annual cost (FAC) of the solar dryer is EUR 49.38, reflecting the equal yearly cost of the capital investment over the dryer's anticipated lifespan, considering both capital and operational expenses. Further, the sinking fund factor (SFF) calculates how much money must be placed away a year, assuming a particular rate of interest, in order to amass a specific amount of money over a specific amount of time. Based on this, the ASV was found to be 3.18 and the AMC to be 7.42. Metallic macro-encapsulates with organic paraffin wax (PCM) can also be used as short-term energy storage inducing thermal lag in solar drying systems. Research shows that the double-pass air solar heater system is economically feasible for solar drying operations. This system's associated ASV (annual salvage value) and AMC (Annual maintenance operational cost) were found to be 3.13 and 7.31, respectively [76]. The payback period for this dryer setup is calculated as approximately five years. The payback period depends on the interest rates and associated costs and savings. Literature suggests that this period could be as low as six–nine [93] months to as high as 4.69 years, per recent review recommendations [94]. Also, the capital cost of solar dryers may vary from 100–2000 US dollars, with a lifespan of 10–25 years [78]. A compilation of the calculated economic parameters is shown in Table 8.

Table 8. Calculated values of economic parameters (EUR)

Parameters	CRF	IC	SV	FAC	SFF	ASV	AMC	AC
Values	0.177	279	55.8	49.38	0.057	3.18	7.422	53.62

### 5.6.5. Environmental assessment results

Considering the radiation value of 755 W/m<sup>2</sup> and the working hours as 10 hours for those without PCM case and 15 hours for those with the PCM case, the average thermal efficiency is considered as 30%, and the number of working days is 150 days. The energy payback time (EBPT) calculated without the PCM condition is 4.03, whereas with PCM is 3.08. Research shows that energy payback could be critical in finding the best suitable hybridization of solar dryers. For instance, Saini et al. [95] evaluated a greenhouse solar dryer under forced mode integrated with four different types of photovoltaic (PV) technologies. The EBPT ranged from (0.39-1.13), and the lowest EBPT combination was proposed as the best feasible model. The low EBPT value of with PCM scenario in our study thus justifies the utility of PCMs for efficient drying conditions of wood fuels. The CO<sub>2</sub> emissions per year, considering a lifetime of 5 years, is calculated as 64.09 kg per year. Similarly, with PV hybrid models, CO<sub>2</sub> emission (in kg) was found to be in the range of (40.96-141.73) kg [95]. The specific energy consumption was calculated considering the wet basis average final moisture content of 15% to average initial moisture content of 45%. The SEC is estimated as 5.22 kWh/kg, which, in the case of the v-groove double pass solar dryer, was calculated as 3.096 kWh/kg [88]. Considering the average exergetic efficiency of 50 %, the sustainability index was found to be 2, which in the case of wind-generated eco-thermal hybrid dryers was (1.28-2.5) [87]. The improvement potential (IP) shows the amount of a system's energy losses. The potential for improvement for various solar dryers varied from 0.047 to 0.094 kW [96]. The lack of productivity (LOP) was 6.85 and the IP as 0.058 kW, which falls under recommended range.

### 5.6.6. Critical Observations

Energy and exergy efficiencies of the drying system are crucial, yet only a few studies on wood fuels considered calculating them. A few works with their distinct hybrid configuration and outcomes are presented in Table 9. Wood fuels as raw materials usually contain around 60% of wet basis (wb) moisture, and ideally, good quality fuels should be in the range of (5-15)% of moisture content (wb). Alberto *et al.* [91] studied solar greenhouse drying with samples of (*Pinus pinaster*) 2.68 cm half-length having an average initial moisture content of 50% kept in two piles. Solar greenhouse dryers were found to be more effective than open-air drying when drying was accomplished quickly and thoroughly by balancing the moisture content of the wood chips with the moving air. This implies that within the first 24 to 48 hours of drying, the moisture should be reduced to levels that are close to 30%. The present study results reveal that for around 22 hrs of consistent drying time, a significant drop of 34%, 29%, and 31% moisture content (wet-basis)

## 5. EXPERIMENTS WITH PHASE CHANGE MATERIAL

was observed for woodchips, pellets, and sawdust, respectively. To achieve faster drying for large volumes of wood, particularly in solar kilns, the most common hybridization is done with commercial paraffin wax. The PCM is chosen on the basis of the dryer operating temperature. The PCM-integrated dryer's efficiency can be further increased using an electrical heat exchanger [38]. Khouya and Draoui [11] carried out research in a hybrid kiln using several PCMs. According to the findings, the thermal storage unit's mode of operation, board thickness, mass flow rate, and recycling heat process all have an impact on drying time. Additionally, compared to a drying technique without recovered heat, adopting an air recycling process reduced the amount of energy provided to the system and the drying time by approximately 47%. The present study also reveals that by using PCM, the average thermal efficiency increased from 19.75% to 23.85%, which might be further increased using electrical-heat exchanger. The high average thermal energy efficiency in (with PCM) scenario supports utilizing coconut oil as thermal energy storage material. The cost of heating 1 kg of hot air is an important criterion for an economically sustainable dryer with 7 Hrs/Day operational hybrid PCM dryer, it was evaluated as 0.0074 US dollars [76], in the present study, this value is 0.0058 EUR. EPBT for greenhouse dryers was 1.14 years, and CO<sub>2</sub> emission per year is 17.6 kg per year for drying tomato flakes[83] as compared to 1.13 years releasing 64.09 kgs of CO<sub>2</sub> per year in the present study. However, the next investigations will attempt large-volume experiments and CFD simulations to better understand the associated physical parameters.

Table 9. Solar drying of distinct wood fuels under different drying conditions.

<b>Solar Dryer</b>	<b>Wood Fuel</b>	<b>PCM</b>	<b>Drying Time (hours)</b>	<b>Temperature range (°C)</b>	<b>Initial and Final Moisture content</b>	<b>Average Energy Efficiency (%)</b>	<b>Ref.</b>
Solar greenhouse dryer	Woodchips	-	19	30.70-55.90	50-10	-	[91]
Solar-electrical dryer	Redpine wood stacks	Commercial PCM RT55	168	40-90	0.8-0.1 (kg <sub>wb</sub> /kg <sub>db</sub> )	79	[38]
Solar Kiln with PCM	Red pine, Spruce and Beech wood	RT64 (Paraffin), RT82 (Paraffin) and Erythritol (Alcoholic sugar)	600	47-94	0.5-0.1 (kg <sub>wb</sub> /kg <sub>db</sub> )	47	[11]
Solar Kiln with PCM	Wood stacks	Paraffin wax	07	30-70	70-6	-	[97]

## 5. EXPERIMENTS WITH PHASE CHANGE MATERIAL

Present study (without PCM)	Woodchips	-	22	18-70	45-16	19.75
	Pellets				37-12	
	Sawdust				39-10	
Present study (with PCM)	Woodchips	Coconut oil	22	18-70	45-11	23.85
	Pellets				37-08	
	Sawdust				39-06	

### 6. SOLAR DRYING POTENTIAL IN HUNGARY: TRENDLINE ASSESSMENT WITH A CASE STUDY

#### 6.1. Scope of renewable energy in Hungary

Today, the energy security concern is a global issue and seeks global cooperation to tackle emerging energy scarcity. The concerns regarding energy production are not only limited to developing countries. However, there are challenges to meet CO<sub>2</sub> emissions, and a sustainable environment cannot be left behind. In such a case, renewable energy sources emerged as a promising solution at the beginning of the 21st century. The emergence of various non-conventional energy sources opened the doors of cooperation among nations as well. The Visegrád Countries in the Central-European region are example of countries with mutual interests that should look beyond boundaries to develop emerging energy sectors. Renewable sources are not yet as user-friendly or economically viable as the conventional fossil fuel-based energy market. The mutual agreements could speed the innovations related to various renewable sources among nations. The European Commission's NECP reports highlight the effectiveness of V4 nations with some recommendations, which were highlighted in this study. In this study, each country, namely Poland, the Czech Republic, Slovakia, and Hungary, is discussed regarding their current energy status in renewable sources [98] [99]. The EU aims to increase the share of renewable energy consumption; the target value is 32% [100]. The National Energy and Climate Plans (NECP) reflect the renewable energy percentage share for V4 countries as Poland (23%), Hungary (21%), Czech Republic (22%), and Slovakia (19.2%), respectively by 2030. Thus, according to the current scenario, V4 nations should look for new potentials and analyze their renewable energy production strategy. Figure 25. shows a comprehensive recent status picture of the share of renewable sources in energy consumption of the V4 Countries [101].

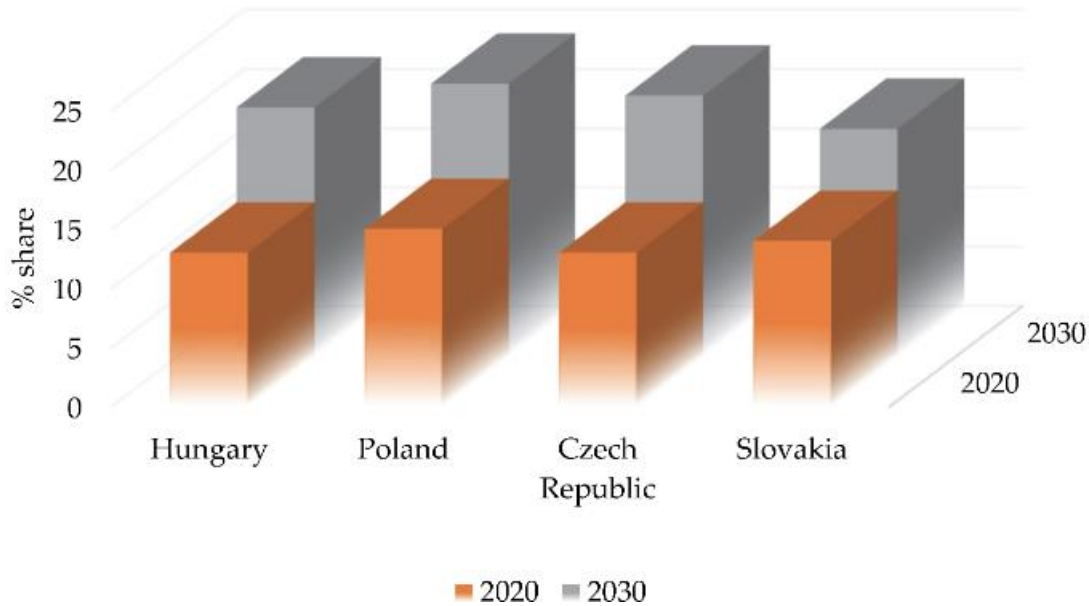


Figure 25. Share of energy from renewable sources in final gross consumption of energy in V4 Countries NECP and future expectations by 2030 [102]

The primary energy consumption through RES in Hungary is 21% by the year 2030. The existing policies forecast the electricity-producing capacity in Hungary will be more than 4000 MW in the coming decade. The production capacity is estimated to be exceeding 6500 GWh, and more than 70% of which will be harnessed through photovoltaics [98]. A recent study in Poland (which receives solar radiation of 1000 kWh/m<sup>2</sup>/year) was conducted to understand potential solar energy technology (SET) utilization as per EU directives. Results suggested some new innovative SET applications with rotating solar towers and artificial photosynthesis [103]. RES and its production's cohesiveness mainly revolve around supply security, energy-saving, and environmental protection with sustainability. These three parameters are essential for the long-term energy independence goals of Hungary [104]. The percentage share was selected as a growth parameter to observe the recent growth in various RES production trends. The last decade's share in percentage is depicted in Figure 26. Based on the available data, the analysis was performed to generate the regressive trendlines. The other significant sources apart from solar in Hungary are biomass, biogas, wind, and hydro. Among these sources, biomass has been a major RES in energy production over the last decade. The results show that the percentage share of biomass has reduced drastically from 67.4% to 48.1%. On the other hand, the other bio-based source increased a bit from 3.9% to 8.8%. Wind and hydro maintained their share somehow in the end. In contrast, solar energy emerged with the biggest growth from almost negligible share to a relevant share of 16.6%. Solar share in the last decade grew from almost 0

to 16%. If the same trends are observed, it could reach more than 30% if the given conditions remain the same. Also, new technological advancements could affect long-term goals.

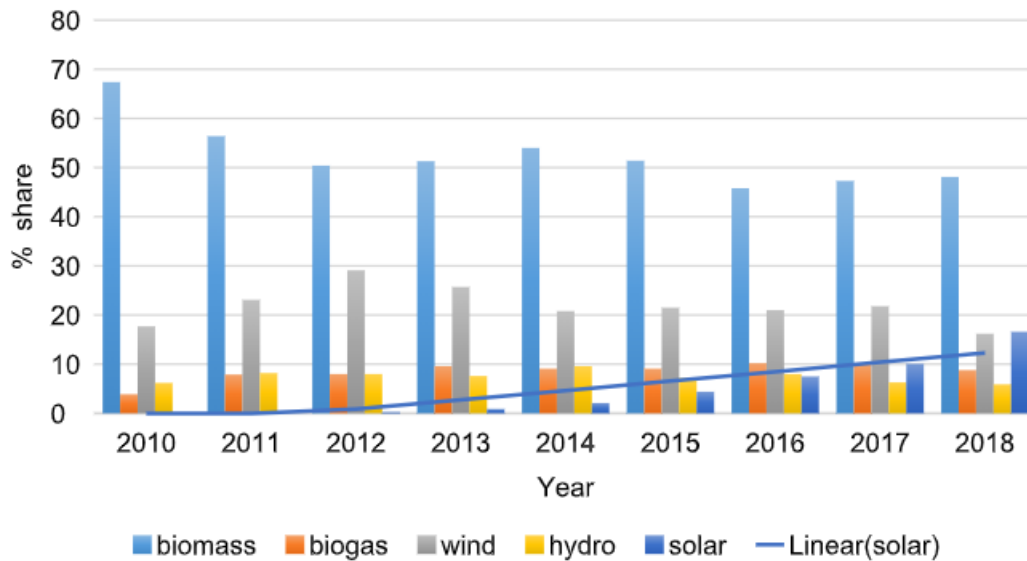


Figure 26. Growth trendline of solar energy share in Hungary (2010-2018) [based on the data of the Hungarian Central Statistical Office]

## 6.2. Trendline assesment of solar potential in Hungary and its neighbour countries

There are certain parameter which affect the solar PV potential analysis of any country or region. Among the several factors the solar irradiance, temperature profiles, weather conditions play a significant role [105]. Understanding the regional potential of PV-based energy generation geographical maps and thermal profiling could be an important tool in making accurate predictions for the regions energy capability [106]. Site specific irradiance forecast supported with temperature profiling helps in understandingthe forecast for PV regional potential. The sum of the energy falling on a surface on earth for a given time period is called Irradiation. The power or instantaneous energy rate received by a surface area on earth is known as Irradiance and is generally calculated on an hourly basis. The irradiance is correlated with cloud cover predictions.Thus, correct analysis of irradiance can be considered in compliance with the sky cover [107]. For understanding the irradiance distribution of the visegrad countries, the PV-GIS interactive tool was used to observe the distribution in four countries [108]. The capital cities, namely Warsaw, Bratislava, Prague and Budapest, were considered irradiance in the respective countries. The Figure 27. gives a brief estimation of horizontal and direct irradiance values in the four countries over the period of 2005-2016. The Monthly solar radiation data analysis reveals

## 6. SOLAR POTENTIAL IN HUNGARY-TRENDLINE ASSESSMENT

that the irradiance of Warsaw, Bratislava, and Prague lies below the range of 200 Kwh/m<sup>2</sup> even during the peak value months. On the contrary, for Budapest, Hungary, it could be observed that during the peak irradiance months, the values cross the range of 200 Kwh/m<sup>2</sup>. The evident higher values reveals higher solar potential of the Hungarian region.

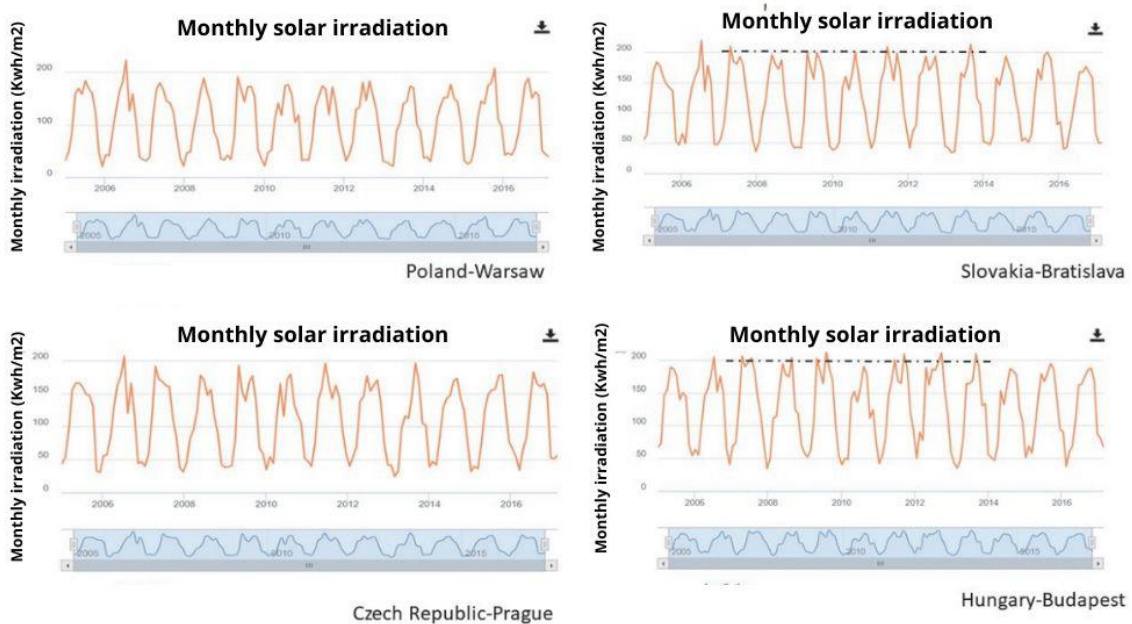


Figure 27. Solar Irradiation trendline of monthly values in capital cities of visegrad countries (2005-2016) [108]

Along with Irradiation data performance of grid, connected PV systems also play an important role in analyzing solar potential. European commission PV-GIS tool gives a monthly energy output for a fixed angle PV system. Figure 28. (a) gives an estimate of energy output throughout the year in kWh. We analyzed the capital cities of the four nations on their respective capital cities. It can be seen that Bratislava (Slovakia) and Budapest (Hungary) gives an output of more than 125 kWh during the peak summer. Whereas for Warsaw (Poland) and Prague (Czech Republic) somehow managed to reach the output of 125kWh during summer. The analysis is based on database of PVGIS-SARAH with slope angle of 35 Degrees. Figure 28 (b) shows solar park presence in various regions of Hungary based on power capacity. In that picture is also highlighted area with higher potential and with lesser solar parks

## 6. SOLAR POTENTIAL IN HUNGARY-TRENDLINE ASSESSMENT

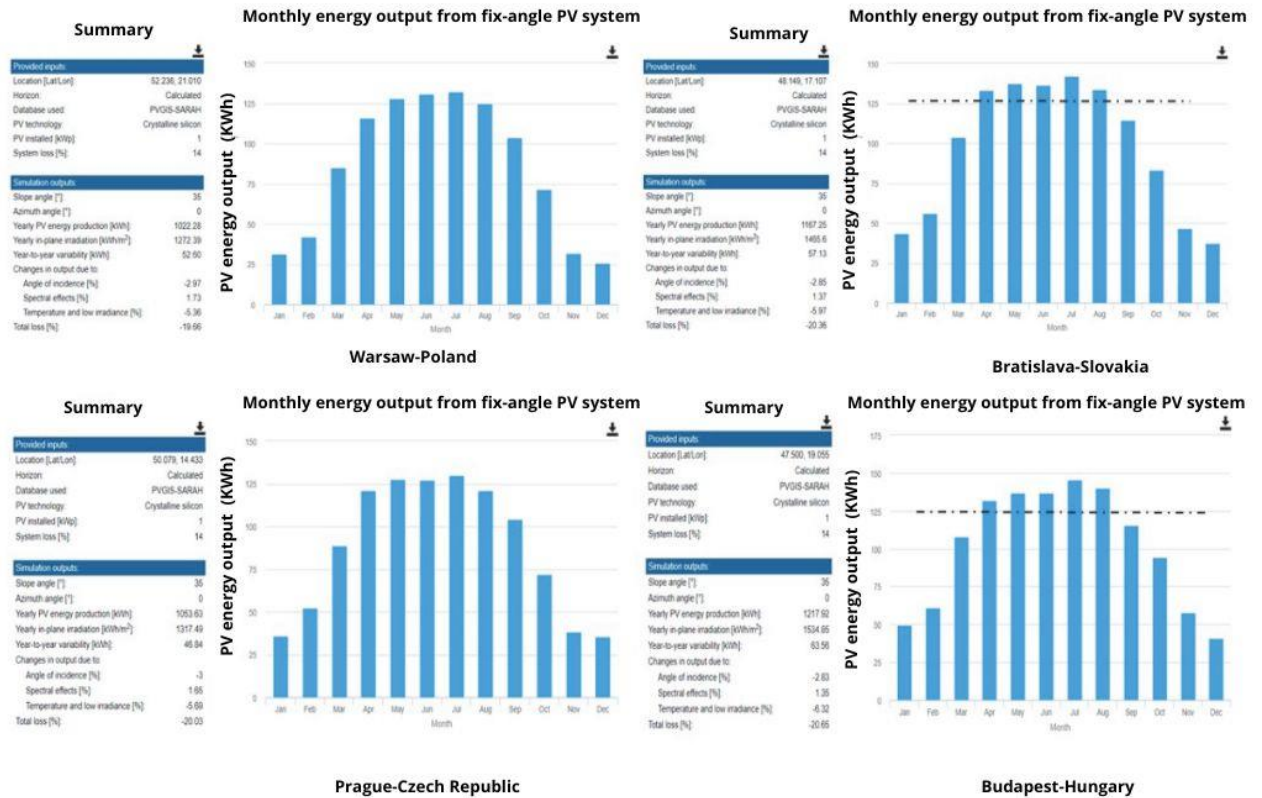


Figure 28. (a) Performance of Grid connected PV with energy output from fixed angle PV system in the capital cities of Visegrad Countries [based on the European Commission PV GIS analysis tool updated in 2019] [108]

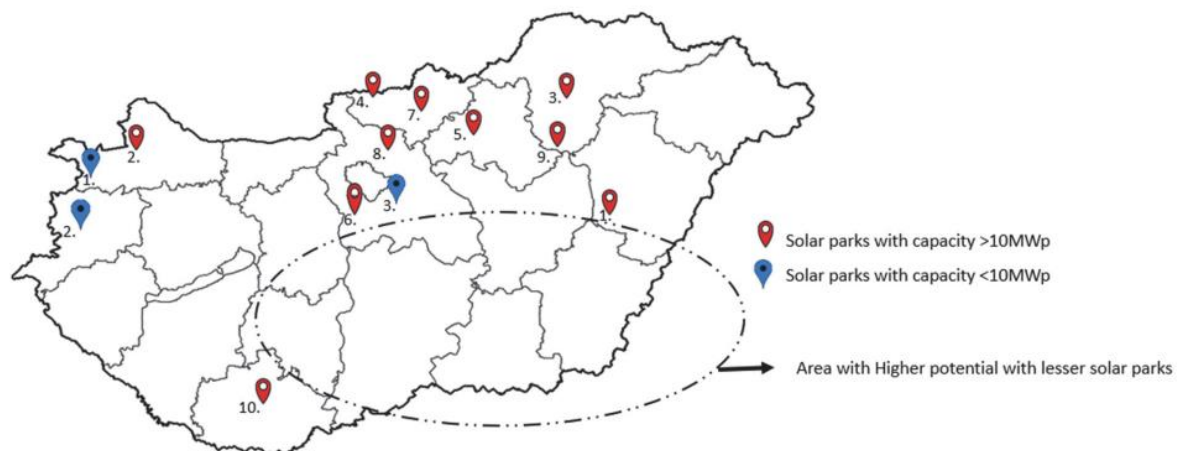


Figure 28. (b) Solar park presence in various regions of Hungary based on power capacity.

### **6.3. Case Study: Real-time Data Assessment of a boiler plant in Miskolc, Hungary**

This section presents a case study with data assessment from a boiler plant in Miskolc, Hungary, using wood chips as fuel. The intent is to provide insights into the real-time assessment of critical factors, such as moisture content, calorific value, production rates, and trendlines. It is well-known that the moisture content affects the calorific value, thus influencing the overall efficiency of the plant operation. Henceforth, the possible remedies are discussed to maintain the quality of wood chips utilizing solar dryers.

#### **6.3.1. Calorific value and moisture content of wood as biofuel**

Biomass withholds energy from them chemically. During combustion, the conversion of this chemical energy into heat occurs. The energy released during combustion is known as biomass's calorific value. This calorific value of the fuel could be determined in two ways, i.e., experimentally or through approximate methods. Among these methods, the experimental approach is costlier as it requires expensive instrumentation. Therefore, approximate methods are more commonly used for determining calorific values [109].

Generally, wood chips are stored in piles at the boiler storage plant. It is well known that boiler efficiency is directly proportional to the quality of fuel, which ensures good combustion. A good combustion fuel, in turn, suggests that it has a high calorific value. Gejdos et al. [110] investigated the storage and quality of wood chops for an experimental duration of 15 months. The extensive study reported that the calorific value was found to be higher on the lowermost part of the wood chip piles. In contrast, the ash content of the fuel was higher in the uppermost section. It is interesting to comprehend these results from the storage viewpoint for the wood chips. Figure 10. presents a general representation of the net calorific value of fuels used in boilers. It must be noted that these data do not consider the latent heat of vaporization.

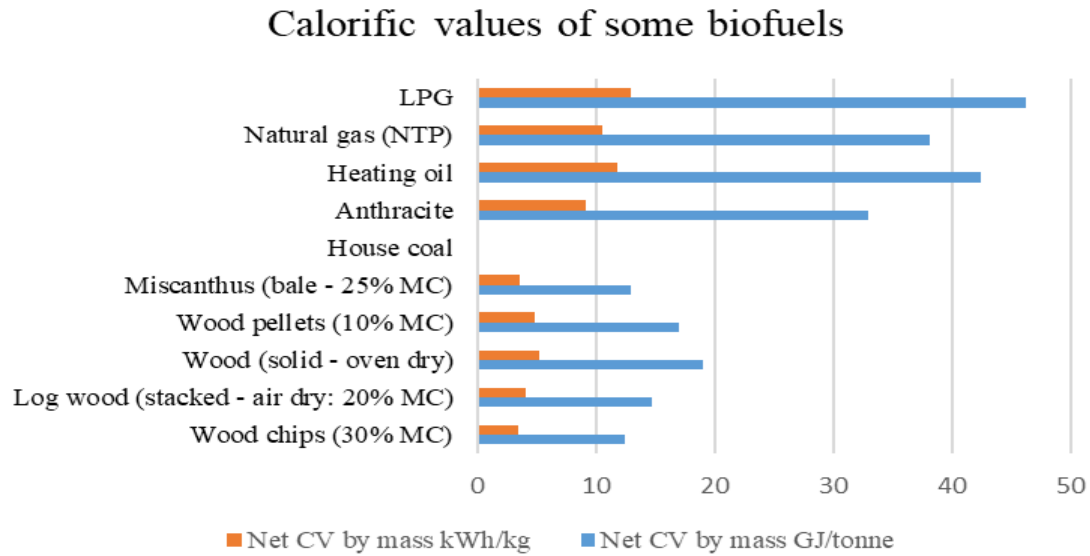


Figure 29. Typical calorific value of biomass fuels (based on data from Forest research, UK accessed on (23-02-2022) [111].

### 6.3.2. Calorific value and moisture content of wood as biofuel

In boiler operations, the moisture content of wood chips is an important parameter that determines the efficiency of the process. Generally, wood chips absorb a lot of moisture during winter and storage and transportation. Such moisture absorption would result in severe problems for the boiler furnace. Therefore, prediction and estimation of moisture content in wood chip samples become inevitable before feeding it in boilers. The moisture content is only a technical parameter, but the amount of moisture influences the supply cost. Therefore, it is essential for the suppliers of wood chips during pre-delivery and critical for operators before feeding the fuel to remove unwanted moisture. Traditionally SEP (Standard Error of Performance) is an estimate to calculate the moisture content from several samples. There are other bulk measurements, such as radio frequency measurements. These kinds of measurements are promising but not controlled for measuring moisture content in bulk samples of wood chips. The SEP method uses the below formula in Equation (45) to compute moisture content [112].

$$SEP = \sqrt{\frac{1}{(N-1)} \sum_{i=1}^N (e_i - \bar{e})^2} \quad (45)$$

Dzurenda and Banski [113] presented a model to understand the parameters affecting the Heat losses and the thermal efficiency of the boiler due to moisture content present in the wood chips

used as fuel in the boiler. The thermal efficiency of the boiler can be calculated using Equation (46) where  $\xi_i$  is the summation of all the heat losses due to flue gasses, chemical unburned carbon loss, mechanical unburned carbon loss, and the loss due to radiation of heat from the surface of boiler to the ambient space.

$$\eta_b = \frac{P}{mQ_n} 100 = 100 - \sum \xi_i \quad (46)$$

### 6.3.3. Trendline analysis: Moisture content and calorific value

To assess the relation between moisture content and calorific value, the authors have collected real-time data from the BIOENERGY MISKOLC Kft. boiler plant in Miskolc, Hungary. The data gathered is for four months, i.e., from December 2020 to March 2021, which is primarily the winter season operation cycle of the plant, as shown in Figure 30. As observed from the calorific plot value (MJ/kg) concerning moisture content (%), calorific value and moisture content are a mirror image of each other. The plot reflects that the data recorded were accurate and obeyed the trend; the calorific value decreases as moisture content increases. This plot shows that the moisture content rarely goes below 20% and mostly fluctuates between 30 – 40%. However, the moisture content in this range is not recommended for the efficient operation of the boiler [114].

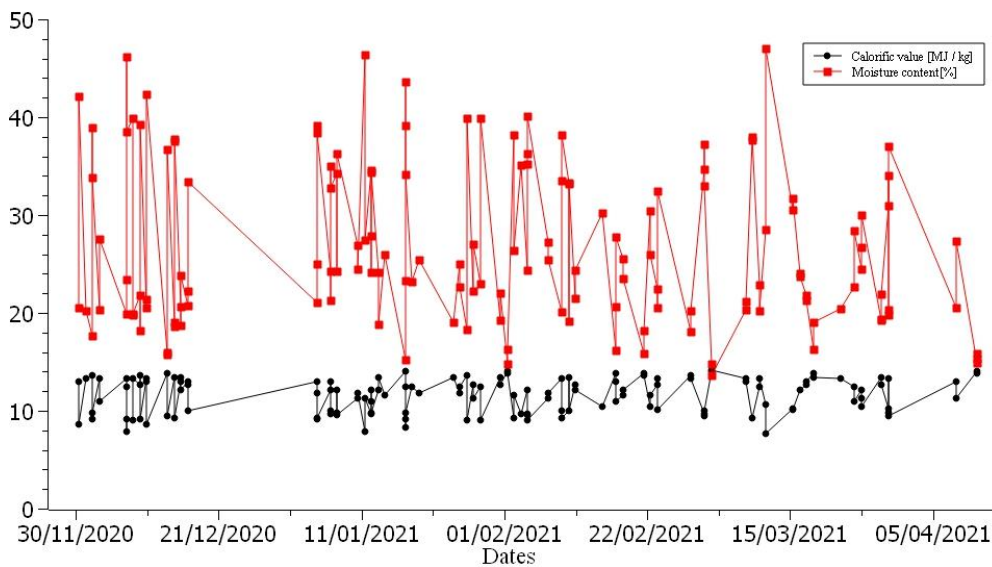


Figure 30. Graphical representation of data collected from the boiler plant for the calorific value and moisture content (duration 01-12-2020 to 06-04-2021) Source – BIOENERGY MISKOLC Kft., Miskolc, Hungary.

### 6.3.4. Trendline analysis: Production, consumption, and operations

Analogous to the Trendline analysis of moisture content and calorific value, the production, fuel consumption, and operating hours data are collected for analysis. The obtained data is presented visually in the form of a Trendline analysis representing the cumulative values from December to April, as shown in Figure 31. As observed, the production is highest during December and January. During these months, the fuel consumption and operating hours remain almost constant. From the analyzed data, it is evident that solar drying could help in reducing the moisture content in fuel, especially during the peak winter season.

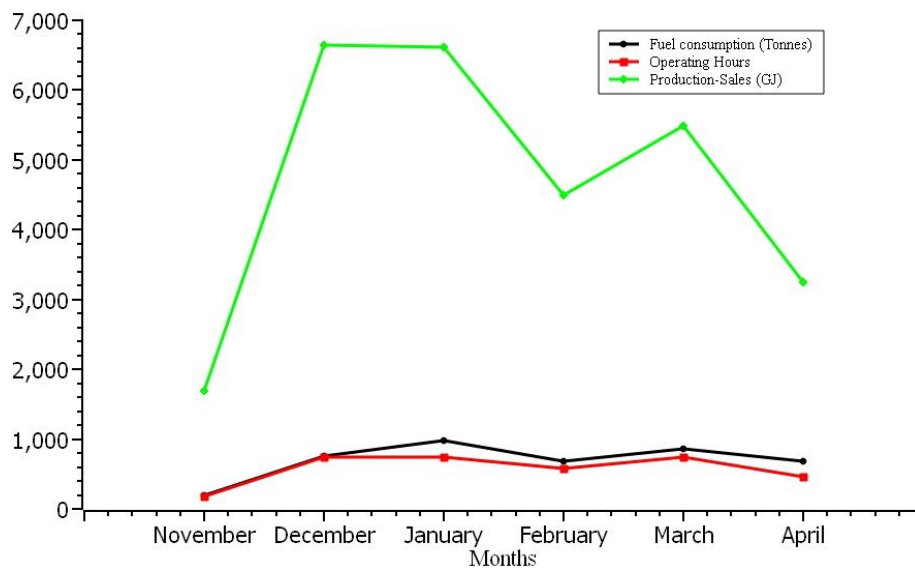


Figure 31. Graphical representation of data collected from the boiler plant for the Production, Fuel Consumption and Operating Hours (Duration November 2020 to April 2021) Source-BIOENERGY MISKOLC Kft. Miskolc, Hungary.

### 6.3.5. Identification of possible remedies via. solar drying

Storage of wood or wood chips is of primary concern for assuring quality or fuel efficiency in boiler operations. The solar energy potential of Hungary in the Central European region is higher than the neighbouring countries [115]. This untapped potential could enhance wood fuel quality with solar drying technology. For any wood type/species, the storage season plays an important role in ensuring the quality as it directly reflects in the moisture content and net calorific value. It is recommended that the storage span should not extend more than 3 – 4 months, as there is no significant energy gain after this period [116]. Ahmadiania et al. [117] proposed an interesting investigation for storing forest wood chips in piles with a self-heating mechanism. In the self-heating concept, due to the porosity inside the chip piles, the vapor pressure gradient increases due to the temperature gradient. It must be noted that pile size and porosity are essential factors

## 6. SOLAR POTENTIAL IN HUNGARY-TRENDLINE ASSESSMENT

in such drying processes. A lab-scale experimental set up was prepared to study the drying behavior of wood chips of grade EN14961 in Miskolc, Hungary [72]. Results show that natural convection dryer reached about 35 °C during peak hours. Also, the moisture content dropped to 25% in experiments performed during the winter season [6]. However, it becomes more complex in large-scale implementation. Based on the comprehensive review conducted and by comparing other models, through this review, the authors propose a solar drying solution with a hybrid model with three distinct choices, as shown in Figure 32. Further investigations can be performed on these three models on the lab scale to determine the best choice for supporting the drying of wood fuel during storage in the winter season.

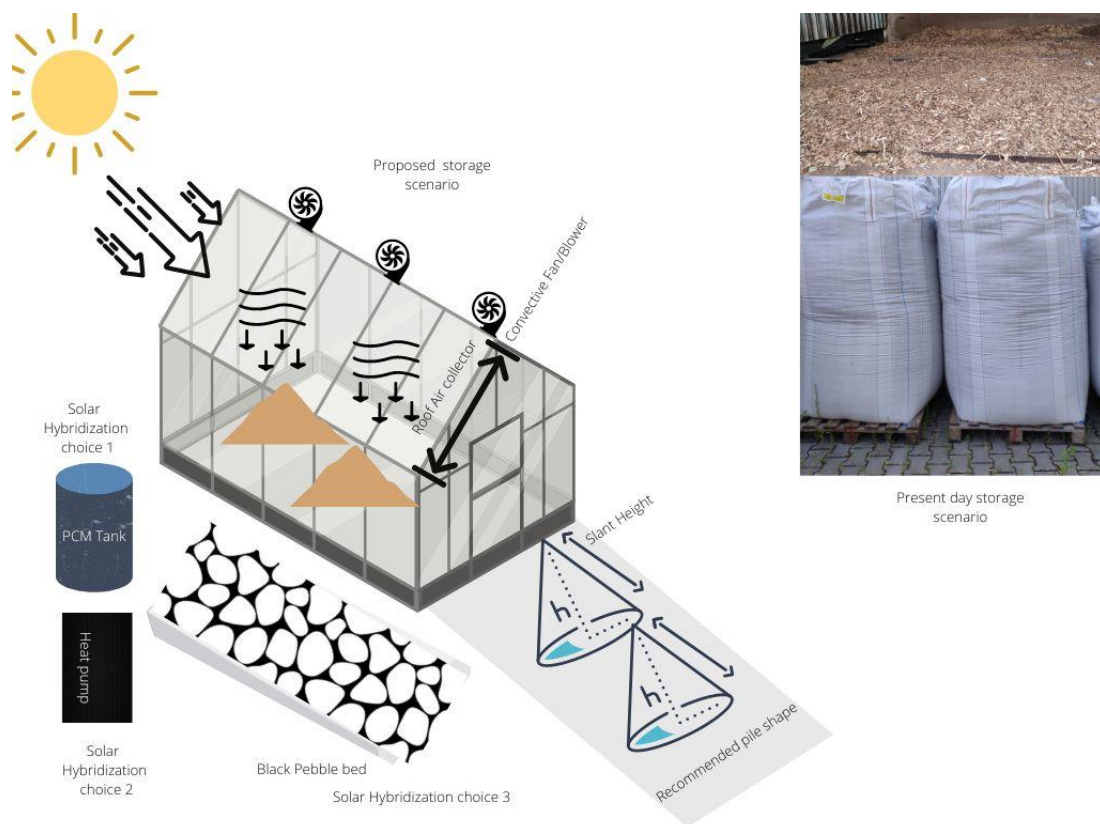


Figure 32. Proposed scenario for the solar drying of wood chips in plant with available hybridization choices for continuous drying during the storage.

### 7. THESES-NEW SCIENTIFIC RESULTS

**T1-** The forced convection solar cabinet dryer exhibited a temperature difference of 10–20 °C between its inlet and outlet, reaching a maximum temperature of 60°C and achieving an average overall energy efficiency ranging from 19.04% to 33.2%. Notably, sawdust and pellets demonstrated superior drying rates compared to woodchips.

**T2-** The use of Artificial Neural Network (ANN) models to predict final moisture content of wood fuels has not been explored before. The present ANN model with  $R^2$  value of 0.99, it successfully predicted final moisture content, displaying strong predictive capabilities. This suggests the potential for scaling up solar drying processes with additional resources.

**T3-** A novel hybrid dryer with PCM and artificial sun (halogen lamps) was developed to avoid intermittent irradiation. The dryer reached a maximum temperature of 70°C, retained useful heat for 3 hours after radiation switch-off, and showed exergy efficiencies ranging between 13.1% and 14.8%. PCM conditions significantly increased exergy amounts, reaching 0.012 kW.

**T4-** For, the hybrid dryer with PCM, the final moisture content of wood fuels was recorded at 11% for wood chips, 8% for pellets, and 6% for sawdust. Economic assessments estimated a lifespan of approximately five years, with a cost of 0.0058 EUR per kg of hot air, resulting in an annual emission of 64.09 kgs of CO<sub>2</sub>. Solar drying of wood fuels demonstrated reduced energy losses and CO<sub>2</sub> emissions, highlighting its environmental benefits.

**T5-** Concentrated solar parks with nearly 10 Megawatts capacity were observed in the northeastern region, with untapped potential identified in the southern and eastern areas (assessment based on the time period in years from 2010-2020). Eastern cities exhibited comparable photovoltaic outputs to western and northern counterparts. This data analysis serves as a valuable resource for government agencies and industrial planners in identifying solar power opportunities.

## 8. FUTURE SCOPE

Several technical parameters jeopardize the design development and optimization of wood drying. The intermittent nature of solar irradiation availability makes it inevitable to distinguish the design constraints for different types of wood products. For example, the solar drying of tropical species of wood in the African continent requires additional considerations of thermal energy storage compared to Australia's prevalent solar kilns. Such constraints are briefly discussed in Section 3.2. In design-based differentiation, the utility and vivid range of available thermal storage mediums play a significant role. However, selecting optimal media, products, and energy calculations requires regressive study and understanding their specific behavior.

Nevertheless, extensive research on numerical modeling and simulation using computational software has emerged as a savior for researchers. New models can be designed using C++, FORTRAN, CFD, MILP, MATLAB, etc., to understand the moisture removal rate with time-dependent equations. A lot more technical acumen can be achieved in investigating novel possible thermal storage mediums to integrate solar drying systems for both large and small-scale utilities. From the reported advancements and available literature, we provide an assessment of technologies that can be used in solar drying of wood drying with associated merits and demerits in Table 10.

Table 10. Merit and demerit assessment of advancements in technologies related to solar drying of wood fuel.

Sl. No.	Technological advancement in solar dryers	Merits	Demerits
1.	Use of photovoltaics and thermal combination	It can help replace auxiliary heaters with renewable	Construction and maintenance of

- |   |   |   |
|---|---|---|
|   | <p>sources (PV/T) and reduce CO<sub>2</sub> emissions. Also, it helps in stable drying conditions with thermal efficiency as high as 50% (approximately).</p>   | <p>glass-to-glass PV/T panel arrangements can be costly for a few applications. Modelling and energy storage of the electrical heater in combined form is yet to be investigated.</p>           |
| <p>2. Use of packed bed for thermal storage</p>                 | <p>The fibre saturation point of the wood can be attained in reduced time as when the MC reaches (fibre saturation point) FSP; it requires a faster drying rate which normal open-air drying could not support.</p> | <p>The black pebbles with higher heat storage capacity are unavailable in all locations. The setup of the dryer must be strongly built to withhold the pebbles in large quantities.</p>         |
| <p>3. Use of PCM for energy storage</p>                         | <p>Higher drying rates can be achieved with a suitable selection of the PCM based on the melting point when it matches the minimal and maximal output temperatures of the drying system.</p>                        | <p>The length, width, and centre distance of wood boards should be considered while selecting the PCM, as due to the difference in drying rates, residual stresses may occur on the boards.</p> |
| <p>4. Use of heat pumps as combined source of energy supply</p> | <p>Heat pumps can be used as a single energy storage source or could also be combined</p>   | <p>A heat pump requires a temperature gradient</p>  |

- 
- |   |  |
|---|--|
| with a concentrated PV/T setup. When used in combination can reduce drying time by 18%. | to work continuously on its compressor. Hence, it is recommended to be used in high-volume drying chambers with combined PV/T.   |
| 5. Use of greenhouse dryers for wood storage  | Greenhouse designs could use single glazing alone or double glazing. It can be modelled standalone or in semi-greenhouse form with faster drying rates. Glazing materials such as plexiglass-glass or plastic glass are readily available and can be constructed at lower costs. |
|   | Relatively lower thermal efficiency in comparison to other models. Even semi-greenhouse dryers increase the drying efficiency by only 5-10%.   |
- 

### 8.1. Future prospects on industrial utility

Much of the reported work on wood-fired boilers is on design and operation-related optimizations. Mermoud et al. [118] compared 2 Megawatt (large) and 0.65 Megawatt (small) wood boilers for efficiency and emissions factors. When the efficiency of the two boilers was compared, it was discovered that the load did not influence their efficiency. A consistent value was reflected for both boilers over the whole load range, even during standby times (83% for the 2MW boiler and 90% for the 0.65 MW boiler). On the other hand, due to the necessary increase in the extra air, CO emissions significantly worsened at low loads. Heat transfer models commonly study heat transfer phenomena during gasification [119]. ANSYS-FLUENT is used for CFD simulation of velocity, temperature, and density distributions to visualize the combustion process [120]. However, little work has been reported on the influence of moisture content in wood fuel and its impact on industrial boiler efficiency. Removing moisture from the woody biomass feedstock is inevitable for

efficient industrial energy production [121]. Optimally dried biomass improves the calorific value and boiler efficiency and lowers flue gas emissions. Investigations suggest that low-grade waste heat from power plants could also supplement drying. For example, Hanning et al. [122] calculated that a 100 MW (Megawatt) power plant could produce enough waste heat to dry the feedstock for a 40 MW plant. This study successfully reduced 60% (on a wet-basis) moisture content to as low as 10%. Similarly, new investigations can attempt to integrate the heat source with solar energy. Extensive review work has been carried out on the prospects of integrating solar air heating systems in the industrial sector. The study suggests solar drying systems can reduce energy consumption by 15% to 80% and carbon emissions by 20% to 80%, respectively [123]. There is untapped potential in achieving the best quality fuel from wood feedstock by controlling the moisture content through solar drying. To date, the EU has encouraged its member states to utilize forest wood for energy generation. As a result, wood is now being burned in numerous European countries' power plants. The European Parliament approved the Renewable Energy Directive's most recent modification (RED). The European Union's renewable energy objective was raised to 45%. The European Parliament also decided in September 2022 how wood burning and biofuels should be encouraged and included in calculating renewable energy targets with certain limitations [124]. The Dutch government, which imports over two metric million tons of wood pellets annually, presented its biomass application policy to the Dutch Parliament in 2022. By 2030, the nation hopes to phase out coal and produce 55% of its electricity from renewable sources [125]. Large-scale Danish combined heat and power (CHP) facilities have mostly switched from burning fossil fuels to woody biomass in recent years. In Spain and Austria, federal incentives exist in addition to central incentives [126]. In contrast, for low-level consumption, customers purchasing highly efficient wood or pellet stoves or larger home biomass heating systems in the USA may be entitled to claim a 30% tax credit, with a ceiling of \$2,000 per year, based on the unit's total cost (purchase and installation) [127]. Moving on to south Asia, Vietnam has seen a sharp increase in wood pellet output over the previous five years. The nation is now the second-largest exporter of wood pellets worldwide. However, most Vietnamese tropical wood imports are regarded as "high-risk" in terms of the legality of their source due to intense competition [128]. Due to these difficulties, a cleaner energy transition also necessitated coordinated, scientifically informed global solutions and the global nature of wood supply and woodfuel concerns.

## 8.2. Future research direction

The solar drying of wood fuels can play a vital role in addressing the increasing demand for wood products. Kumar et al. [102] recently developed a lab-scale dryer to measure the solar drying energy and exergy efficiency of three distinct wood fuels, i.e., woodchips, sawdust, and pellets. The results were found promising. According to environmental studies, a recent review suggests solar dryers have a strong potential for reducing carbon dioxide. Additionally, most of the analyzed situations had acceptable payback periods for these systems, demonstrating their economic advantage [129]. Favorable policies and promotions for solar drying combined with the collaboration of local/regional producers can boost the trade of dried products [130]. Policies related to supporting solar drying must be investigated. Furthermore, the carbon footprint of dryers was found to be low for dryers with high temperatures and low flow rate drying air design [131]. The supply chain analysis of the future solar dryer ecosystem can be improved using business model tools like a business canvas and value proposition models [132]. The discounted cash flow  $V_p$  could be used to undertake an economic assessment as mentioned in equation (47) [133]. The projected return on investment must also be examined.

$$V_p = \sum_{f=1}^n \left[ \frac{I_i}{(1+i)^n} - \frac{G_i}{(1+i)^n} \right] \quad (47)$$

Starting when the dryer works at its highest capacity and full-time, the investment's recovery and profitability are achievable; otherwise, it will be underutilized and produce economic losses, as do conventional dryers. For economical and performance reasons, the dryers' primary components can be changed. For example, the hot air trapping system can be covered in Plexiglas (PMMA). Similarly, more raw materials could be examined. Another critical possible future research direction is evaluating the CO<sub>2</sub> emissions (kg/year). Tagne et al. [108] performed calculations on carbon emissions and found solar drying of firewood on an industrial scale can be environment-friendly.

However, we found that limited studies have assessed the sustainability and economic parameters of solar-drying wood products. One possible reason could be limitations of data availability on environmental factors or financial pricing of products. This holds the potential that further research works can add this dimension to the overall optimization process of dryers as shown in Figure 33. It becomes more relevant to do an economic assessment of wood dryers because of their large volume storage capacity.

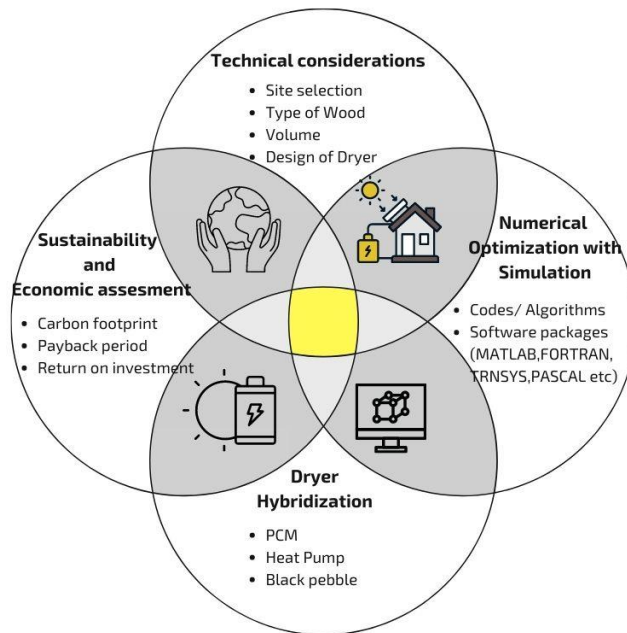


Figure. 33. Schematic representation of the four most important dimensions of research to be considered in future for solar drying assessment of wood fuel.

Another intriguing avenue for future research lies in exploring the potential effects of solar drying on thermochemical treatments such as torrefaction, gasification, or pyrolysis applied to various types of woody biomass. Investigating the influence of moisture content and drying temperature on these processes could yield valuable insights into enhancing the overall efficiency and sustainability of bioenergy production. By pre-drying woody biomass using solar energy, it may be possible to optimize the feedstock characteristics for thermochemical treatments, leading to improved energy yields and reduced emissions. Understanding the intricate interplay between solar drying parameters and subsequent thermochemical conversion processes could pave the way for more efficient and environmentally friendly bioenergy production systems. This research could contribute significantly to the development of cleaner and more sustainable alternatives to traditional fossil fuels, addressing pressing energy and environmental challenges.

**ACKNOWLEDGMENTS**

---

**REFERENCES**

- [1] A. H. Elsheikh, S. W. Sharshir, M. Abd Elaziz, A. E. Kabeel, W. Guilan, and Z. Haiou, “Modeling of solar energy systems using artificial neural network: A comprehensive review,” *Sol. Energy*, vol. 180, pp. 622–639, 2019, doi: <https://doi.org/10.1016/j.solener.2019.01.037>.
- [2] N. H. Helwa, H. A. Khater, M. M. Enayet, and M. I. Hashish, “Experimental Evaluation of Solar Kiln for Drying Wood,” *Dry. Technol.*, vol. 22, no. 4, pp. 703–717, Jan. 2004, doi: 10.1081/DRT-120034258.
- [3] A. Mujumdar, P. Perré, and R. Keey, “Drying of Wood: Principles and Practices,” *Handb. Ind. Drying, Fourth Ed.*, no. July, pp. 797–846, 2014, doi: 10.1201/b17208-44.
- [4] E. E. Thybring, M. Fredriksson, S. L. Zelinka, and S. V. Glass, “Water in Wood: A Review of Current Understanding and Knowledge Gaps,” *Forests*, vol. 13, no. 12, 2022, doi: 10.3390/f13122051.
- [5] H. A. Khater, N. H. Helwa, M. M. Enayet, and M. I. Hashish, “Optimization of Solar Kiln for Drying Wood,” *Dry. Technol.*, vol. 22, no. 4, pp. 677–701, Jan. 2004, doi: 10.1081/DRT-120034257.
- [6] K. Baibhaw, G. L. Szepesi, and Z. Szamosi, “Design and Development of natural convective solar dryer,” *Multidiscip. Sci.*, vol. 11, no. 4, pp. 144–150, 2021, doi: <https://doi.org/10.35925/j.multi.2021.4.18>.
- [7] M. Simo-Tagne, R. Rémond, Y. Rogaume, A. Zoulalian, and B. Bonoma, “Modeling of coupled heat and mass transfer during drying of tropical woods,” *Int. J. Therm. Sci.*, vol. 109, pp. 299–308, 2016, doi: <https://doi.org/10.1016/j.ijthermalsci.2016.06.012>.
- [8] M. Simo-Tagne, A. Zoulalian, R. Rémond, and Y. Rogaume, “Mathematical modelling and numerical simulation of a simple solar dryer for tropical wood using a collector,” *Appl. Therm. Eng.*, vol. 131, pp. 356–369, 2018, doi:

- <https://doi.org/10.1016/j.applthermaleng.2017.12.014>.
- [9] B. Lamrani, A. Khouya, and A. Draoui, “Energy and environmental analysis of an indirect hybrid solar dryer of wood using TRNSYS software,” *Sol. Energy*, vol. 183, no. March, pp. 132–145, 2019, doi: 10.1016/j.solener.2019.03.014.
- [10] A. Khouya, “Energy analysis of a combined solar wood drying system,” *Sol. Energy*, vol. 231, pp. 270–282, 2022, doi: <https://doi.org/10.1016/j.solener.2021.11.068>.
- [11] A. Khouya and A. Draoui, “Computational drying model for solar kiln with latent heat energy storage: Case studies of thermal application,” *Renew. Energy*, vol. 130, pp. 796–813, 2019, doi: 10.1016/j.renene.2018.06.090.
- [12] S. N. Ugwu, B. O. Ugwuishiwu, O. V Ekechukwu, H. Njoku, and A. O. Ani, “Design, construction, and evaluation of a mixed mode solar kiln with black-painted pebble bed for timber seasoning in a tropical setting,” *Renew. Sustain. Energy Rev.*, vol. 41, pp. 1404–1412, 2015, doi: <https://doi.org/10.1016/j.rser.2014.09.033>.
- [13] A. Khouya, “Modelling and analysis of a hybrid solar dryer for woody biomass,” *Energy*, vol. 216, p. 119287, 2021, doi: 10.1016/j.energy.2020.119287.
- [14] Z. F. Sun, C. G. Carrington, and P. Bannister, “Dynamic modelling of the wood stack in a wood drying kiln,” *Chem. Eng. Res. Des.*, vol. 78, no. 1, pp. 107–117, 2000, doi: 10.1205/026387600526942.
- [15] M. Hasan, M. Zhang, W. Wu, and T. A. G. Langrish, “Discounted cash flow analysis of greenhouse-type solar kilns,” *Renew. Energy*, vol. 95, pp. 404–412, 2016, doi: <https://doi.org/10.1016/j.renene.2016.04.050>.
- [16] X. Chi *et al.*, “Effects of air-assisted solar drying on poplar lumber drying processes in sub frigid zone regions,” *Dry. Technol.*, pp. 1–11, May 2022, doi: 10.1080/07373937.2022.2068571.
- [17] Y. J. David Luna, Jean-Pierre Nadeau, “Solar timber kilns: State of the art and foreseeable developments,” *Renew. Sustain. Energy Rev. Elsevier*, vol. 13, p. pp.1446-1455, 2009, doi: 10.1016/j.rser.2008.08.017.
- [18] H. U. Emelue, N. Omehe, P. Oghome, and K. Amanze, “Design and Construction of Cabinet Solar Dryers,” vol. 5, no. 3, pp. 270–284, 2015, doi: 10.9734/BJAST/2015/9433.
- [19] S. Malakar, V. K. Arora, and P. K. Nema, “Design and performance evaluation of an

- evacuated tube solar dryer for drying garlic clove,” *Renew. Energy*, vol. 168, pp. 568–580, 2021, doi: <https://doi.org/10.1016/j.renene.2020.12.068>.
- [20] R. Daghigh, R. Shahidian, and H. Oramipoor, “A multistate investigation of a solar dryer coupled with photovoltaic thermal collector and evacuated tube collector,” *Sol. Energy*, vol. 199, pp. 694–703, 2020, doi: <https://doi.org/10.1016/j.solener.2020.02.069>.
- [21] L. Ge and G.-S. Chen, “Control modeling of ash wood drying using process neural networks,” *Optik (Stuttg.)*, vol. 125, no. 22, pp. 6770–6774, 2014, doi: <https://doi.org/10.1016/j.ijleo.2014.07.091>.
- [22] A. Kharaghani, K. H. Le, T. T. H. Tran, and E. Tsotsas, “Reaction engineering approach for modeling single wood particle drying at elevated air temperature,” *Chem. Eng. Sci.*, vol. 199, pp. 602–612, 2019, doi: <https://doi.org/10.1016/j.ces.2019.01.042>.
- [23] B. Lamrani and A. Draoui, “Thermal performance and economic analysis of an indirect solar dryer of wood integrated with packed-bed thermal energy storage system: A case study of solar thermal applications,” *Dry. Technol.*, vol. 39, no. 10, pp. 1371–1388, Jun. 2021, doi: [10.1080/07373937.2020.1750025](https://doi.org/10.1080/07373937.2020.1750025).
- [24] M. Simo-Tagne, A. Zoulalian, R. Rémond, and Y. Rogaume, “Mathematical modelling and numerical simulation of a simple solar dryer for tropical wood using a collector,” *Appl. Therm. Eng.*, vol. 131, pp. 356–369, 2018, doi: [10.1016/j.applthermaleng.2017.12.014](https://doi.org/10.1016/j.applthermaleng.2017.12.014).
- [25] H. S. F. Awadalla, A. F. El-Dib, M. A. Mohamad, M. Reuss, and H. M. S. Hussein, “Mathematical modelling and experimental verification of wood drying process,” *Energy Convers. Manag.*, vol. 45, no. 2, pp. 197–207, 2004, doi: [https://doi.org/10.1016/S0196-8904\(03\)00146-8](https://doi.org/10.1016/S0196-8904(03)00146-8).
- [26] M. Hasan and T. A. G. Langrish, “Time-valued net energy analysis of solar kilns for wood drying: A solar thermal application,” *Energy*, vol. 96, pp. 415–426, 2016, doi: <https://doi.org/10.1016/j.energy.2015.11.081>.
- [27] F. Thibeault, D. Marceau, R. Younsi, and D. Kocaefe, “Numerical and experimental validation of thermo-hygro-mechanical behaviour of wood during drying process,” *Int. Commun. Heat Mass Transf.*, vol. 37, no. 7, pp. 756–760, 2010, doi: <https://doi.org/10.1016/j.icheatmasstransfer.2010.04.005>.
- [28] M. Autengruber, M. Lukacevic, and J. Füssl, “Finite-element-based moisture transport

- model for wood including free water above the fiber saturation point,” *Int. J. Heat Mass Transf.*, vol. 161, p. 120228, 2020, doi: <https://doi.org/10.1016/j.ijheatmasstransfer.2020.120228>.
- [29] D. Luna, J.-P. Nadeau, and Y. Jannot, “Model and simulation of a solar kiln with energy storage,” *Renew. Energy*, vol. 35, no. 11, pp. 2533–2542, 2010, doi: <https://doi.org/10.1016/j.renene.2010.03.024>.
- [30] S. Pang, “Mathematical Modeling of Kiln Drying of Softwood Timber: Model Development, Validation, and Practical Application,” *Dry. Technol.*, vol. 25, no. 3, pp. 421–431, Mar. 2007, doi: 10.1080/07373930601183751.
- [31] N. Bekkioui, “Performance comparison and economic analysis of three solar dryer designs for wood using a numerical simulation,” *Renew. Energy*, vol. 164, pp. 815–823, 2021, doi: <https://doi.org/10.1016/j.renene.2020.09.126>.
- [32] N. Bekkioui, S. El hakiki, A. Rachadi, and H. Ez-Zahraouy, “One-year simulation of a solar wood dryer with glazed walls in a Moroccan climate,” *Renew. Energy*, vol. 155, pp. 770–782, 2020, doi: <https://doi.org/10.1016/j.renene.2020.03.131>.
- [33] B. Lamrani and A. Draoui, “Thermal performance and economic analysis of an indirect solar dryer of wood integrated with packed-bed thermal energy storage system: A case study of solar thermal applications,” *Dry. Technol.*, vol. 0, no. 0, pp. 1–18, 2020, doi: 10.1080/07373937.2020.1750025.
- [34] M. Hasan and T. A. G. Langrish, “Performance Comparison of Two Solar Kiln Designs for Wood Drying Using a Numerical Simulation,” *Dry. Technol.*, vol. 33, no. 6, pp. 634–645, Apr. 2015, doi: 10.1080/07373937.2014.968254.
- [35] M. Bell, G. Carrington, R. Lawson, and J. Stephenson, “Socio-technical barriers to the use of energy-efficient timber drying technology in New Zealand,” *Energy Policy*, vol. 67, pp. 747–755, 2014, doi: <https://doi.org/10.1016/j.enpol.2013.12.010>.
- [36] M. Simo-Tagne and L. Bennamoun, “Numerical study of timber solar drying with application to different geographical and climatic conditions in Central Africa,” *Sol. Energy*, vol. 170, pp. 454–469, 2018, doi: <https://doi.org/10.1016/j.solener.2018.05.070>.
- [37] M. Simo-Tagne, M. C. Ndukwu, and M. N. Azese, “Experimental Modelling of a Solar Dryer for Wood Fuel in Epinal (France),” *Modelling*, vol. 1, no. 1, pp. 39–52, 2020, doi: 10.3390/modelling1010003.

- 
- [38] B. Lamrani and A. Draoui, "Modelling and simulation of a hybrid solar-electrical dryer of wood integrated with latent heat thermal energy storage system," *Therm. Sci. Eng. Prog.*, vol. 18, p. 100545, 2020, doi: <https://doi.org/10.1016/j.tsep.2020.100545>.
- [39] M. C. Ndukwu and L. Bennamoun, "Potential of integrating Na<sub>2</sub>SO<sub>4</sub> · 10H<sub>2</sub>O pellets in solar drying system," *Dry. Technol.*, vol. 36, no. 9, pp. 1017–1030, 2018, doi: [10.1080/07373937.2017.1366506](https://doi.org/10.1080/07373937.2017.1366506).
- [40] M. C. Ndukwu, D. Onyenwigwe, F. I. Abam, A. B. Eke, and C. Dirioha, "Development of a low-cost wind-powered active solar dryer integrated with glycerol as thermal storage," *Renew. Energy*, vol. 154, pp. 553–568, 2020, doi: <https://doi.org/10.1016/j.renene.2020.03.016>.
- [41] M. Diago, A. C. Iniesta, A. Soum-Glaude, and N. Calvet, "Characterization of desert sand to be used as a high-temperature thermal energy storage medium in particle solar receiver technology," *Appl. Energy*, vol. 216, pp. 402–413, 2018, doi: <https://doi.org/10.1016/j.apenergy.2018.02.106>.
- [42] A. Martínez González, R. Lesme Jaén, and E. E. Silva Lora, "Thermodynamic assessment of the integrated gasification-power plant operating in the sawmill industry: An energy and exergy analysis," *Renew. Energy*, vol. 147, pp. 1151–1163, 2020, doi: <https://doi.org/10.1016/j.renene.2019.09.045>.
- [43] N. Vanzetti, G. Corsano, and J. M. Montagna, "Integrated scheduling of the drying process in a sawmill," *Comput. Chem. Eng.*, vol. 153, p. 107407, 2021, doi: <https://doi.org/10.1016/j.compchemeng.2021.107407>.
- [44] L. Blanco-Cano, A. Soria-Verdugo, L. M. Garcia-Gutierrez, and U. Ruiz-Rivas, "Evaluation of the Maximum Evaporation Rate in Small-Scale Indirect Solar Dryers," *J. Sol. Energy Eng. Trans. ASME*, vol. 138, no. 2, pp. 1–4, 2016, doi: [10.1115/1.4032351](https://doi.org/10.1115/1.4032351).
- [45] O. A. Babar, A. Tarafdar, S. Malakar, V. K. Arora, and P. K. Nema, "Design and performance evaluation of a passive flat plate collector solar dryer for agricultural products," *J. Food Process Eng.*, vol. 43, no. 10, 2020, doi: [10.1111/jfpe.13484](https://doi.org/10.1111/jfpe.13484).
- [46] O. J. Alamu, C. N. Nwaokocha, and O. Adunola, "Design and Construction of a Domestic Passive Solar Food Dryer," *Leonardo J. Sci.*, no. 16, pp. 71–82, 2010.
- [47] H. E. Ñ, "Experimental energy and exergy analysis of a double-flow solar air heater having different obstacles on absorber plates," vol. 43, pp. 1046–1054, 2008, doi: <https://doi.org/10.1016/j.renene.2008.03.016>.

- 10.1016/j.buildenv.2007.02.016.
- [48] Ā. Kurtbas and A. Durmus, “Efficiency and exergy analysis of a new solar air heater,” vol. 29, pp. 1489–1501, 2004, doi: 10.1016/j.renene.2004.01.006.
- [49] G. Habtay, M. A. Al-Neama, J. Buzas, and I. Farkas, “Experimental Performance of Solar Air Heaters for Drying Applications,” *Eur. J. Energy Res.*, vol. 1, no. 5, pp. 4–10, 2021, doi: 10.24018/ejenergy.2021.1.5.29.
- [50] S. Hatami, G. Payganeh, and A. Mehrpanahi, “Energy and exergy analysis of an indirect solar dryer based on a dynamic model,” *J. Clean. Prod.*, vol. 244, p. 118809, 2020, doi: <https://doi.org/10.1016/j.jclepro.2019.118809>.
- [51] D. Bahrehmand, M. Ameri, and M. Gholampour, “Energy and exergy analysis of different solar air collector systems with forced convection,” *Renew. Energy*, vol. 83, pp. 1119–1130, 2015, doi: <https://doi.org/10.1016/j.renene.2015.03.009>.
- [52] T. K. Abdelkader, Q. Fan, E. S. Gaballah, S. Wang, and Y. Zhang, “Energy and Exergy Analysis of a Flat-Plate Solar Air Heater Artificially Roughened and Coated with a Novel Solar Selective Coating,” *Energies*, vol. 13, no. 4, 2020, doi: 10.3390/en13040997.
- [53] H. Krabch, R. Tadili, and A. Idrissi, “Design, realization and comparison of three passive solar dryers. Orange drying application for the Rabat site (Morocco),” *Results Eng.*, vol. 15, p. 100532, 2022, doi: <https://doi.org/10.1016/j.rineng.2022.100532>.
- [54] V. Rasooli Sharabiani, M. Kaveh, R. Abdi, M. Szymanek, and W. Tanaś, “Estimation of moisture ratio for apple drying by convective and microwave methods using artificial neural network modeling,” *Sci. Rep.*, vol. 11, no. 1, p. 9155, 2021, doi: 10.1038/s41598-021-88270-z.
- [55] P. P. Singh, S. Singh, and S. S. Dhaliwal, “Multi-shelf domestic solar dryer,” *Energy Convers. Manag.*, vol. 47, no. 13–14, pp. 1799–1815, 2006, doi: 10.1016/j.enconman.2005.10.002.
- [56] A. K. Kushwah, M. K. G. Gaur, A. K. Kumar, and P. S. Singh, “Application of ANN and prediction of drying behavior of mushroom drying in side hybrid greenhouse solar dryer : An experimental validation,” vol. 8, no. 2, 2022, doi: 10.18186/thermal.1086189.
- [57] A. Sadadou, S. Hanini, M. Laidi, and A. Rezrazi, “ANN-based Approach to Model MC / DR of Some Fruits Under Solar Drying,” vol. 70, pp. 233–242, 2021.

- 
- [58] B. K. Bala, M. A. Ashraf, M. A. Uddin, and S. Janjai, "Experimental and neural network prediction of the performance of a solar tunnel drier for drying jackfruit bulbs and leather," *J. Food Process Eng.*, vol. 28, no. 6, pp. 552–566, 2005, doi: 10.1111/j.1745-4530.2005.00042.x.
- [59] S. Tiwari, "ANN and mathematical modelling for moisture evaporation with thermal modelling of bitter gourd flakes drying in SPVT solar dryer," *Heat Mass Transf.*, vol. 56, no. 10, pp. 2831–2845, 2020, doi: 10.1007/s00231-020-02886-x.
- [60] J. F. Hinojosa, S. F. Moreno, and V. M. Maytorena, "Low-Temperature Applications of Phase Change Materials for Energy Storage: A Descriptive Review," *Energies*, vol. 16, no. 7, 2023, doi: 10.3390/en16073078.
- [61] S. Hasbi, K. Y. Leong, K. Z. K. Ahmad, A. R. Norwazan, and M. S. Saharudin, "Development of Coconut Oil/Capric Acid Eutectic Phase Change Material with Graphene as Latent Thermal Energy Storage," *Int. J. Automot. Mech. Eng.*, vol. 20, no. 1, pp. 10247–10257, 2023, doi: 10.15282/ijame.20.1.2023.07.0792.
- [62] L. Safira, N. Putra, T. Trisnadewi, E. Kusriani, and T. M. I. Mahlia, "Thermal properties of sonicated graphene in coconut oil as a phase change material for energy storage in building applications," *Int. J. Low-Carbon Technol.*, vol. 15, no. 4, pp. 629–636, 2020, doi: 10.1093/ijlct/ctaa018.
- [63] C. A. Saleel, "A review on the use of coconut oil as an organic phase change material with its melting process, heat transfer, and energy storage characteristics," *J. Therm. Anal. Calorim.*, vol. 147, no. 7, pp. 4451–4472, 2022, doi: 10.1007/s10973-021-10839-7.
- [64] C. A. Saleel, M. A. Mujeebu, and S. Algarni, "Coconut oil as phase change material to maintain thermal comfort in passenger vehicles: An experimental analysis," *J. Therm. Anal. Calorim.*, vol. 136, no. 2, pp. 629–636, 2019, doi: 10.1007/s10973-018-7676-y.
- [65] A. Afzal *et al.*, "Human thermal comfort in passenger vehicles using an organic phase change material— an experimental investigation, neural network modelling, and optimization," *Build. Environ.*, vol. 180, p. 107012, 2020, doi: <https://doi.org/10.1016/j.buildenv.2020.107012>.
- [66] D. M. Martínez, B. W. Ebenhack, and T. P. Wagner, "Chapter 1 - Introductory concepts," D. M. Martínez, B. W. Ebenhack, and T. P. B. T.-E. E. Wagner, Eds. Elsevier, 2019, pp. 1–33.

- 
- [67] B. Europe, “World Pellet Map.” [Online]. Available: <https://epc.bioenergyeurope.org/about-pellets/pellets-statistics/world-pellet-map/>. [Accessed: 25-Jul-2022].
- [68] D. Almeida and E. Marques, “Solar Drying Acacia- Influence in Pellets Quality :,” in *22nd International Congress of Mechanical Engineering (COBEM 2013)*, 2013, no. Cobem, pp. 6742–6752.
- [69] M. N. A. Hawlader, M. S. Uddin, and M. M. Khin, “Microencapsulated PCM thermal-energy storage system,” *Appl. Energy*, vol. 74, no. 1, pp. 195–202, 2003, doi: [https://doi.org/10.1016/S0306-2619\(02\)00146-0](https://doi.org/10.1016/S0306-2619(02)00146-0).
- [70] A. K. Raj, M. Srinivas, and S. Jayaraj, “A cost-effective method to improve the performance of solar air heaters using discrete macro-encapsulated PCM capsules for drying applications,” *Appl. Therm. Eng.*, vol. 146, pp. 910–920, 2019, doi: <https://doi.org/10.1016/j.applthermaleng.2018.10.055>.
- [71] G. Tsatsaronis, “Definitions and nomenclature in exergy analysis and exergoeconomics,” *Energy*, vol. 32, no. 4, pp. 249–253, 2007, doi: <https://doi.org/10.1016/j.energy.2006.07.002>.
- [72] B. Kumar, L. G. Szepesi, and Z. Szamosi, “Drying behaviour observations for wood chips of grade EN14961,” *Multidiszcip. tudományok*, vol. 11, no. 4, pp. 151–156, 2021, doi: [10.35925/j.multi.2021.4.19](https://doi.org/10.35925/j.multi.2021.4.19).
- [73] B. Kumar, G. Szepesi, Z. Szamosi, and G. Krámer, “Analysis of a Combined Solar Drying System for Wood-Chips, Sawdust, and Pellets,” *Sustainability*, vol. 15, no. 3, 2023, doi: [10.3390/su15031791](https://doi.org/10.3390/su15031791).
- [74] A. El Khadraoui, S. Bouadila, S. Kooli, A. Guizani, and A. Farhat, “Solar air heater with phase change material: An energy analysis and a comparative study,” *Appl. Therm. Eng.*, vol. 107, pp. 1057–1064, 2016, doi: [10.1016/j.applthermaleng.2016.07.004](https://doi.org/10.1016/j.applthermaleng.2016.07.004).
- [75] S. Bouadila, S. Kooli, M. Lazaar, S. Skouri, and A. Farhat, “Performance of a new solar air heater with packed-bed latent storage energy for nocturnal use,” *Appl. Energy*, vol. 110, pp. 267–275, 2013, doi: <https://doi.org/10.1016/j.apenergy.2013.04.062>.
- [76] A. K. Raj, M. Srinivas, and S. Jayaraj, “A cost-effective method to improve the performance of solar air heaters using discrete macro-encapsulated PCM capsules for drying applications,” *Appl. Therm. Eng.*, vol. 146, no. June 2018, pp. 910–920, 2019, doi: <https://doi.org/10.1016/j.applthermaleng.2018.10.055>.

- 10.1016/j.applthermaleng.2018.10.055.
- [77] A. Ghiami and S. Ghiami, “Comparative study based on energy and exergy analyses of a baffled solar air heater with latent storage collector,” *Appl. Therm. Eng.*, vol. 133, pp. 797–808, 2018, doi: 10.1016/j.applthermaleng.2017.11.111.
- [78] B. Kumar, G. Szepesi, and Z. Szamosi, “Optimisation techniques for solar drying systems: a review on modelling, simulation, and financial assessment approaches,” *Int. J. Sustain. Energy*, vol. 42, no. 1, pp. 182–208, Dec. 2023, doi: 10.1080/14786451.2023.2185870.
- [79] M. Edalatpour, A. Kianifar, K. Aryana, and G. N. Tiwari, “Energy, exergy, and cost analyses of a double-glazed solar air heater using phase change material,” *J. Renew. Sustain. Energy*, vol. 8, no. 1, p. 15101, Jan. 2016, doi: 10.1063/1.4940433.
- [80] A. Kianifar, S. Zeinali Heris, and O. Mahian, “Exergy and economic analysis of a pyramid-shaped solar water purification system: Active and passive cases,” *Energy*, vol. 38, no. 1, pp. 31–36, 2012, doi: <https://doi.org/10.1016/j.energy.2011.12.046>.
- [81] T. Alam, R. P. Saini, and J. S. Saini, “Experimental investigation on heat transfer enhancement due to V-shaped perforated blocks in a rectangular duct of solar air heater,” *Energy Convers. Manag.*, vol. 81, pp. 374–383, 2014, doi: <https://doi.org/10.1016/j.enconman.2014.02.044>.
- [82] J. Banout, P. Ehl, J. Havlik, B. Lojka, Z. Polesny, and V. Verner, “Design and performance evaluation of a Double-pass solar drier for drying of red chilli (*Capsicum annum L.*),” *Sol. Energy*, vol. 85, no. 3, pp. 506–515, 2011, doi: <https://doi.org/10.1016/j.solener.2010.12.017>.
- [83] O. Prakash and A. Kumar, “Environomical analysis and mathematical modelling for tomato flakes drying in a modified greenhouse dryer under active mode,” *Int. J. Food Eng.*, vol. 10, no. 4, pp. 669–681, 2014, doi: 10.1515/ijfe-2013-0063.
- [84] A. M. Zachariah, Richu Taher Maatallah, “Environmental and economic analysis of a photovoltaic assisted mixed mode solar dryer with thermal energy storage and exhaust air recirculation,” *Int. J. Energy Res.*, no. July, pp. 1–13, 2020, doi: 10.1002/er.5868.
- [85] “Australia’s independent guide to creating sustainable homes for the future.,” 2023. [Online]. Available: <https://www.yourhome.gov.au/materials/embodied-energy>. [Accessed: 10-Apr-2023].
- [86] Andrew Alcorn, “Embodied energy and CO2 coefficientd for NewZealand building

- materials,” *Cent. Build. Perform. Res. Victoria Univ. Wellingt.*, no. November, pp. 4–16, 2001.
- [87] M. C. Ndukwu *et al.*, “Assessment of eco-thermal sustainability potential of a cluster of low-cost solar dryer designs based on exergetic sustainability indicators and earned carbon credit,” *Clean. Energy Syst.*, vol. 3, no. October, p. 100027, 2022, doi: 10.1016/j.cles.2022.100027.
- [88] A. Hassan, A. M. Nikbahkt, Z. Welsh, P. Yarlagadda, S. Fawzia, and A. Karim, “Experimental and thermodynamic analysis of solar air dryer equipped with V-groove double pass collector: Techno-economic and exergetic measures,” *Energy Convers. Manag. X*, vol. 16, no. September, p. 100296, 2022, doi: 10.1016/j.ecmx.2022.100296.
- [89] L. Szabó and A. Szaniszló, “Solar power plant station in fishland,” *Int. Rev. Appl. Sci. Eng.*, vol. 8, pp. 37–43, 2017, doi: 10.1556/1848.2017.8.1.6.
- [90] M. Simo-tagne and M. Ndi-azese, “Thermal , economic , and environmental analysis of a novel solar dryer for firewood in various temperate and tropical climates,” *Sol. Energy*, vol. 226, no. August, pp. 348–364, 2021, doi: 10.1016/j.solener.2021.08.060.
- [91] A.-J. Perea-Moreno, A. Juaidi, and F. Manzano-Agugliaro, “Solar greenhouse dryer system for wood chips improvement as biofuel,” *J. Clean. Prod.*, vol. 135, pp. 1233–1241, 2016, doi: <https://doi.org/10.1016/j.jclepro.2016.07.036>.
- [92] C. Coskun, M. Bayraktar, Z. Oktay, and I. Dincer, “Energy and exergy analyses of an industrial wood chips drying process,” *Int. J. Low-Carbon Technol.*, vol. 4, no. 4, pp. 224–229, Dec. 2009, doi: 10.1093/ijlct/ctp024.
- [93] K. R. Arun, M. Srinivas, C. A. Saleel, and S. Jayaraj, “Active drying of unripened bananas (Musa Nendra) in a multi-tray mixed-mode solar cabinet dryer with backup energy storage,” *Sol. Energy*, vol. 188, no. July, pp. 1002–1012, 2019, doi: 10.1016/j.solener.2019.07.001.
- [94] A. Kamarulzaman, M. Hasanuzzaman, and N. A. Rahim, “Global advancement of solar drying technologies and its future prospects: A review,” *Sol. Energy*, vol. 221, pp. 559–582, 2021, doi: <https://doi.org/10.1016/j.solener.2021.04.056>.
- [95] V. Saini, S. Tiwari, and G. N. Tiwari, “Environ economic analysis of various types of photovoltaic technologies integrated with greenhouse solar drying system,” *J. Clean. Prod.*, vol. 156, pp. 30–40, 2017, doi: <https://doi.org/10.1016/j.jclepro.2017.04.044>.

- [96] A. Fudholi, K. Sopian, M. Y. Othman, M. H. Ruslan, and B. Bakhtyar, “Energy analysis and improvement potential of finned double-pass solar collector,” *Energy Convers. Manag.*, vol. 75, pp. 234–240, 2013, doi: <https://doi.org/10.1016/j.enconman.2013.06.021>.
- [97] S. Kumar and V. S. Kishankumar, “Thermal energy storage for a solar wood drying kiln: estimation of energy requirement,” *J. Indian Acad. Wood Sci.*, vol. 13, no. 1, pp. 33–37, 2016, doi: 10.1007/s13196-016-0162-x.
- [98] European Commission, “NECP HUNGARY, 2018.” [Online]. Available: [https://ec.europa.eu/energy/sites/ener/files/documents/ec\\_courtesy\\_translation\\_hu\\_necp.pdf](https://ec.europa.eu/energy/sites/ener/files/documents/ec_courtesy_translation_hu_necp.pdf).
- [99] European Commission, “NECP of European countries.” [Online]. Available: [https://ec.europa.eu/energy/topics/energy-strategy/national-energy-climate-plans\\_en](https://ec.europa.eu/energy/topics/energy-strategy/national-energy-climate-plans_en).
- [100] Eurostat DATA, “No Title,” 2020. [Online]. Available: <https://ec.europa.eu/eurostat/cache/infographs/energy/bloc-4c.html>.
- [101] J. Dyduch and A. Skorek, “Go South! Southern dimension of the V4 states’ energy policy strategies – An assessment of viability and prospects,” *Energy Policy*, vol. 140, no. 9, pp. 1689–1699, 2020, doi: 10.1016/j.enpol.2020.111372.
- [102] R. Energy, “Renewables in National Energy and Climate Plans of Visegrad countries Challenging the low ambition,” vol. 1, 2020.
- [103] J. Barwicki, M. Kuboń, and A. Marczuk, “New Developments of Solar Energy Utilization in the Aspect of EU Directives,” *Agric. Eng.*, vol. 21, no. 2, pp. 15–24, 2017, doi: 10.1515/agriceng-2017-0012.
- [104] A. Talamon, “Global renewable energy trends and Hungary,” *Int. Rev. Appl. Sci. Eng.*, vol. 3, no. 1, pp. 81–85, 2012, doi: 10.1556/irase.3.2012.1.10.
- [105] G. Pintér, H. Zsiborács, N. H. Baranyai, A. Vincze, and Z. Birkner, “The economic and geographical aspects of the status of small-scale photovoltaic systems in hungary-a case study,” *Energies*, vol. 13, no. 13, 2020, doi: 10.3390/en13133489.
- [106] G. A. Vokas, G. C. Zoridis, and K. V. Lagogiannis, “Single and Dual Axis PV Energy Production over Greece: Comparison between Measured and Predicted Data,” *Energy Procedia*, vol. 74, pp. 1490–1498, 2015, doi: 10.1016/j.egypro.2015.07.798.
- [107] S. Park, Y. Kim, N. J. Ferrier, S. M. Collis, R. Sankaran, and P. H. Beckman, “Prediction

- of Solar Irradiance and Photovoltaic Solar Energy Product Based on Cloud Coverage Estimation Using Machine Learning Methods,” *Atmosphere (Basel)*, vol. 12, no. 3, p. 395, 2021, doi: 10.3390/atmos12030395.
- [108] European Commission, “PHOTOVOLTAIC GEOGRAPHICAL INFORMATION SYSTEM.” [Online]. Available: [https://re.jrc.ec.europa.eu/pvg\\_tools/en/](https://re.jrc.ec.europa.eu/pvg_tools/en/).
- [109] M. Erol, H. Haykiri-Acma, and S. Küçükbayrak, “Calorific value estimation of biomass from their proximate analyses data,” *Renewable Energy*, vol. 35, no. 1, pp. 170–173, 2010, doi: 10.1016/j.renene.2009.05.008.
- [110] M. Gejdoš, M. Lieskovský, M. Slančík, M. Němec, and Z. Danihelová, “Storage and fuel quality of coniferous wood chips,” *BioResources*, vol. 10, no. 3, pp. 5544–5553, 2015, doi: 10.15376/biores.10.3.5544-5553.
- [111] Forest research, “Typical calorific Values.” [Online]. Available: <https://www.forestresearch.gov.uk/tools-and-resources/fthr/biomass-energy-resources/reference-biomass/facts-figures/typical-calorific-values-of-fuels/>. [Accessed: 23-Feb-2022].
- [112] J. Nyström and E. Dahlquist, “Methods for determination of moisture content in woodchips for power plants - A review,” *Fuel*, vol. 83, no. 7–8, pp. 773–779, 2004, doi: 10.1016/j.fuel.2003.11.002.
- [113] L. Dzurenda and A. Banski, “Influence of moisture content of combusted wood on the thermal efficiency of a boiler,” *Arch. Thermodyn.*, vol. 38, no. 1, pp. 63–74, 2017, doi: 10.1515/aoter-2017-0004.
- [114] I. Czupy, F. Szűcs, and A. Vágvölgyi, “Technical Problems of Wood Chips Utilization,” *IOP Conf. Ser. Earth Environ. Sci.*, vol. 159, p. 12038, 2018, doi: 10.1088/1755-1315/159/1/012038.
- [115] B. Kumar *et al.*, “Trendline assessment of solar energy potential in hungary and current scenario of renewable energy in the visegrád countries for future sustainability,” *Sustain.*, vol. 13, no. 10, 2021, doi: 10.3390/su13105462.
- [116] M. A. Brand, G. I. Bolzon de Muñoz, W. F. Quirino, and J. O. Brito, “Storage as a tool to improve wood fuel quality,” *Biomass and Bioenergy*, vol. 35, no. 7, pp. 2581–2588, 2011, doi: <https://doi.org/10.1016/j.biombioe.2011.02.005>.
- [117] S. Ahmadinia *et al.*, “Forest chip drying in self-heating piles during storage as affected by

- temperature and relative humidity conditions,” *Fuel*, vol. 324, p. 124419, 2022, doi: <https://doi.org/10.1016/j.fuel.2022.124419>.
- [118] F. Mermoud, A. Haroutunian, J. Faessler, and B. Lachal, “Impact of load variations on wood boiler efficiency and emissions,” *Arch. Des Sci.*, vol. 41, no. 0, pp. 27–38, 2015.
- [119] I. Klačková, I. Zajačko, R. Lenhard, I. Gritsuk, and D. Wiecek, “Simulation of wood biomass combustion in hot water boiler,” *IOP Conf. Ser. Mater. Sci. Eng.*, vol. 776, no. 1, p. 12033, 2020, doi: 10.1088/1757-899x/776/1/012033.
- [120] S. Echi, A. Bouabidi, Z. Driss, and M. S. Abid, “CFD simulation and optimization of industrial boiler,” *Energy*, vol. 169, pp. 105–114, 2019, doi: <https://doi.org/10.1016/j.energy.2018.12.006>.
- [121] D. C. Bianchini and F. J. Simioni, “Economic and risk assessment of industrial wood chip drying,” *Sustain. Energy Technol. Assessments*, vol. 44, p. 101016, 2021, doi: <https://doi.org/10.1016/j.seta.2021.101016>.
- [122] H. Li, Q. Chen, X. Zhang, K. N. Finney, V. N. Sharifi, and J. Swithenbank, “Evaluation of a biomass drying process using waste heat from process industries: A case study,” *Appl. Therm. Eng.*, vol. 35, pp. 71–80, 2012, doi: <https://doi.org/10.1016/j.applthermaleng.2011.10.009>.
- [123] A. Lingayat, R. Zachariah, and A. Modi, “Current status and prospect of integrating solar air heating systems for drying in various sectors and industries,” *Sustain. Energy Technol. Assessments*, vol. 52, p. 102274, 2022, doi: <https://doi.org/10.1016/j.seta.2022.102274>.
- [124] K. Richter, “EU Parliament votes to limit support for wood burning,” 2022.
- [125] S. Bolla, Bob , Flach, “Report Name : EU Wood Pellet Annual I . Summary Member State governments .,” *GAIN*, no. April, 2022.
- [126] D. Lesinsky, “ANALYSIS OF EXISTING INCENTIVES IN EUROPE FOR HEATING,” *Eur. Environ. Bureau*, no. December, 2020.
- [127] HPBA, “Wood and Pellet Heater Investment Tax Credit,” 2022.
- [128] fern, “EU BIOMASS-INCENTIVES MADNESS REACHES VIETNAM,” Nov-2022.
- [129] E. H. Bani Hani, M. Alhuyi Nazari, M. E. H. Assad, H. Forootan Fard, and A. Maleki, “Solar dryers as a promising drying technology: a comprehensive review,” *J. Therm. Anal. Calorim.*, vol. 147, no. 22, pp. 12285–12300, 2022, doi: 10.1007/s10973-022-

- 11501-6.
- [130] V. Goel, S. Bhattacharyya, R. Kumar, S. K. Pathak, V. V Tyagi, and R. P. Saini, “Identification of barriers and drivers to implementation of solar drying technologies,” *J. Therm. Anal. Calorim.*, 2022, doi: 10.1007/s10973-022-11631-x.
- [131] M. Beigi, M. Torki, F. Khoshnam, and M. Tohidi, “Thermodynamic and environmental analyses for paddy drying in a semi-industrial dryer,” *J. Therm. Anal. Calorim.*, vol. 146, no. 1, pp. 393–401, 2021, doi: 10.1007/s10973-020-09968-2.
- [132] B. Kumar, L. Berényi, Z. Szamosi, and G. L. Szepesi, “Business model analysis for the scope of entrepreneurship in a solar drying field in the European region,” *Entrep. Raw Mater. Sect.*, pp. 85–92, 2022, doi: 10.1201/9781003259954-9.
- [133] J. Q. Olguín, M. E. F. López, and y J. C. T. Urías, “ECONOMIC ASSESSMENT OF A WOOD SOLAR DRYER,” vol. 2, no. 7, pp. 97–104.

---

---

## LIST OF PUBLICATIONS RELATED TO THE TOPIC OF THE RESEARCH FIELD

- [1] Kumar, Baibhaw, Gábor Szepesi, Zoltán Szamosi, and Gyula Kramer. Analysis of a Combined Solar Drying System for Wood-Chips, Sawdust, and Pellets. *Sustainability*.15 (3):1791. (2023) MTMT: 33582995 <https://doi.org/10.3390/su15031791> Q1(3.8)
- [2] Kumar, Baibhaw, Raj K, Arun, Gábor Szepesi and Zoltán Szamosi. A conspectus review on solar drying of wood: regional and technical contrivances. *J Therm Anal Calorim.* (1-25) (2023). MTMT: 33721596 <https://doi.org/10.1007/s10973-023-12093-5> Q2 (4.75)
- [3] Kumar, Baibhaw, Gábor Szepesi and Zoltán Szamosi. Optimisation techniques for solar drying systems: a review on modelling, simulation, and financial assessment approaches, *International Journal of Sustainable Energy*, 42:1, 182-208, (2023) MTMT: 33714404 DOI: 10.1080/14786451.2023.2185870 (Q2)
- [4] Kumar, Baibhaw, Gábor Szepesi, Zsolt Čonka, Michal Kolcun, Zsolt Péter, László Berényi, and Zoltán Szamosi. Trendline Assessment of Solar Energy Potential in Hungary and Current Scenario of Renewable Energy in the Visegrád Countries for Future Sustainability, *Sustainability*, Vol.13, issue 10, P 5462, (2021) MTMT: 32017468 <https://doi.org/10.3390/su13105462> Q1 (3.8)
- [5] Kumar, Baibhaw, Gábor Szepesi and Zoltán Szamosi. Drying behaviour observations for wood chips of grade en14961, *Multidiszciplináris tudományok: a Miskolc egyetem közleménye* 11: 4 pp.151-156.,6p. (2021) MTMT:31937254 <https://doi.org/10.35925/j.multi.2021.4.19>
- [6] Kumar, Baibhaw, Gábor Szepesi and Zoltán Szamosi. Design and development of natural convective solar dryer, *Multidiszciplináris tudományok: a Miskolc egyetem közleménye* 11: 4 pp.144-150., 7p. (2021) MTMT: 31931131 <https://doi.org/10.35925/j.multi.2021.4.18>
- [7] Kumar, Baibhaw, László Berényi, Gábor Szepesi and Zoltán Szamosi. Business model analysis for the scope of entrepreneurship in a solar drying field in the European region. *ENTREPRENEURSHIP IN THE RAW MATERIALS SECTOR*, 85. (2022). MTMT:32740220 <http://dx.doi.org/10.1201/9781003259954-9>